SLOSHING MOTION OF WATER

IN A

MOONPOOL

by

J. MADHANI BSc(Hons) Civil Engineering

A THESIS SUBMITTED IN PARTIAL FULFILMENT OF MASTER

OF SCIENCE IN MARINE TECHNOLOGY

(OFFSHORE ENGINEERING)

University of Strathclyde
Department of Ship & Marine
Technology
Glasgow

November 1985

CONTENTS

SUMMARY

This thesis is concerned with the sloshing motion of water in a moonpool. It is a relatively new problem, that is particularly predominant in moonpools with relatively large dimensions. The problem is further complicated by the additional behaviour of vertical oscillation. It is inevitable that large moonpools will be needed as offshore technology advances, therefore making a problem an important one. The research involves two parts, the theoretical and experimental study.

The theoretical study consists of idealising the moonpool to a two dimensional system, represented by two surface piercing parallel barriers at a distance 2a apart. The barriers are forced to undergo roll motion which in turn generates waves. These travelling waves are travelling in opposite directions to each other and have the same amplitude and period, and thus can be expressed in terms of a standing wave. This is mathematically achieved by applying the theory of wavemaking, and therefore the wave amplitude at the side wall can be evaluated at near resonant conditions.

The experimental study comprises of comparing the results obtained from the tank and moonpool experiments. The rolling motion creates the sloshing waves in both cases, in addition the vertical oscillation in the moonpool is produced by generating waves at one end of the towing tank. Apart from highlighting influencing parameters, the resonant frequencies obtained from these experiments are then compared with the theoretical values. Experiments in demonstrating the effect of increasing damping with the aid of baffles are also conducted.

This is an important aspect which is very necessary if operations in launching and retrieving are to be carried out efficiently and safely.

ACKNOWLEDGEMENTS

The project was initiated and supervised by Dr. Lee of Strathclyde University and I am indebted to him for his assistance and support.

I would also like to gratefully acknowledge the following members of staff in building the model and helping to set up the experiments:

D. Clelland (Research Assistant),
W. West (Senior Technician),
I. Bellingham (Technician) and
A. Thompson (Technician).

LIST OF FIGURES AND TABLES

1.0 INTRODUCTION

The advance in offshore exploration has demanded a need for effective and efficient support. One aspect which is vital to this support is the ability to launch and retrieve diving bells, submersibles and equipment. This is often achieved via an open moonpool. In the past, moonpools employed for launching and retrieving subsea units have been generally designed with small dimensions, suitable for subsea units such as diving bells. Although the moonpool system has many advantages over other handling systems, i.e. side and stern handling (see Lee [1]), there is a major drawback, this being the water column in the moonpool can oscillate as much as four times or more than the outside waves in certain conditions. This particular aspect has received much attention in the past few years.

Due to advancement in Offshore Technology, the need for deploying larger subsea units with regular or irregular shapes has arisen and handling these calls for a larger moonpool which can also be used for a variety of other purposes i.e. 'a Multipurpose Moonpool'. Although the vertical oscillation continues to be a problem, the increasing size of the moonpool allows for the free surface to exhibit greater movement, thus making the sloshing motion of the moonpool significant. The combination of vertical oscillation and sloshing motion will indeed lead to hazzards in launching and retrieving operations.

Another aspect of sloshing is that it can cause high local structural loads. A similar problem of sloshing in liquid cargo tanks has received considerable attention. The situation is identical, in that the water in the tank responds to the ship's motions and when the excitation is near the natural fundamental frequency of the water, this results in violent waves. The motion subsequent to this excitation will mainly depend upon the depth of water (h) and the width of tank (L). The low draft case (for $h/L < 0.21$) is characterised by the formation of hydraulic jumps and travelling waves for excitation periods around resonant. At higher draft ($h/L \geqslant 0.21$) large standing waves are usually formed in the resonant range. Furthermore it is understood that the free surface of a liquid under forced oscillation has an infinite number of natural frequencies. However it is the lowest mode that has the likelihood of being excited since the prevailing frequencies of ship's motion are relatively low.

The phenomenon of water sloshing in moonpools is very complicated. Apart from the many parameters such as size and geometrical shape of the moonpool, there are the non-linear effects such as the free surface and at the fluid-side wall interface. Being a relatively new problem, it has not received any serious effort in research. It must also be stated that sloshing in tanks has not been successfully solved despite the fact that it has received much attention.

With the above in mind, plus the limited time available, particular emphasis was placed on experimental studies.

The format of the thesis basically comprises of ten chapters. The aims of the project are stated in Chapter 2. In Chapter 3 the Literature Review investigates and highlights previous work which has been conducted in this field. As sloshing in moonpools is a relatively new problem, to date there has been little or no work recorded. Thus most of the work expressed in the Literature Review is on related topics i.e. sloshing in tanks. Chapter 4 discussed the project approach, both from a theoretical and experimental aspect. The theoretical aspect consists of simplifying the sloshing motion in a moonpool to a parallel surface piercing barriers undergoing roll motion, and the approach to solving the problem was accomplished by applying the wavemaker theory. Furthermore, the resonant frequencies of the sloshing motion were calculated. The experimental study generally consisted of making comparisons between the sloshing motion in a moonpool with a tank.

The in-depth theoretical study is carried out in Chapter 5. Here the problem is formulated by modelling the moonpool with vertical barriers and applying the assumption/ boundary conditions. The solution to the problem is obtained by considering waves generated by one barrier and adding it to the waves created by the neighbouring barrier. The barriers are moving in phase with one another. The addition of these waves basically constitute a standing wave which can be mathematically expressed by using the wavemaker theory. The final part of this chapter involves calculating the resonant frequencies by using a general formula for natural frequency and substituting the relevant resonant terms.

In chapter 6 the Experimental Study involves employing a two-dimensional model tank with a removeable bottom which was attached to a roll forcing mechanism. This feature allowed the model in addition to a tank to be used as a moonpool which was located and fitted in a towing tank. The experiment consisted of performing a series of runs by activating the roll forcing mechanism at varying speeds. This in turn excited the water within the tank/moonpool and therefore enabled the wave height to be measured via a wave probe which was connected to a pen recorder chart. Additional experiments were conducted with baffles inserted in the model to introduce damping and hence investigate the outcome. Furthermore, waves were generated in the towing tank to create vertical oscillation in the moonpool. This meant that overall the resonant frequencies for pure sloshing, vertical oscillation and the coupling effect of the two could be measured. The results obtained from the experiments are shown at the end of this chapter. This also includes a summary of Experimental Results and Observations. A brief description on the character of fluid tank/moonpool behaviour with a set of photographs taken during the experiments are in Chapter 7.

Chapter 8 involves discussions on the experimental and theoretical studies and Chapter 9 mentions areas which require further research. Finally, the outcome of the work conducted for this thesis is concluded in Chapter 10.

2.0 AIMS OF THE PROJECT

The main aim of this project is to investigate the behaviour of sloshing in moonpools with relatively large dimensions and obtain a basic knowledge and understanding of the problem.

More specifically the aims are:

1. To carry out experiments to compare the phenomenon of water sloshing in a moonpool with the same in a closed container.

2. To develop a simple theoretical model of moonpool sloshing and verify it through experimental results.

3. To explore methods of reducing sloshing motion.

3.0 LITERATURE REVIEW

In the past, analytical studies of liquid motion in rigid containers has been subjected to numerous investigations. The majority of the present and past work are based on simplified potential flow. Two classes of solutions have been established from this theory, i.e. the linear and non-linear solutions. It is obvious that the linear solutions are the simplest in that the equation is linearised by neglecting the second order term. In the case of non-linear solution, the assumption in neglecting the second-order term cannot be made. Hence this entails a more complex solution involving either the Power Series or the Numerical methods. A great deal of non-linear studies of liquid sloshing have stemmed from Moisiev's theory (See ref.[2]).

Faltinsen [3] studied the effect of sloshing in rectangular tanks. The theoretical study uses the non-linear perturbation technique. This mathematical model is an extension of Moisiev's theoretical work. In his analysis, Faltinsen considers the depth of fill to be moderate to large and assumes small amplitude roll motions of containers. In a more recent paper, Faltinsen [4] applied a boundary integral technique in favour of the finite element or finite difference technique. The problem was formulated for sway only and uses the distribution of sources on the boundaries and free surface in order to determine the potential at any point in the fluid. This method is very cumbersome and not entirely successful when comparisons were made with the experiments. To account for this error, Faltinsen performed an additional theoretical study based on another mathematical model.

This was achieved by using a small fictitious term which was added in the dynamic free surface condition and the mathematical model was completed by the usual process of satisfying the boundary conditions and separating the variables. This was purely for a transient case, i.e. free vibrations.

The shallow-depth case has been investigated by Chu and Ying [5], Chester [6], Verhagen and Wijngaarden [7] and Wijngaarden [8]. The solution is derived by using a perturbation method. The linear theory of acoustics which is also known as the shallow water wave theory in the area of hydrodynamics, is used. It predicts a single hydraulic jump of constant strength which moves periodically back and forth in the container.

Theoretical and experimental study of ship-roll stabilisation tanks have been conducted by Chu and co-workers [9]. Although the results of the theoretical study were not comparable with the experimental study, the work provides useful information on experimental techniques. During the experiments the movement of free surface was mapped at discrete intervals in time with small angles of roll oscillation. A detailed description was also given on the general character of tank fluid behaviour.

Demirbilek [10] studied Energy Dissipation sloshing waves in a rolling tank. He mentions that viscous in sloshing plays an important role and therefore this should not be ignored. Due to the fact that there has been relatively little work on the effect of viscosity in sloshing, the paper introduces a linear theory of viscous liquid sloshing and formulates a boundary value problem subject to the appropriate conditions. Viscosity is included in the problem formulation.

Demirbilek formulates the problem on the basis of absolute and apparent accelerations. Absolute accelerations consisted of Euler's equation of motion, and apparent accelerations were defined as a combination of translational, centrifugal, Euler and Coriolis accelerations. The purpose of introducing these fictitious accelerations was to account for the translational and rotational motion of the moving co-ordinate system. The formulation was completed by the usual conditions, and supposingly allowed for viscosity by incorporating the effects into the dynamic free surface boundary conditions. (The actual process was not published).

The mathematical solution involves expressing the velocity potential Φ in terms of hyperbolic functions and trigonometric functions in order to express the waves in the tank. This was incorporated into an infinite Fourier series-type solution. The outcome of this study provided useful information in the relation of viscous dissipation with Reynolds and Froude numbers which were expressed in terms of the tank dimensions. Furthermore, this allows the prediction of the fact that as the draft increases less viscous energy is dissipated.

The theory of wavemaking was first introduced by Haverlock [11]. The principle formula was derived by considering the motion of the water surface to consist of travelling waves together with local disturbance. This type of solution is one which may have possible application to the waves produced in water by the small oscillations of a solid body. A standing wave can be considered as the superimposition of two travelling waves of the same amplitude and same period, travelling in opposite directions.

With this in mind, the theory of wavemaking can be used to express the standing waves and local disturbances which, for example, occurs in the moonpool when excited by the roll motion of the vessel.

Bass and co-workers [12] investigated the effect of Liquid Loads in LNG cargo tanks. The paper presents the results of a research study to develop LNG tank design methodology for loads resulting from LNG sloshing. The experiment comprised of gathering sloshing data from scaled models with a range of fill depths, excitation frequencies, amplitudes and tank wall pressure measurements. Emphasis has been made on slosh induced dynamic wall pressures which is of concern when considering the structural strength of tanks.

Sloshing in tanks is a complicated problem and this problem has not been successfully solved. Indeed, sloshing coupled with vertical oscillation adds further complication to the problem. To date there has been no work recorded in this field. This means that the literature review reveals only parallel studies which have been undertaken and have a similar pattern of behaviour and perhaps in some way may be related.

4.0 PROJECT APPROACH

The approach involves the theoretical and experimental study. In view of critical review more emphasis is given to the latter.

1. Theoretical Study

Waves generated in the moonpool by the rolling motion are similar to those waves caused by two parallel surface-piercing barriers undergoing roll motion. In turn, the two barrier problem can be solved by considering waves generated by each barrier. The approach to solving the problem is accomplished by applying the wavemaker theory. Hence the simplification of a moonpool problem to a two barrier problem allows this approach to be taken.

2. Experimental Study

Pure sloshing which is the result of a liquid in a tank undergoing roll motion is a long standing and well established problem which has received much attention. The motion of the water in the moonpool with relatively large dimensions is still in the primary stages of investigation. Whether these two problems have similar characteristics still has to be studied. The effects of vertical oscillation on the sloshing in moonpools are also unknown. The obvious approach in tackling these unknown aspects are to make comparisons.

Making comparisons between the two cases not only allows these particular aspects to be highlighted but it will enhance the fundamental understanding of the problem.

Furthermore, it will also determine the parameters which play an important role in the sloshing behaviour of water in moonpools. With this in mind, the experimental study will comprise of a rectangular tank undergoing roll oscillation which will represent a purely sloshing behaviour, and a rectangular open moonpool section immersed in a towing tank undergoing the same excitation.

As the moonpool increases in size, it is inevitable that some form of damping will be necessary to ensure that operations in launching and retrieving can be safely carried out. Therefore additional experiments are also carried out to demonstrate the effects of increasing damping with the aid of baffles.

5.0 THEORETICAL STUDY

5.1 INTRODUCTION

When a body is immersed in water and undergoes the roll motion, this results in waves being generated. The principle of wavemaking has been extensively studied (see ref. [11], [12] and [13] and has been applied to a wide range of wavemakers such as flap type, wedge type and so on.

Basically, the wavemaker theory represents the waves generated in two parts: travelling waves which propogate in the X-direction (see fig. 5.1) and local disturbances which decay as the distance from the wavemaker increases. If a second barrier is placed at a distance 2a and experiences roll motion (assuming small amplitude roll), there will be two progressive periodic waves of the same period and amplitude but travelling in the opposite direction. This results in a formation of a standing wave.

When considering the moonpool, it is expected that the roll motion will produce standing waves as in the case of a tank. On this basis of similarity, the wavemaker theory will be applied to the moonpool problem; bearing in mind that this approach has never been attempted.

5.2 FORMULATION OF THE PROBLEM

Consider a two-dimensional carestian co-ordinate system with its origin at the undisturbed free surface on the centreline of the moonpool with y positively downwards. The width of the infinitely long barriers (moonpool) is 2a while the depth of immersion is h. The moonpool is forced to oscillate harmonically in rolling mode with small amplitude at frequency W (see fig. 5.2).

Assumptions and Boundary Conditions

The amplitude of motion of the barriers is assumed to be small so that the equations can be linearised. With this approximation, the horizontal fluid velocity at $x = \pm a$ is equal to the component of the velocity of the moonpool (barriers). Viscosity and surface tension are neglected. Consider the following:

(a) Fluid is incompressible and flow is irrotational so that there exists a velocity potential which satisfies Laplace equation.

$$\partial^2\Phi/\partial x^2 + \partial^2\Phi/\partial y^2 = 0 \quad \ldots\ldots\ldots\ldots(1)$$

(b) The linearised free surface condition is given by:

$$K\phi + \frac{\partial \phi}{\partial y} = 0 \qquad \text{at} \quad y=0 \;\ldots\ldots\ldots\ldots (2)$$

For further information on (a) and (b) see Appendix III and ref. [14, 15].

(c) Body Boundary Conditions

$$\frac{\partial \phi}{\partial x} = \pm \; U(y) \; \text{Cos} \; wt \qquad \text{at} \quad x = \pm a$$

where U(y) is the horizontal component of the velocity at any point (a,y) on the barriers and w is the frequency of moonpool rotation. See also ref. [12, 13].

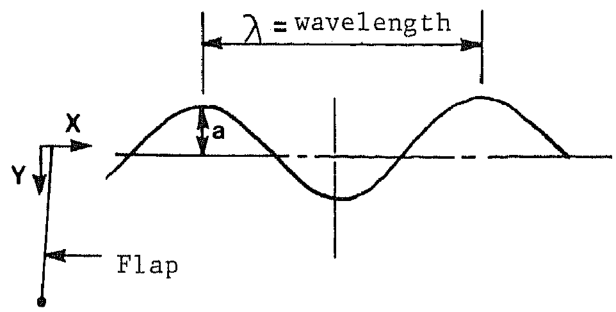

Fig. 5.1 Flap Type Wavemaker

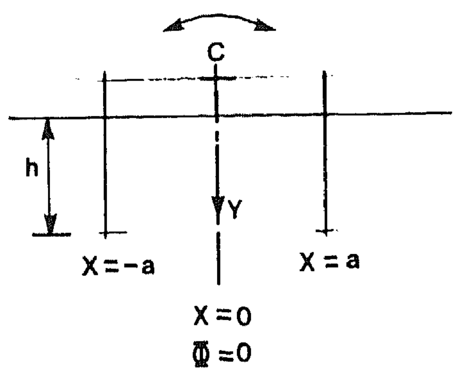

(C is centre of rotation)

Fig. 5.2 (Two Barriers Representing a Moonpool)

5.3 SOLUTION

The expression for Φ being the velocity potential which satisfies the conditions in 5.2 are in the form as shown below:

$$\Phi = \Phi_1 + \Phi_2 \quad \ldots\ldots\ldots\ldots\ldots\ldots\ldots\ldots\ldots\ldots \quad (4)$$

where Φ_1 represents Standing Waves and Φ_2 local oscillations (i.e. at x = a oscillations at x = -a disappears and vice versa).

Thus $$\Phi_1 = \frac{2A}{K} \text{ Cosh Ky SinKa Coswt} \quad \ldots\ldots\ldots\ldots \quad (5)$$

$$\Phi_2 = \frac{An}{Kn} \text{ Cos Kny } (e^{-Kn(a+x)} + e^{In(x-a)}) \text{ Coswt} \quad \ldots \quad (6)$$

The constants A and An are chosen to satisfy equation (3) (see 5.2)

K, Kn are wave numbers such that $K = 2\pi/\lambda$ and $Kn = 2\pi\frac{(2n-1)}{\lambda}$ where λ is the wavelength and n is an integer.

By applying the boundary conditions and solving the equations in the manner as shown in Appendix II, the constants A and An can be determined.

i.e. $$A = \frac{2WeS \operatorname{Cosh} Kh}{Kh \operatorname{Cos}^2 Ka (\operatorname{Sin}Kh \operatorname{Cosh} Kh + Kh)} \qquad \text{........(7)}$$

and $$An = \mp \frac{2WeS \operatorname{Cos}Knh}{Knh\, e^{-Kn2a} (\operatorname{Sin}Knh \operatorname{Cos}Knh + Knh)} \qquad \text{........(8)}$$

where h = draft (m)

S = amplitude of roll motion (m)

2a = width of moonpool (m)

We = frequency of excitation (rad/s)

(see Appendix II for further details)

By substituting (7) and (9) into (5) and (6) yields

$$\Phi_1 = \frac{4\ We\ S \operatorname{Cosh}Kh \operatorname{Cosh}Ky \operatorname{Sin}Kx \ \operatorname{Cos} wt}{K^2 h \operatorname{Cos}^2 Ka (\operatorname{Sinh}Kh \operatorname{Cos}Kh + Kh)}$$

The surface elevation is given by

$$\zeta = \frac{1}{g} \partial\Phi/\partial t \qquad \text{..................................(9)}$$

At x = a

$$1\zeta 1 = \frac{2We}{h} S \operatorname{Sin} wt\ (w) \frac{2\operatorname{Cosh}Kh \operatorname{Sin}Ka}{K^2 \operatorname{Cos}Ka (\operatorname{Sinh}Kh \operatorname{Cos}Kh + Kh)} +$$

$$\sum_{n=1}^{\infty} \frac{\operatorname{Cos}Knh}{Kn^2 (\operatorname{Sin}Knh \operatorname{Cos}Knh + Knh)} \qquad \text{..................................(10)}$$

the resonant frequency is given by

$$Wn = (Kn\ g \tanh Knh)^{1/2}$$

The lowest mode is most likely to be excited,
i.e. n = 1 therefore:

$$W = \left[\frac{2\pi}{\lambda} \; g \tanh \frac{2\pi}{\lambda} h\right]^{1/2} \quad \ldots\ldots\ldots\ldots\ldots\ldots\ldots\ldots (12)$$

At resonance, assuming that $\lambda = 4a$ and substituting in equation (10) yields

$|\eta| \to \infty$, i.e. the amplitude of wave approaches infinity, at near resonance conditions.

Thus the frequency of resonant is such that its wavelength is 4a.

Hence from equation (12) yields

$$W_{RES} = \left[\frac{\pi g}{2a} \; \tanh \frac{h\pi}{2a}\right]^{1/2} \quad \ldots\ldots\ldots\ldots\ldots\ldots\ldots\ldots (13)$$

5.4 CALCULATION OF RESONANT FREQUENCIES

(a) Sloshing Motion:

The Resonant Frequencies of the sloshing motion are calculated from equation (13) (5.3) by substituting numerical values for both h and 2a. The results are tabulated below:

ASPECT RATIO (h/2a)	W_{RES} rad/s 2a = 0.5	W_{RES} rad/s 2a = 0.2
0.25	6.36	4.50
0.5	7.52	5.32
1.00	7.84	5.54
1.50	7.85	5.55

(b) Vertical Oscillation

Neglecting non-linearities due to variable mass in the moonpool, the natural frequency for the free undamped moonpool oscillation is given by:

$$Wv = \left[\frac{g}{h+h'}\right]^{1/2} \qquad (14)$$

where h is draught of moonpool, $g = 9.81 m/s^2$ and h is the equivalent length of added water column below moonpool. See ref. [16].

Equation (14) can be rearranged as follows:

$$h = g/Wv^2 - h' \quad \ldots\ldots\ldots\ldots\ldots\ldots\ldots\ldots\ldots\ldots \quad (15)$$

in addition, $h' \propto (At)^{1/2}$ where At equals the cross sectional area of the moonpool.

$$\Rightarrow h' = \text{constant } (At)^{\frac{1}{2}} \quad \ldots\ldots\ldots\ldots\ldots\ldots\ldots\ldots \quad (16)$$

The values of h and Wv are obtained from the experimental study and substituted into equation (15). (See Table 5). This allows h' to be calculated and therefore from equation (16) the constant can be evaluated as shown in Table 1.

TABLE 1

Frequency *Wv (rad/S)	$1/Wv^2$	Draft h (m)	g/Wv^2	h'	$(At)^{1/2}$	Constant
6.91	0.021	0.125	0.206	0.081	0.274	0.30
5.53	0.033	0.250	0.324	0.074	0.274	0.27
6.03	0.028	0.200	0.274	0.075	0.173	0.43
4.9	0.042	0.300	0.412	0.112	0.173	0.65

* See Table 5

Ideally, for an average value, the constant should be evaluated from a much larger sample of data.

However, in order to make comparisons, it is possible to use a constant of 0.41 derived by Fukuda (see ref. [16], bearing in mind that only vertical oscillation is considered).

i.e. $h' = 0.41\ (At)^{1/2}$ .... (17.)

The results calculated from equation (15) using equation (17) are shown in Table 2.

TABLE 2

ASPECT RATIO h/2a	Wv rad/s
0.25	6.43
0.50	5.22
1.00	6.02
1.50	5.70

6.0 EXPERIMENTAL STUDY

6.1 INTRODUCTION

In the past, theoretical studies have been presented in order to tackle the general problem of liquid sloshing in tanks. They are complex in nature, often involving assumptions which tend to divert the problem from a reality to an ideal case. However, liquid sloshing in tanks is regarded as a relatively well established engineering problem, whilst water sloshing in moonpools is a relatively new problem which means that virtually no information is available on this topic.

In order to exploit the limited resources, some useful information can be obtained by comparing the two cases of water sloshing i.e. the tank and the moonpool. This will provide a foundation to a more comprehensive analysis of the problem. Therefore the main aims of the experiments are:

(1) To compare the behaviour of sloshing in a tank with a moonpool when excited by roll motion of the vessel.

(2) To compare the above results with the calculated resonance frequencies.

(3) To explore methods of increasing damping with the aid of baffles.

The roll motion was chosen because out of the six modes of motions it is the most influential mode in sloshing.

6.2 DESCRIPTION OF MODEL

The basic configuration of the model used in performing experiments is shown in fig. 6.2. The two dimensional model was constructed from 13mm plywood with a front perspex panel for viewing. It also has a bottom which can be easily removed. This feature allows the model to be used to represent a liquid tank and a simplified moonpool undergoing roll motion. The dimensions of the model are 500mmL x 700mmh x 150mmW. The experimental arrangement is shown in fig. 6.2, 6.3 and 6.4.

The amplitude of roll of the model was fixed at approximately $3\frac{1}{2}°$. It was not possible due to the restriction on time to carry out a series of experiments with a variation of roll angles.

To accommodate higher aspect ratios, for example h/2a = 1.0, 1.5, it was necessary to reduce the width of the model. This was achieved by constructing two hollow square sections of 150mmL x 150mmW x 700mmh. These sections were wedged inside the model against the sides and held in position by suitable clamps.

Finally, baffles of two different sizes, 20/40mm x 150mmL were cut from thin plastic material and these were to be pressed into place as shown in fig. 6.1.

6.3 INSTRUMENTS USED AND EXPERIMENTAL PROCEDURE

The tank was filled to the required water depth. In the case of the moonpool, the appropriate water depth was achieved by raising or lowering the dexion frame support, see fig. 6.4. The wave probe and the linear variable transformers (LVDT) were calibrated to 0.05v/cm and 0.1v/cm respectively. The signals from these transducers were then recorded on a pen recorder.

The roll forcing mechanism was switched on and once the steady state was achieved (within a minute), the results were taken. The motor was then switched off allowing the motions within the model to subside before generating another excitation frequency in a similar manner.

Experiments Conducted (See Table 3)

(1) Tank forced to roll with varying excitation frequencies.

(2) Tank as in (1) but with damping (baffles).
(For baffle's position see Table 4).

(3) Moonpool forced to roll as in (1).

(4) Moonpool stationary with waves generated* by wavemaker in towing tank to produce vertical oscillations.

(5) Moonpool with waves generated and also forced to roll as in (1) to produce coupling effect.

(6) Moonpool as in (1) but with damping (see Table 4 for baffle's position).

TABLE 3

To show the types of experiment carried out at various aspect ratios.

ASPECT RATIOS			
0.25	0.5	1.0	1.5
1	1	1	1
-	2	-	-
3	3	3	3
4	4	4	4
5	5	5	5
-	6	-	-

Note: Number indicates the type of experiment, as described in main text. See above.

* Waves were generated prior, at and just after resonant frequency due to vertical oscillation.

6.4 MOONPOOL EXPERIMENTS WITH WAVES

Simple harmonic waves of a range of frequencies were generated by the wavemakers, and thus produced an oscillating column of water within the moonpool. The amplitudes of the vertical oscillation were then measured with its corresponding frequencies. The moonpool was externally excited by the roll forcing mechanism during vertical oscillation, and in some cases where time permitted, before and after; the procedure being exactly the same as in 6.3. The third channel from the pen recorder was connected to the wave probe situated outside the vicinity of the moonpool, positioned in phase with the wave probe inside the moonpool. This allowed the ratio of Moonpool Wave amp/wave amp to be calculated.

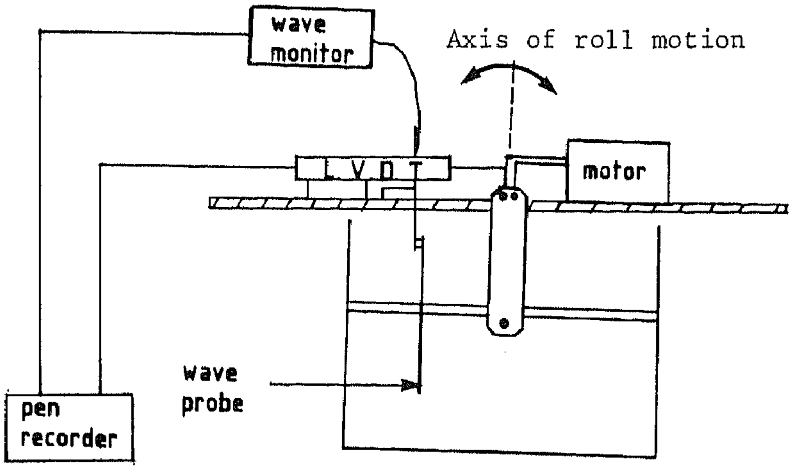

Fig. 6.2 Experimental Arrangement

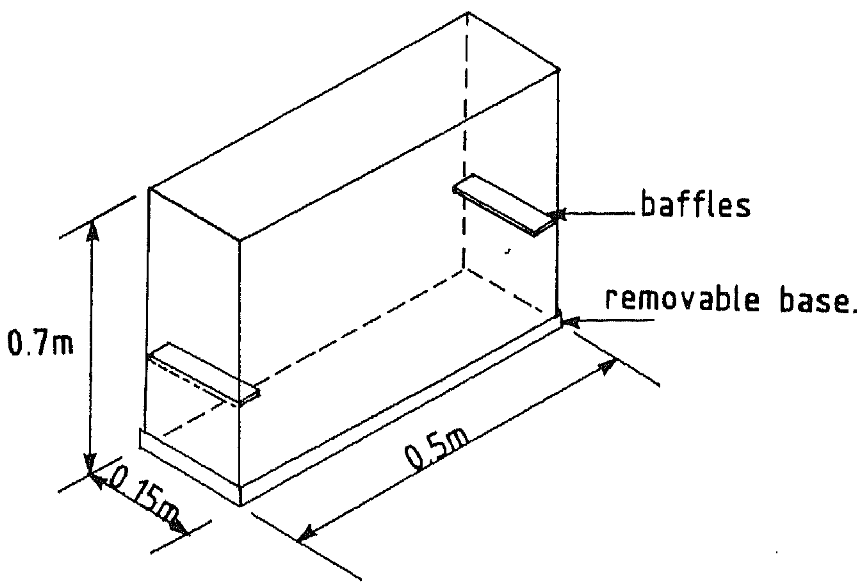

Fig. 6.1 Basic Configuration of the Model

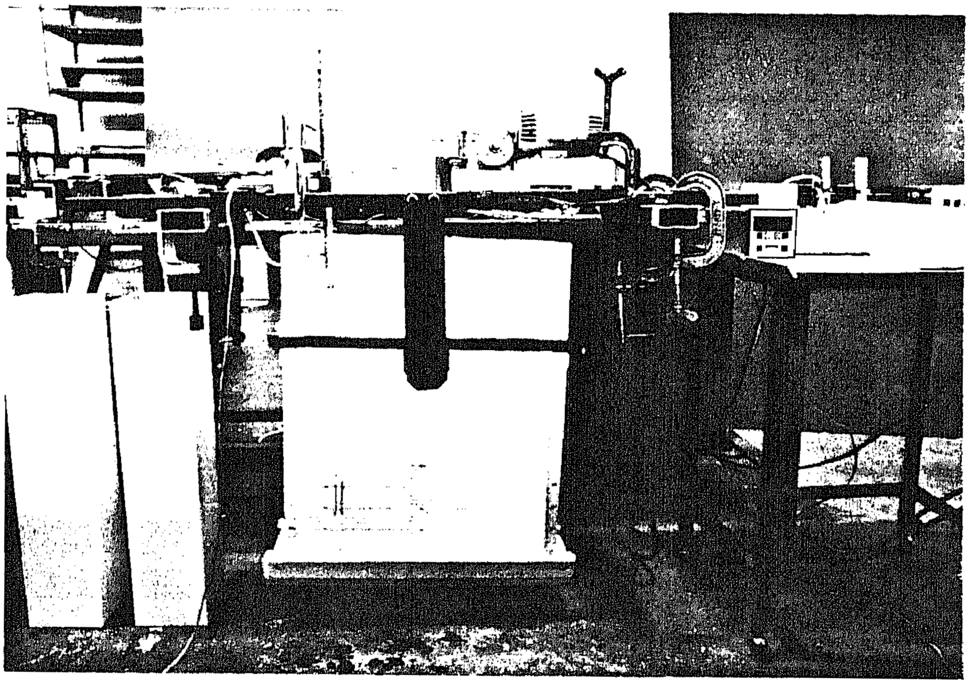

Fig. 6.3 Shows the Arrangement of a Tank Experiment

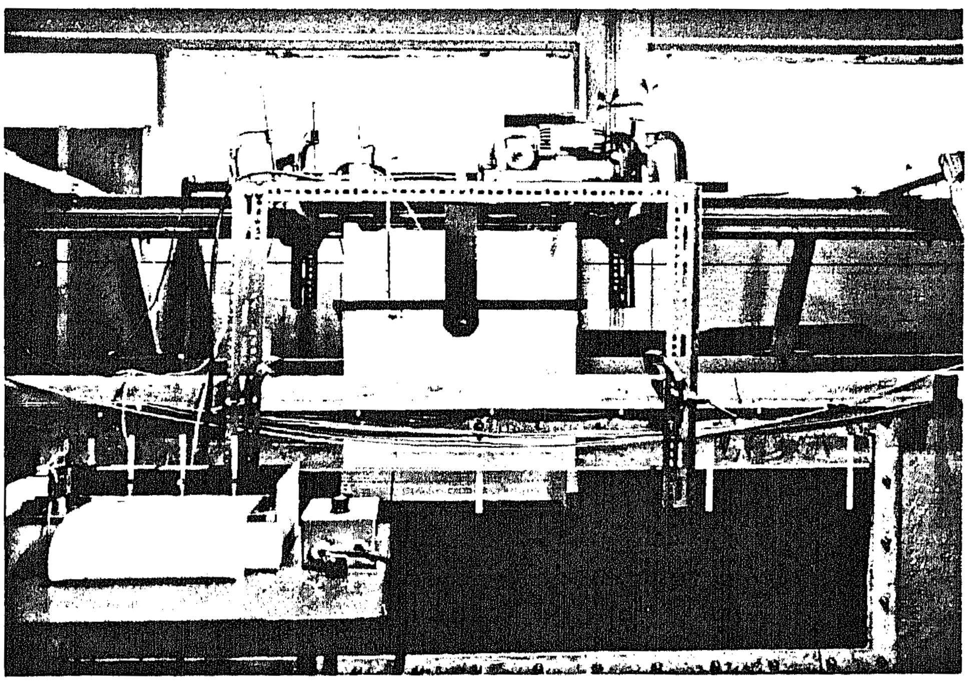

Fig. 6.4 Shows the Arrangement of a Moonpool Experiment

6.5 RESULTS AND COMMENTS

The results from the experimental study allowed comparisons to be made between the tank and moonpool. In addition the resonant frequencies obtained from the experiment were compared with the calculated values. Results from the experiments are plotted on graphs (1-17). On inspecting the graphs it can be seen that the position at resonance lies in the narrow band between the drawn curves. Within this band waves tended to break and thus the data tend to be unreliable. Hence the peaks were not drawn. An example of this behaviour is shown from the output of the pen recorder on fig. A1.1 (Appendix I), clearly illustrating the 'beating' phenomenon. The beating effect purely suggests that the difference between the excitation frequency and natural frequency are close, i.e. approaching resonance conditions and not resonance.

Table 4 tabulates the results obtained from graphs 1-4 and the calculated values of resonant frequencies. For aspect ratio (h/2a) equal to 0.5 the resonant frequency for both the tank and moonpool are very close, to within 7%. Furthermore the calculated values provided a very good approximation in both cases, i.e. within 6% for the tank and 1% for the moonpool. For aspect ratio of 1.0, the resonant frequencies for the tank and moonpool are very close, to within 4%. This also applies to higher aspect ratio (h/2a) equal to 1.5. In addition, the calculated values give a reasonable approximation for the tank and perhaps indicate a slightly better accuracy in favour of the moonpool (see Table 4). Generally the transition from h/2a equal to 1.0 to 1.5 appears to have little effect in the resonant frequency.

Therefore it is apparent that the resonant frequencies with these aspect ratios ($h/2a = 1.0-1.5$) are approaching a maximum limit. This behaviour can be confirmed by investigating the formula as shown below:

$$W_{RES.} = \left[\frac{g\pi}{2a} \tanh \frac{h\pi}{2a}\right]^{1/2}$$

where h = depth of water

$2a$ = width of tank

g = 9.18 m/s

When $\tanh \to 1$ $W_{RES} \to (g\pi/2a)$, i.e. for a particular width, W_{RES} approaches a constant (see graph (17).

At the lower aspect ratio ($h/2a = 0.25$) the resonant frequency of the tank and the moonpool showed a larger percentage difference i.e. 27%, the reason being that in the case of the tank experiment the mass of water can be easily defined due to the solid boundaries. However, the moonpool has a varying mass of water and as a consequence the resonant frequency was found to be higher by 27% in comparison with the tank. Although the theoretical value showed to be in good correlation with the figure obtained from the tank experiment, in the case of the moonpool, the theoretical value was under estimated by as much as 37%. (See Table 4).

The natural frequency of the water was found by allowing the water to oscillate freely after being excited. The results obtained are shown in Table 5, in which comparisons are made with the frequencies at resonance and the theoretical values. It can be seen that the natural frequencies are slightly higher than the excitation frequencies at resonance and also that they are closely related to the theoretical values.

Chapter 7 gives a brief description together with photographs on the pattern of behaviour in which the water in the tank and moonpool were excited. Generally it was observed that as the draft increases, the motion near the bottom gradually subsides. This means that less energy is being dissipated. In addition, the walls of the model provide damping to a greater extent due to a large area of contact with the water. As a result, the frictional stresses are increased. This provides a possible explanation for the reason why the area under the curves shown in graphs 5 and 6 for aspect ratio 1.0 is greater than for the aspect ratio of 1.5.

Two additional sets of tests have been conducted and these will be discussed below:

(a) Moonpool Experiments with Waves

Table 5 shows that the formula for evaluating the frequency at resonance for vertical oscillation produces reasonable results when comparing with the experimental figures.

The coupling effect of the vertical oscillation and the sloshing due to the rolling motion gave a more accurate representation to the practical situation of water motions in moonpools.

It was discovered that, in general, the frequencies at resonances of the sloshing, coupled with vertical oscillation, differed by only a few percent when comparing with pure sloshing (no waves). See Table 7. This indicates that there are no major changes. Observation at low frequencies showed that vertical oscillation dominated the scene. Near resonance the sloshing motion became the noticeable factor (see Chapter 7). The combination of the vertical oscillation and sloshing showed a much larger movement along the side walls of the moonpool and also the nodes of the standing wave at the centre was oscillating. The combination of the frequencies due to vertical oscillation and sloshing produced a beat (see fig. A1.2 Appendix 1), the lower frequency being the vertical oscillation and the higher frequency caused by sloshing.

Although damping at resonance was considerable as in the case of 4cm width baffles (two baffles each side, at water surface and 50/100mm below) it must be emphasised that, as a consequence, a fair amount of turbulence was created. (See Chapter 7). This situation would be problematical especially when the moonpool is used for the launching of subsea units.

The results shown on the graphs (7-13) do not provide an obvious solution but rather a foundation for future work. For example, a combination of baffles could be increased within specified regions, in order to determine the best combinations. The most direct solution would appear to be the insertion of a perforated bulkhead or a porous barrier which should restrict the motions along the side walls.

Further experiments would verify this statement.

(b) Experiments with Baffles

The introduction of baffles generally had two main effects: the amplitudes were considerably reduced (increased damping); it slightly shifted the resonant frequency in a positive direction. See Table 8. The following points were observed:

(1) At resonance the frequencies in the moonpool were slightly higher in comparison to the tank (ranging from 1% to 13%).

(2) The baffles with larger width (4cm) appeared to have a stronger influence in both increasing the resonant frequency and damping.

(3) Baffles inserted between the water surface and 50mm below water surface appeared to be more effective in increasing resonant frequency and damping and more so if the combination of two baffles were employed within these regions. If the baffles were inserted at 100mm below water surface, it is apparent that damping slightly improves. However, this does not have a noticeable effect on the resonant frequency.

Observation suggested that the baffles situated nearer the water surface were subject to a high stress due to water pounding, i.e. slamming loads. This was demonstrated by the fact that during the rolling motion the baffles tended to be dislodged from their positions.

6.6 SUMMARY OF EXPERIMENTAL RESULTS

The following points were observed:

(1) Sloshing phenomenon is characterised by the formation of large amplitude standing waves near resonance.

(2) The resonance frequencies obtained from both the tank and moonpool experiments are within close limits (4-7%) with the exception of h/2a = 0.25 (27%). As the draft in the moonpool decreases, it appears that the varying mass has a noticeable effect.

(3) The coupling effect of sloshing (forced in roll mode) and vertical oscillation (due to waves generated) have virtually the same frequencies as that of pure sloshing (no waves generated).

(4) The experiments show that, at resonance, the frequencies for vertical oscillation are lower than the frequencies for pure sloshing. Although sloshing dominates the scene at resonance, vertical oscillation predominates before and after resonance.

(5) The theoretical values of resonant frequencies are within close agreements with the experimental results for sloshing and vertical oscillation with the exception of low draft i.e. h/2a = 0.25.

(6) It is apparent that at higher aspect ratios (1.0-1.5) the increase in draft results in less energy being dissipated.

(7) An increase in the total width reduces the frequency at resonant.

(8) Theoretical and experimental results show that as the draft increases for a particular width, the frequencies at resonant have a small increment until a point is reached where a steady value is maintained.

(9) At resonant observations suggest that the motions within the model lag by phase angle of approximately $\pi/2$. This indicates that there are viscous effects.

(10) Generally the introduction of baffles provides damping and slightly increases the frequencies at resonant.

Table 4 : SLOSHING DUE TO ROLLING MOTION

EXPERIMENTAL RESULTS - RESONANT FREQUENCIES AND THEORETICAL VALUES

Aspect Ratio h/2a	Experimental Results Resonant Frequencies (rad/s)		Theoretical Values WRES (rad/s)	Percentage difference 3-2/3 x 100%	Difference between theoretical and experimental results	
	Tank	Moonpool			Tank 4-2/4 x 1000%	Moonpool 4-3/4 x 100%
0.25	6.29	8.68	6.36	27.5	1.0	36.5
0.50	7.10	7.62	7.52	6.8	5.6	1.3
1.00	10.57	11.04	12.39	4.2	14.7	10.9
1.50	10.89	11.31	12.47	3.8	12.2	8.9

TABLE 5 : SLOSHING DUE TO ROLLING MOTION

EXPERIMENTAL RESULTS - NATURAL FREQUENCIES

Aspect Ratio h/2a	Experimental Results Natural Frequencies (rad/s)		% Difference between the Natural & Resonant freq. (rad/s)		Theoretical Values Rad/s	Difference between Theoretical & Exp. Results	
	Tank	Moonpool	Tank	Moonpool		Tank 6-2/6x100%	Moonpool 6-3/6x100%
0.25	6.41	8.73	1.9	0.6	6.36	0.8	37.3
0.50	7.54	7.95	5.8	4.2	7.52	0.3	5.7
1.00	12.56	12.02	15.8	8.2	12.39	1.4	3.0
1.50	12.82	12.24	15.1	7.6	12.47	2.8	1.8

Table 6 : VERTICAL OSCILLATION (MOONPOOL EXPERIMENTS WITH WAVE)

Aspect Ratio (h/2a)	Experimental Freq. at Resonance rad/s	Theoretical Values rad/s	Percentage difference %
0.25	6.91	6.43	7.6
0.50	5.53	5.22	9.2
1.00	6.03	6.02	0.2
1.50	4.90	5.10	3.9

Table 7 : EXPERIMENTAL RESULTS OF SLOSHING COUPLED WITH VERTICAL OSCILLATION

Aspect Ratio (h/2a)	Wave Frequency (generated) rad/s /h3	Experimental Results Resonance Frequency (rad/s)		
		Vertical Osc.	Sloshing Coupled with cert. osc.	Pure sloshing (no waves)
0.25	6.91/1.1	6.91	8.61	8.68
0.50	5.03/0.8		7.67	7.62
0.50	5.47/0.87		7.67	7.62
0.50	5.53/0.88	5.53	7.58	7.62
0.50	5.59/0.89		7.95	7.62
0.50	5.66/0.90		7.85	7.62
1.00	5.66/0.90		11.18	11.04
1.00	5.91/0.94		11.64	11.04
1.00	6.03/0.96	6.03	11.26	11.04
1.00	6.16/0.98		11.12	11.04
1.00	6.28/1.0		11.04	11.04
1.50	4.90/0.78	4.90	11.29	11.31

Table 8 : EXPERIMENTS WITH DAMPING : ASPECT RATIO (h/2a) = 0.5

	2cm WIDE								4cm WIDE								
	One baffle each side			Two baffles each side				Three baffles each side	One baffle each side				Two baffles each side				Three baffles each side
	1	5	6	1 & 4	1 & 5	1 & 6	3 & 5	2, 3 & 4	7	1	5	6	1 & 4	1 & 5	1 & 6	3 & 5	2, 3 & 4
Experimental Results																	
Resonance Frequency																	
(1) Rad/s																	
(a) Tank	7.1	-	7.00		7.20	7.20	-	-	-	8.13	7.53	7.04	7.79	7.95	7.95	-	-
(b) Moonpool	8.00	8.00	7.85	7.99	7.99	7.85	7.90	7.66	8.06	8.20	8.06	7.16	8.49	8.62	7.85	8.62	8.34
Perc. Difference (2) between tank & moonpool %	11.33	-	12.1	-	9.9	10.7	-	-	-	8.5	6.6	1.7	8.2	7.8	1.3		
Compared without baffles																	
(3) + higher																	
− lower																	
(a) Tank *1	0	-	-0.1	-	+0.1	-0.05	-	-	-	+1.03	+0.43	-0.06	+0.69	+0.85	+0.85		
%	0		1.4		1.4	0.7				14.5	6.1	0.8	9.7	12	12		
(b) Moonpool *2	+0.38	+0.38	+0.23	+0.63	+0.63	+0.23	+0.28	+0.04	+0.44	+0.58	+0.44	-0.46	+0.87	+1.00	+0.23	+1.00	+0.72
%	5.0	5.0	3.0	8.3	8.3	3.0	3.7	0.5	5.8	7.6	5.8	6.0	11.4	13.1	3.0	13.1	9.4

*1 (1a − 7.1) rad/s
*2 (1b − 7.62) rad/s

Key N.O.	Position of baffles from Water Surface
1	At water surface
2	10mm below
3	20mm below
4	30mm below
5	50mm below
6	100mm below
7	50mm above water surface

USER: CLHV02 FILE: PLOTLIB PLOT NO: 1

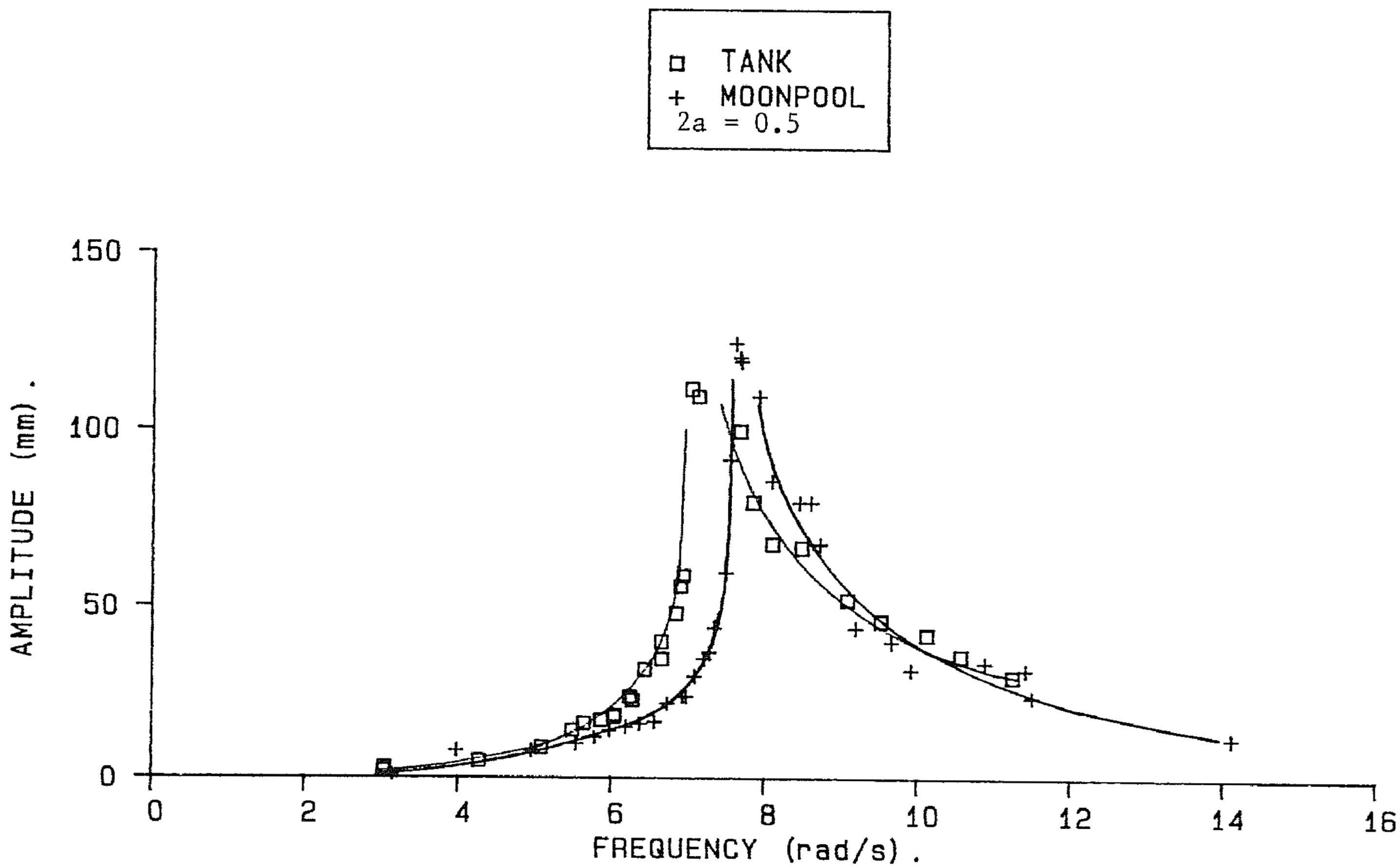

1

A PLOT OF EXCITATION FREQUENCY versus WAVE AMPLITUDE
FOR TANK AND MOONPOOL.
ASPECT RATIO (h/2a) = 0.5.

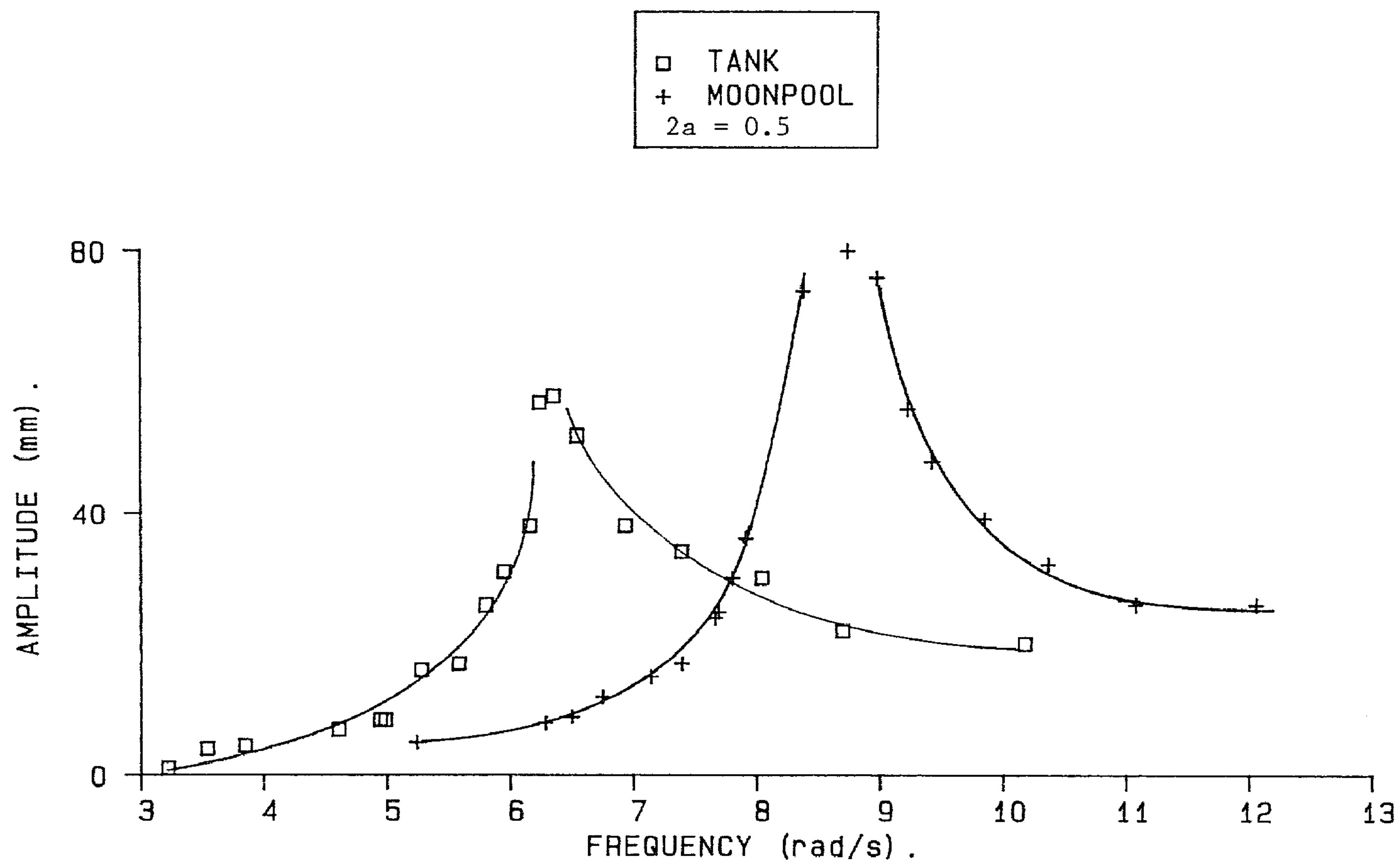

2	A PLOT OF EXCITATION FREQUENCY versus WAVE AMPLITUDE FOR TANK AND MOONPOOL. ASPECT RATIO (h/2a) = 0.25.

USER: CLHV02 FILE: PLOTLIB PLOT NO: 1

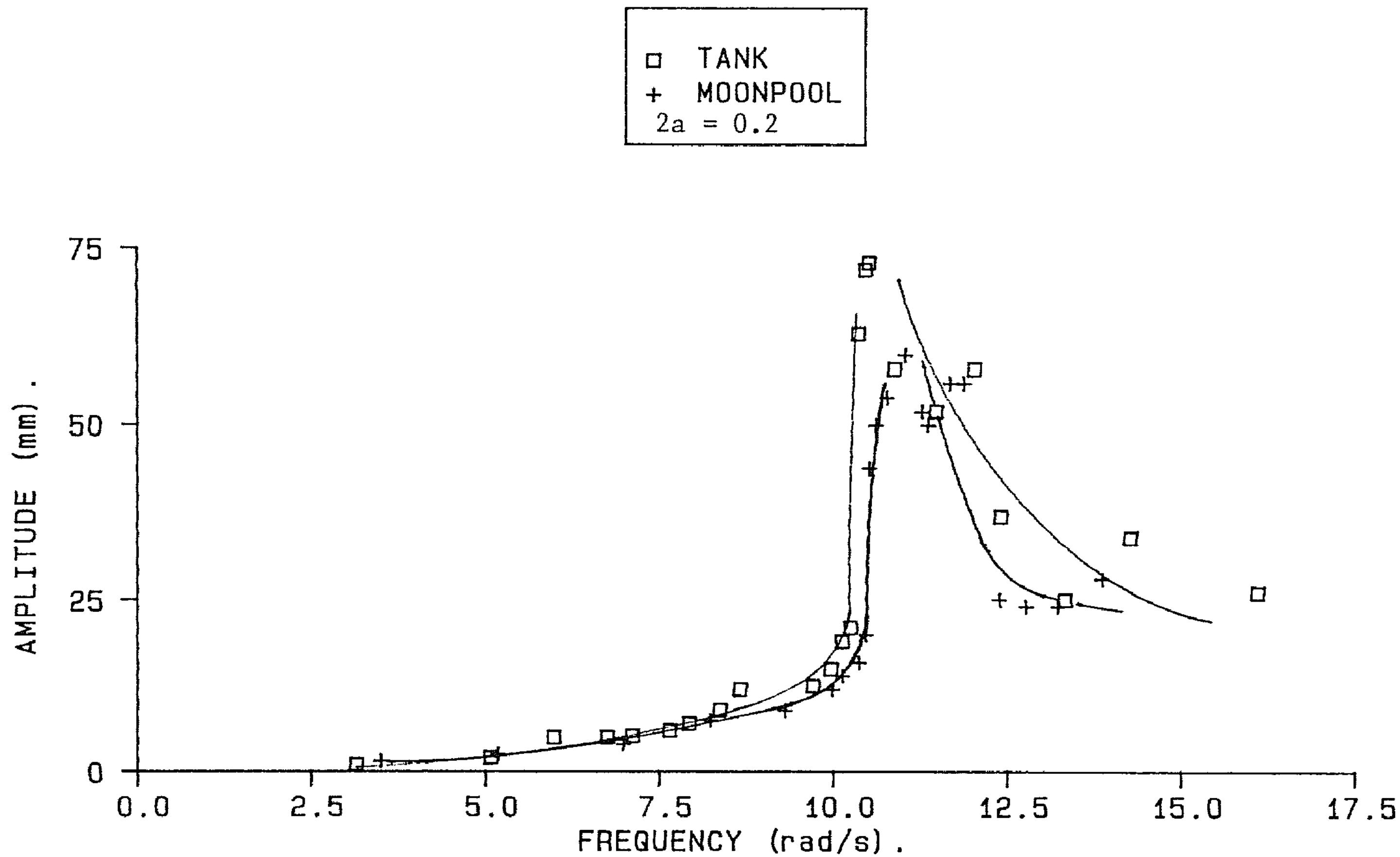

3

A PLOT OF EXCITATION FREQUENCY versus WAVE AMPLITUDE
FOR TANK AND MOONPOOL.
ASPECT RATIO (h/2a) = 1.0.

USER: CLHV02 FILE: PLOTLIB PLOT NO: 1

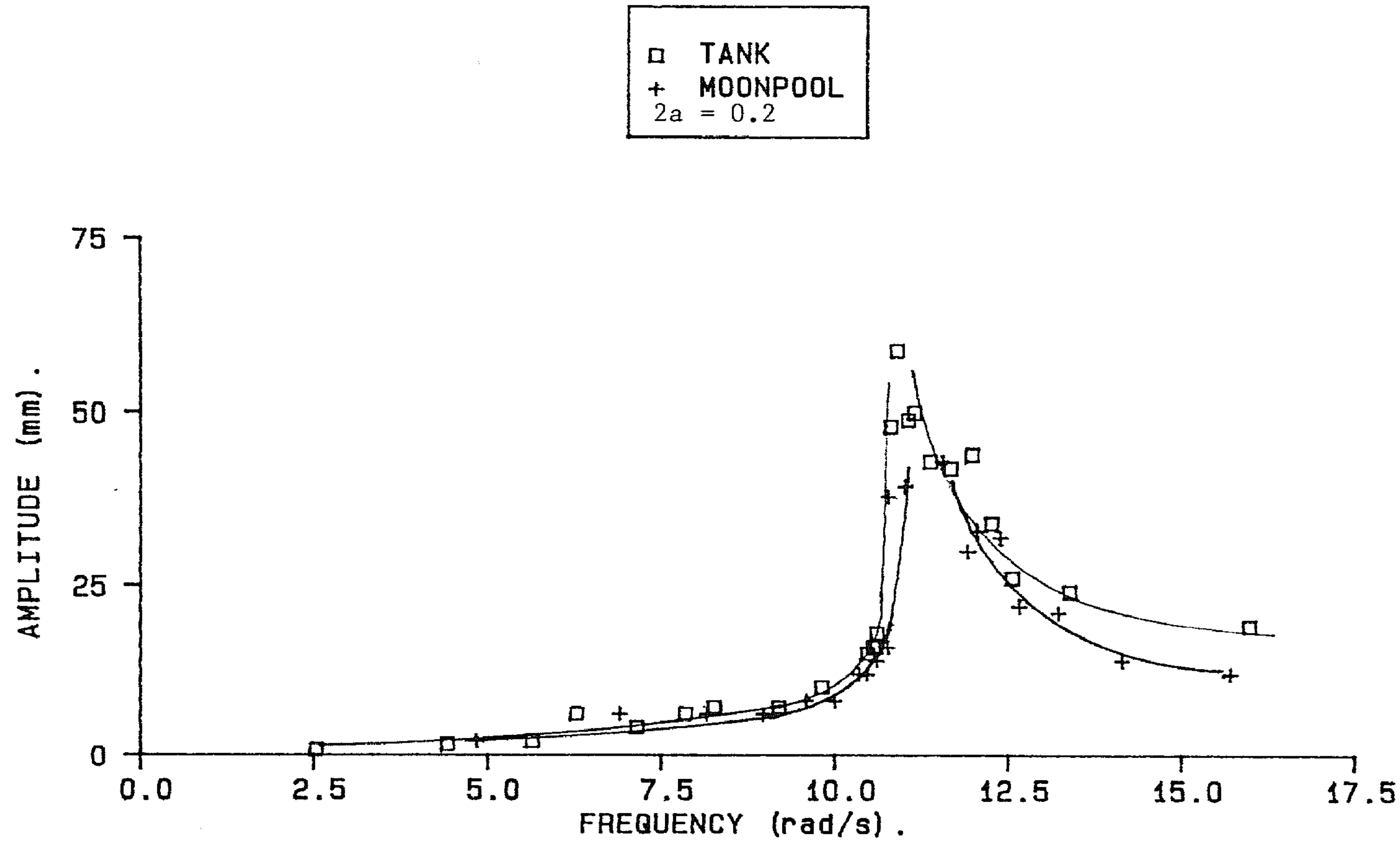

4	A PLOT OF EXCITATION FREQUENCY versus WAVE AMPLITUDE FOR TANK AND MOONPOOL. ASPECT RATIO (h/2a) = 1.5.

USER: CLHV02 FILE: PLOTLIB PLOT NO: 1

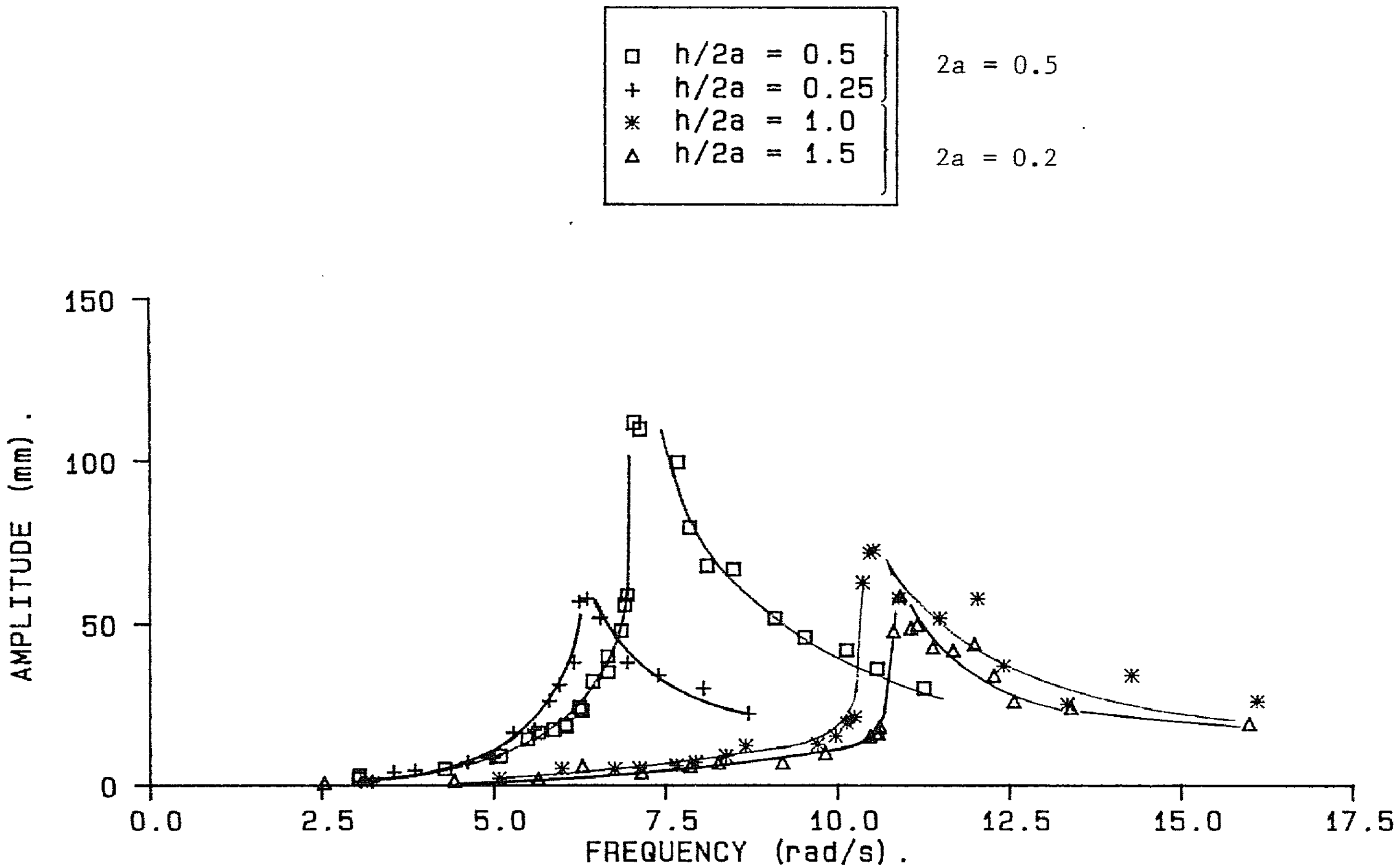

5	A PLOT OF EXCITATION FREQUENCY versus WAVE AMPLITUDE FOR TANK WITH DIFFERENT ASPECT RATIOS.

USER: CLHV02 FILE: PLOTLIB PLOT NO: 1

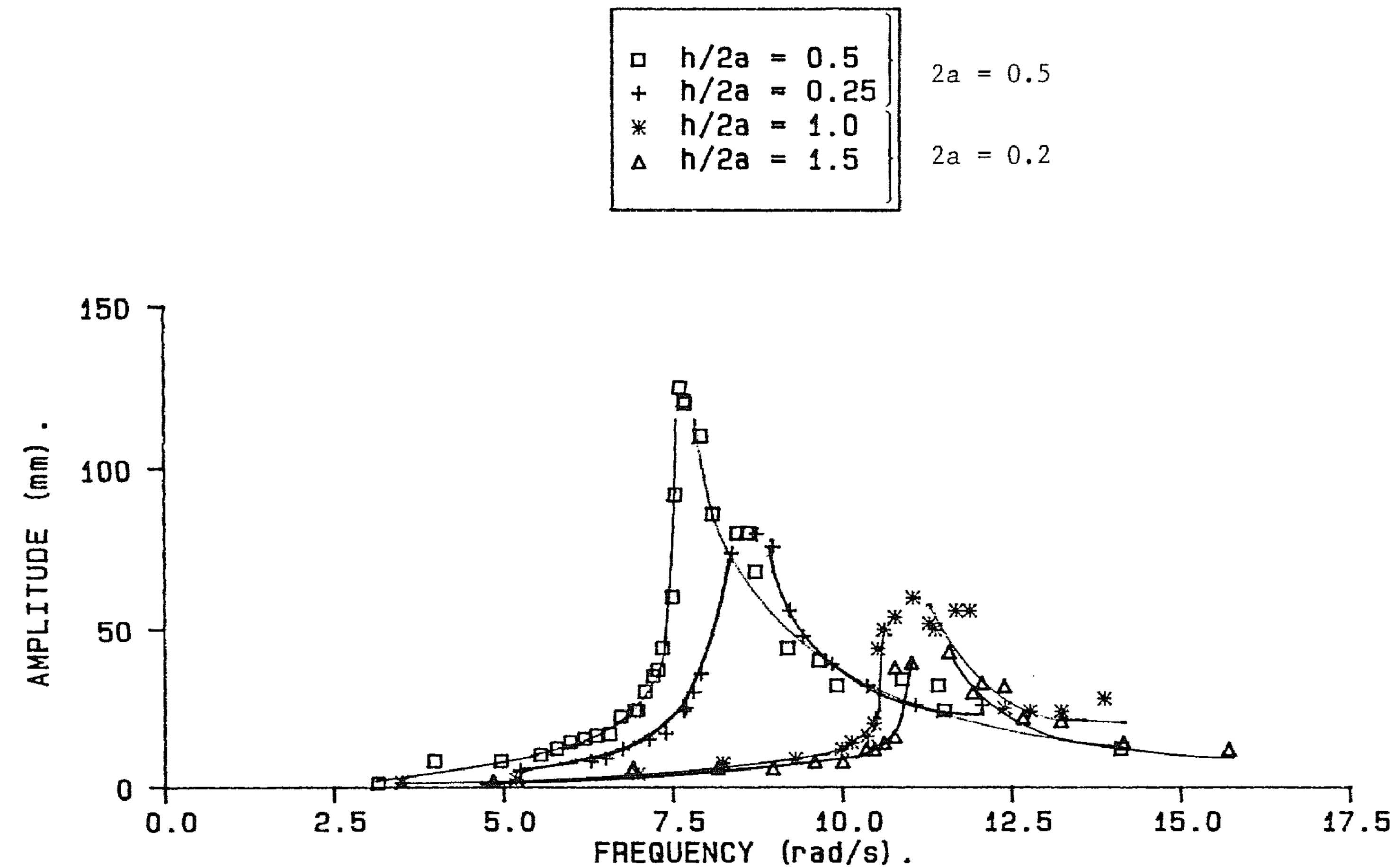

6	A PLOT OF EXCITATION FREQUENCY versus WAVE AMPLITUDE FOR MOONPOOL WITH DIFFERENT ASPECT RATIOS.

USER: CLHV02 FILE: PLOTLIB PLOT NO: 1

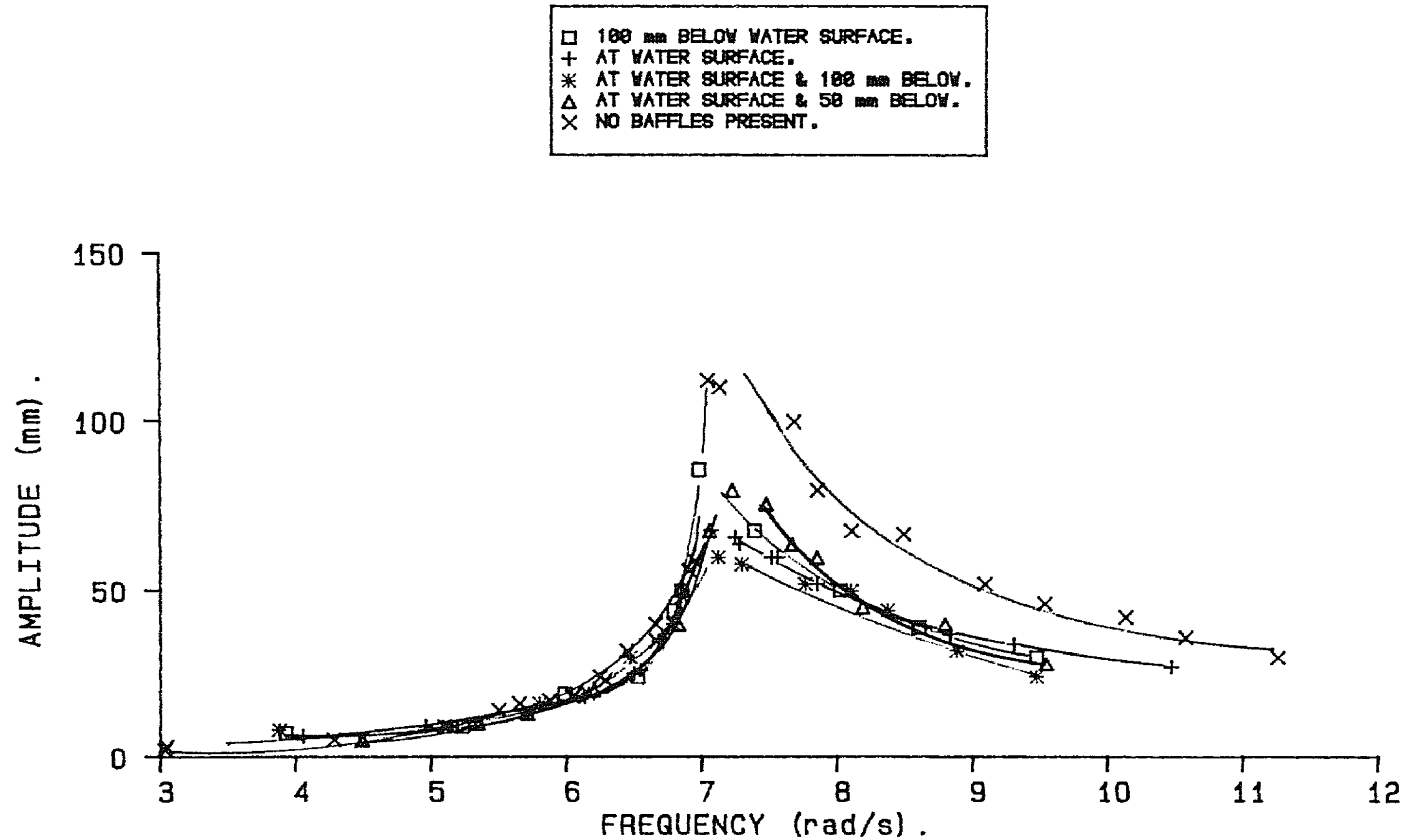

7

A PLOT OF EXCITATION FREQUENCY versus WAVE AMPLITUDE
FOR TANK WITH 2 cm BAFFLES .
ASPECT RATIO (h/2a) = 0.5.

USER: CLHV02 FILE: PLOTLIB PLOT NO: 1

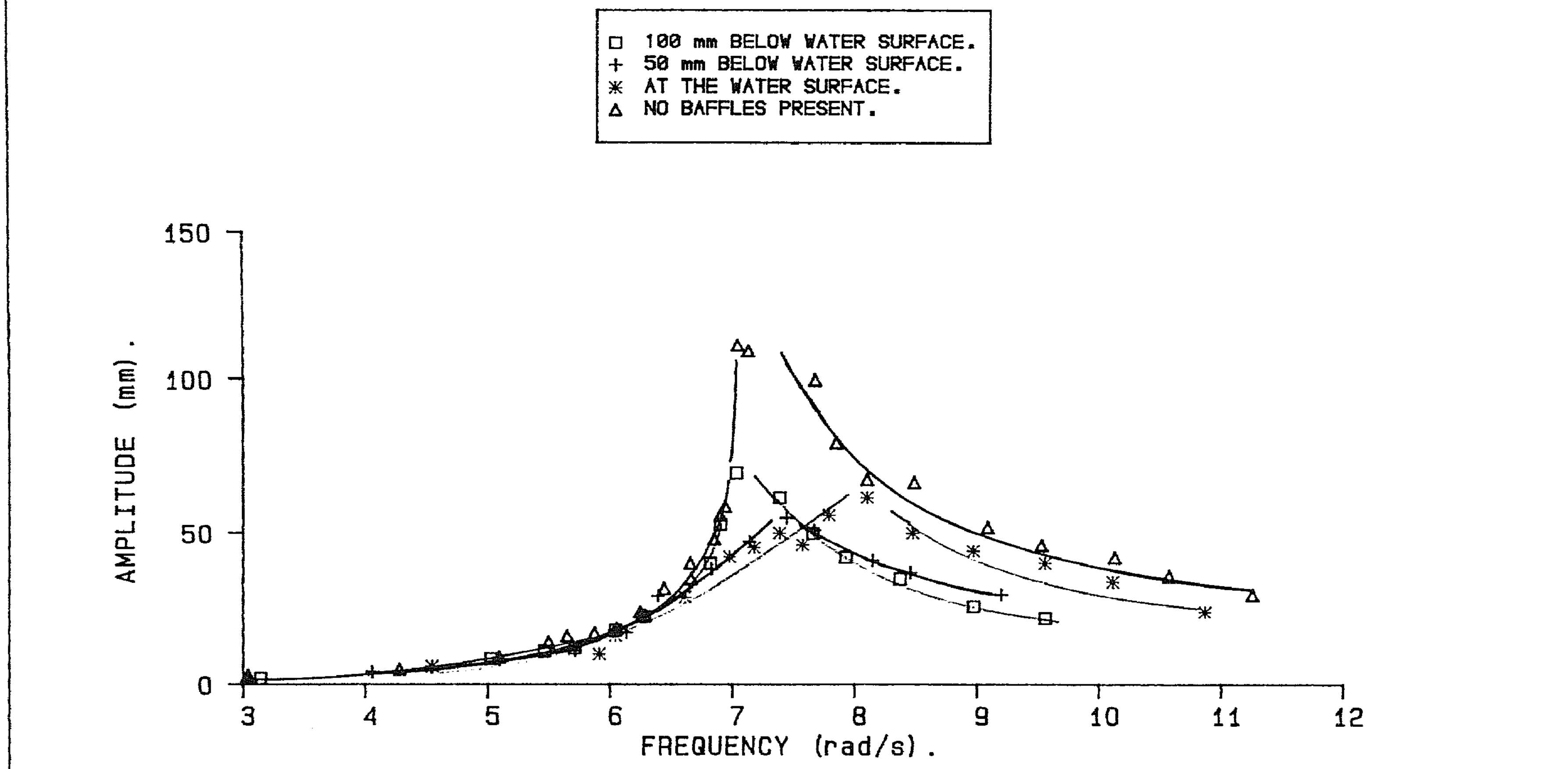

8	A PLOT OF EXCITATION FREQUENCY versus WAVE AMPLITUDE FOR TANK WITH 4cm BAFFLES. ASPECT RATIO (h/2a) = 0.5.

USER: CLHV02 FILE: PLOTLIB PLOT NO: 1

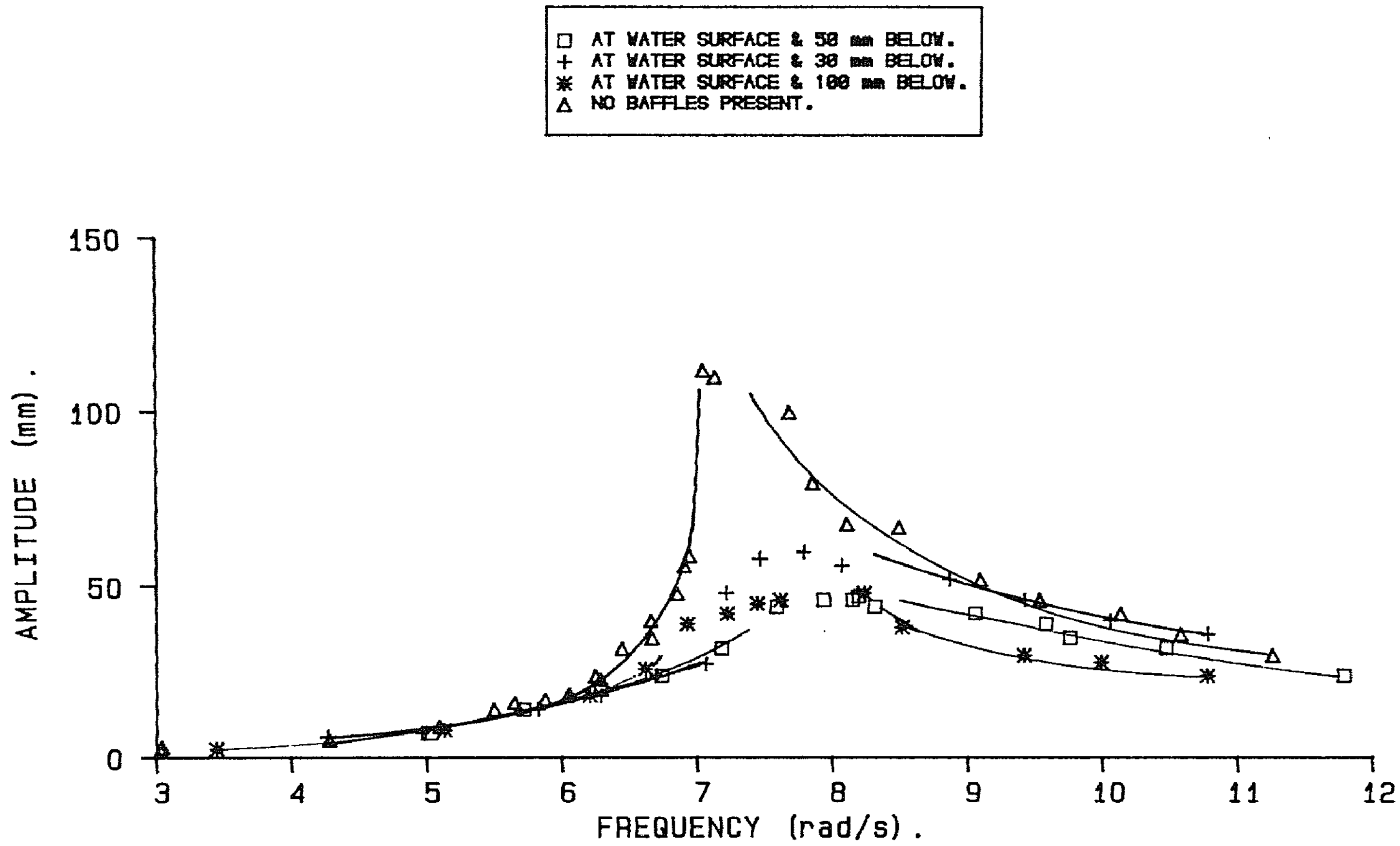

9	A PLOT OF EXCITATION FREQUENCY versus WAVE AMPLITUDE FOR TANK WITH 4CM BAFFLES. ASPECT RATIO (h/2a) = 0.5.

USER: CLHV02 FILE: PLOTLIB PLOT NO: 1

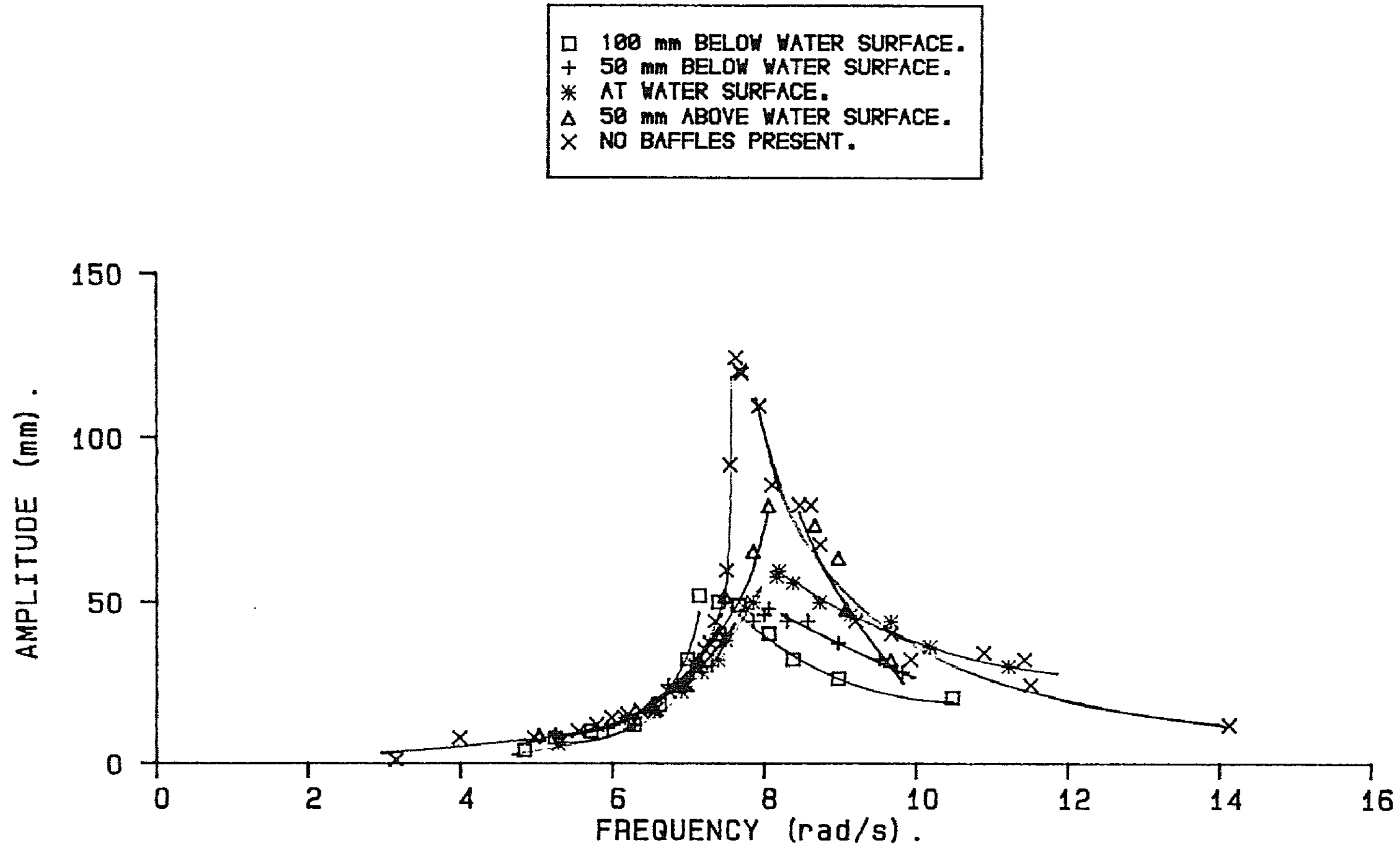

10	A PLOT OF EXCITATION FREQUENCY versus WAVE AMPLITUDE FOR MOONPOOL WITH 4cm BAFFLES. ASPECT RATIO (h/2a) = 0.5.

USER: CLHV02 FILE: PLOTLIB PLOT NO: 1

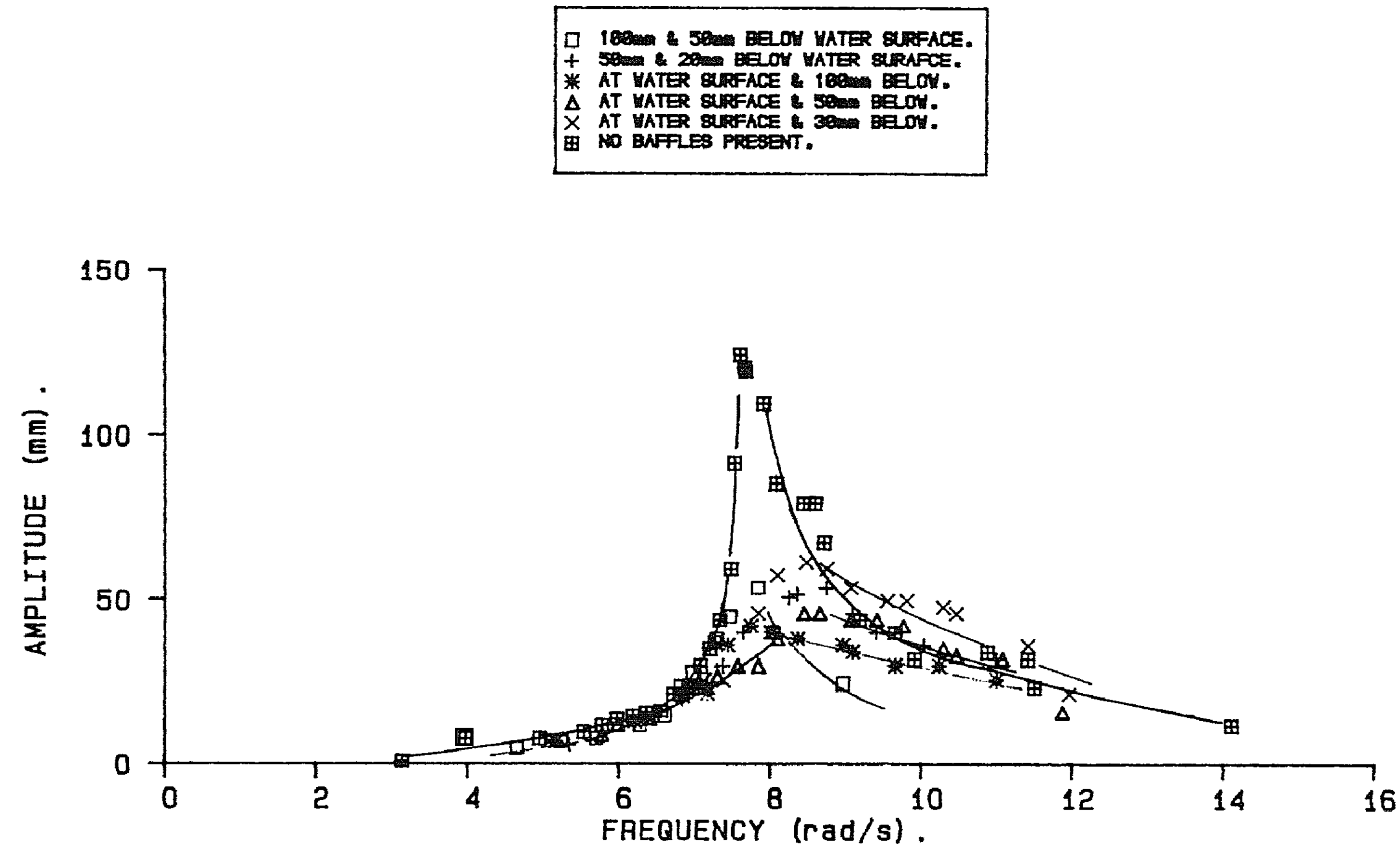

11	A PLOT OF EXCITATION FREQUENCY versus WAVE AMPLITUDE FOR MOONPOOL WITH 4cm BAFFLES. ASPECT RATIO (h/2a) = 0.5.

USER: CLHV02 FILE: PLOTLIB PLOT NO: 1

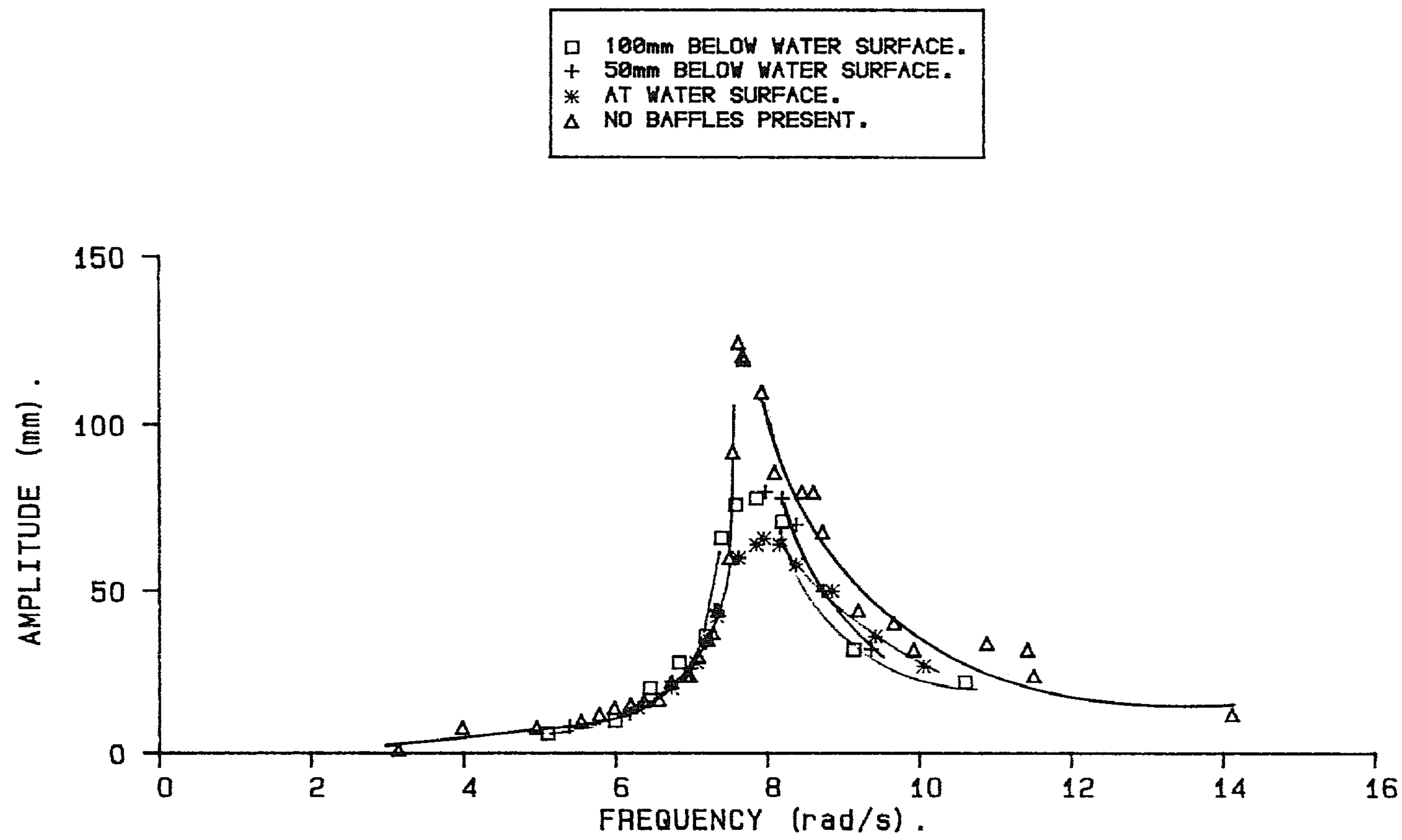

12	A PLOT OF EXCITATION FREQUENCY versus WAVE AMPLITUDE FOR MOONPOOL WITH 2 cm BAFFLES. ASPECT RATIO (h/2a) = 0.5

USER: CLHV02 FILE: PLOTLIB PLOT NO: 1

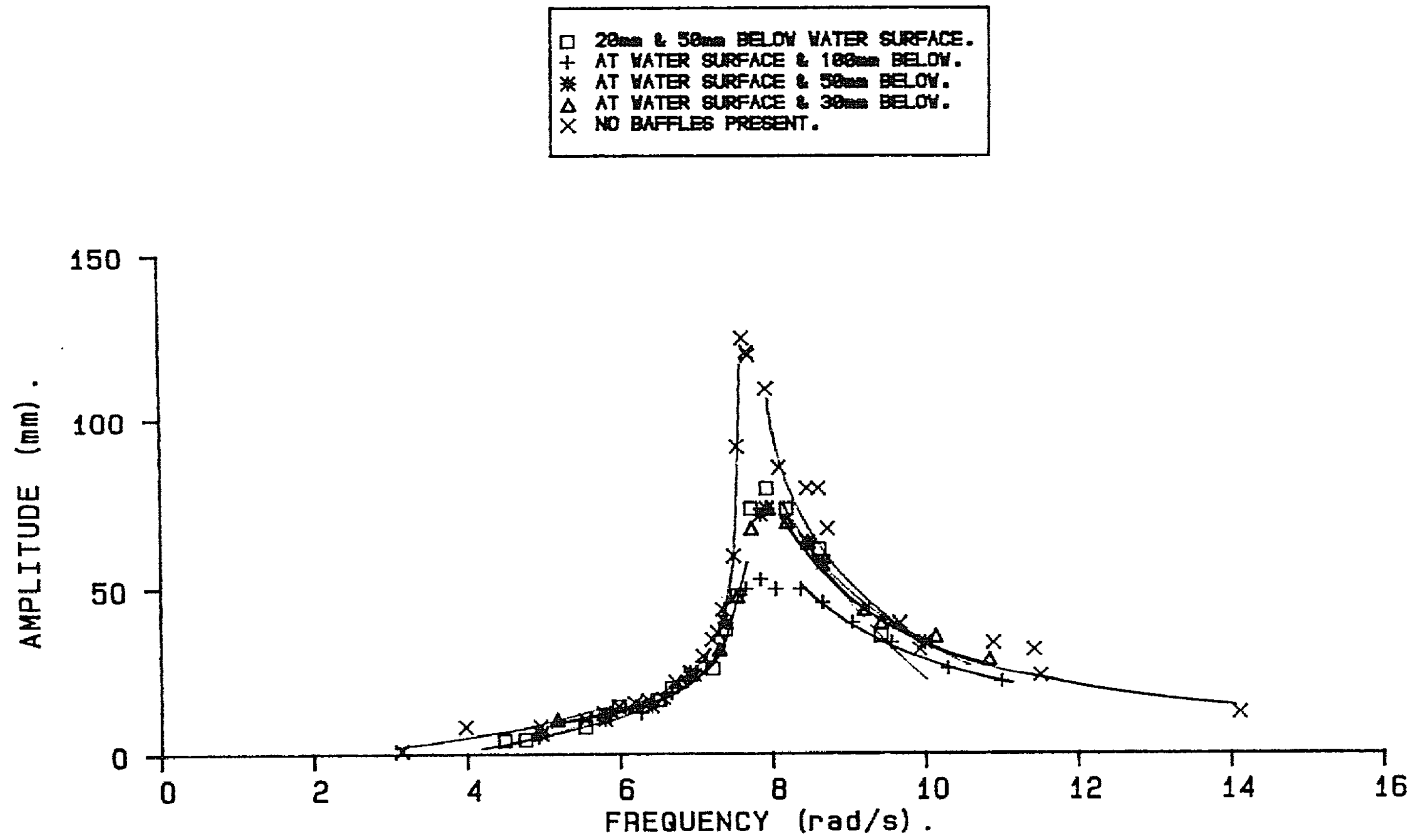

13

A PLOT OF EXCITATION FREQUENCY versus WAVE AMPLITUDE FOR MOONPOOL WITH 2cm BAFFLES. ASPECT RATIO (h/2a) = 0.5.

USER: CLHV02 FILE: PLOTLIB PLOT NO: 1

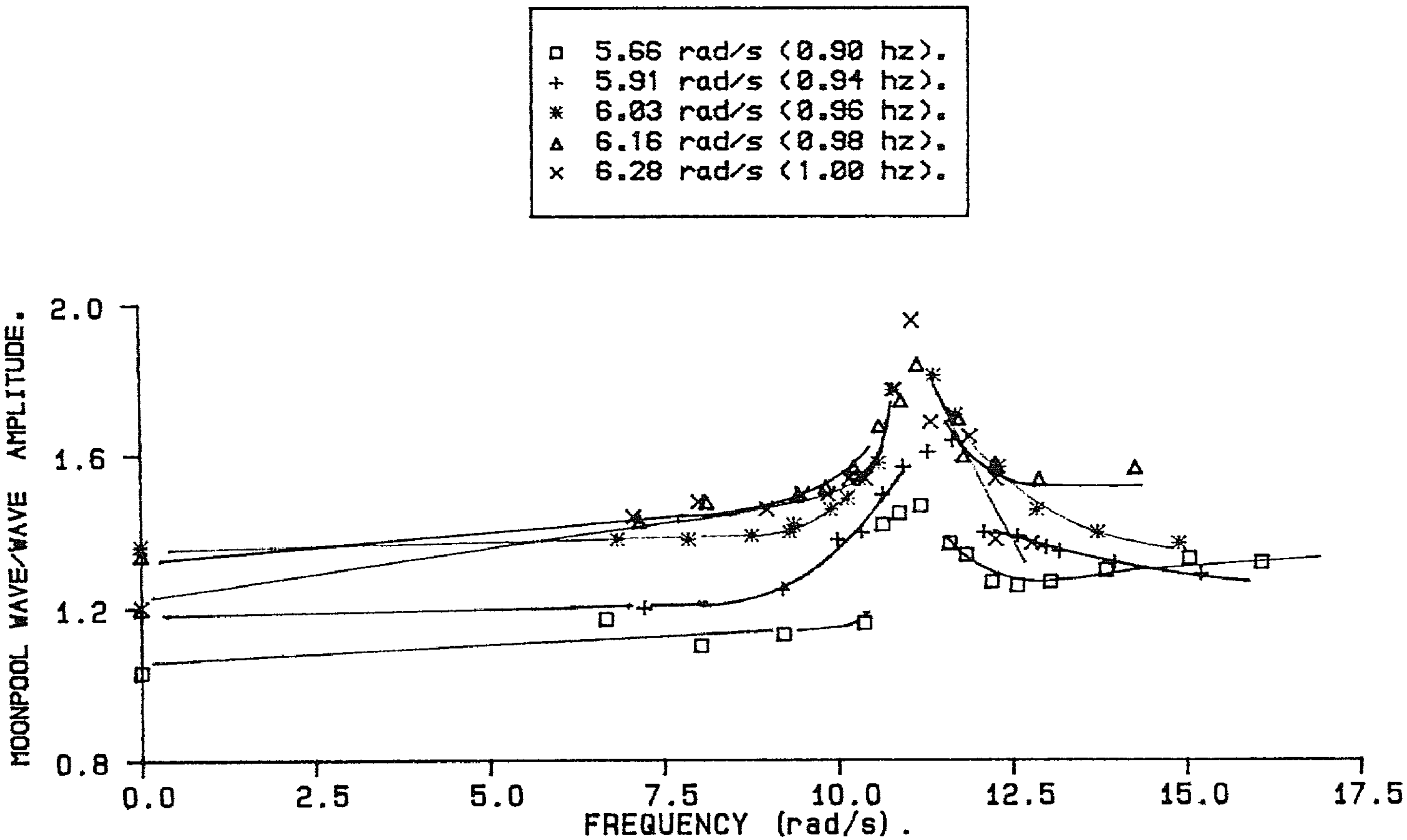

13

A PLOT OF EXCITATION FREQUENCY versus THE RATIO OF MOONPOOL WAVE AMPLITUDE : WAVE AMPLITUDE .
ASPECT RATIO (h/2a) = 1.0.

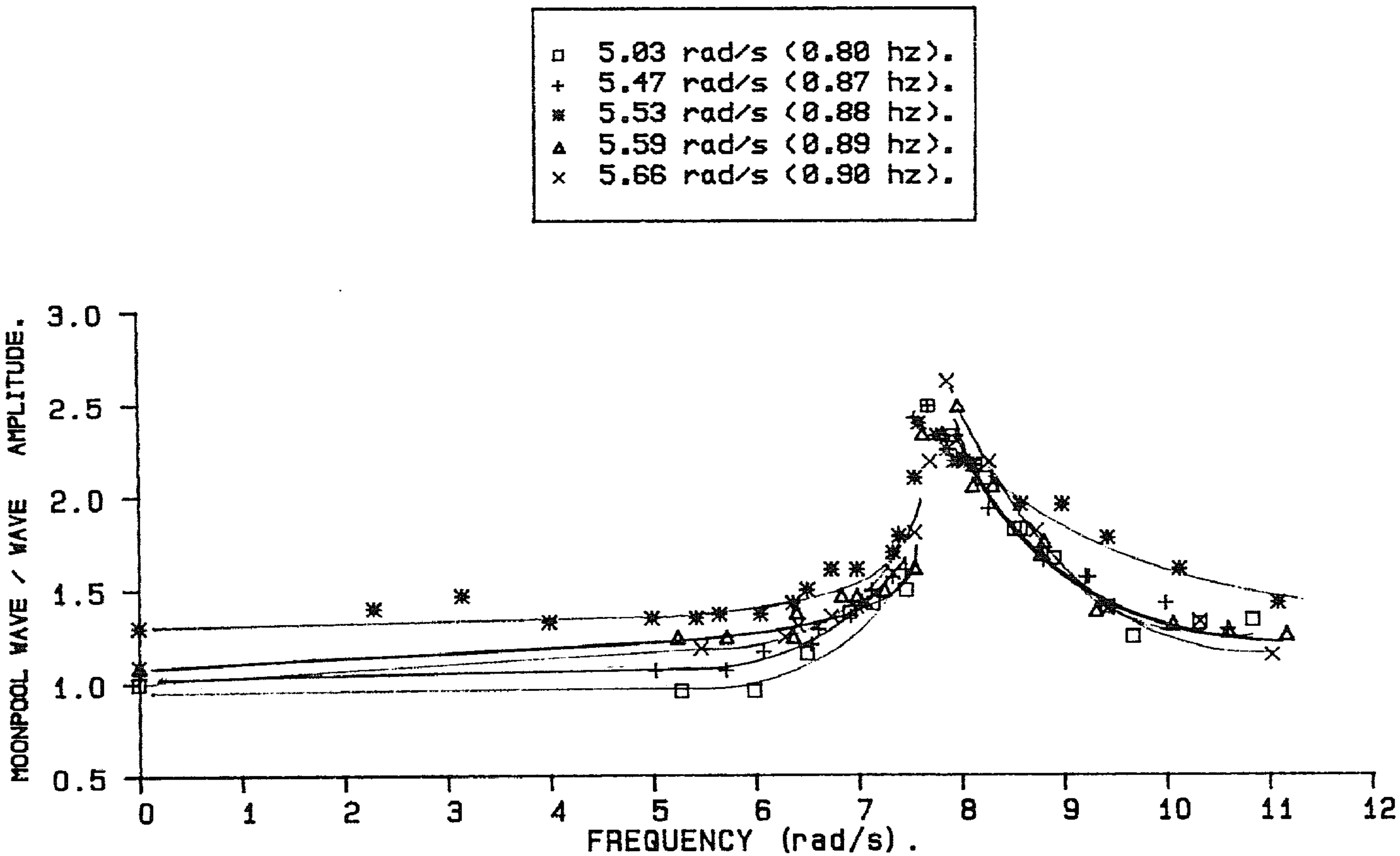

14

A PLOT OF EXCITATION FREQUENCY versus THE RATIO OF MOONPOOL WAVE AMPLITUDE: WAVE AMPLITUDE. ASPECT RATIO (h/2a) = 0.5.

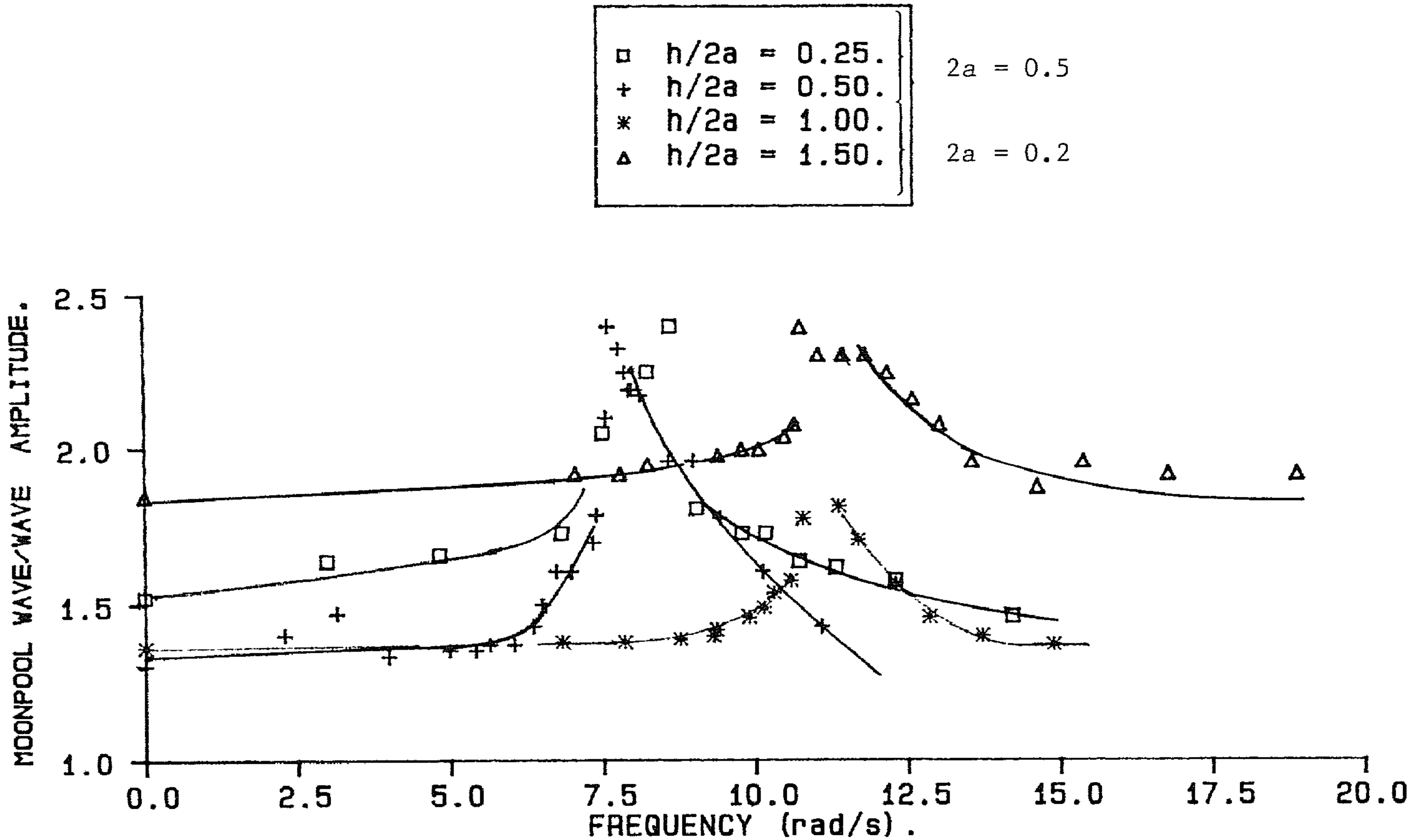

15	A PLOT OF EXCITATION FREQUENCY versus THE RATIO OF MOONPOOL WAVE AMP.: WAVE AMP. (AT RESONANCE OSCILLATION) FOR DIFFERENT ASPECT RATIO.

USER: CLHV02 FILE: PLOTLIB PLOT NO: 1

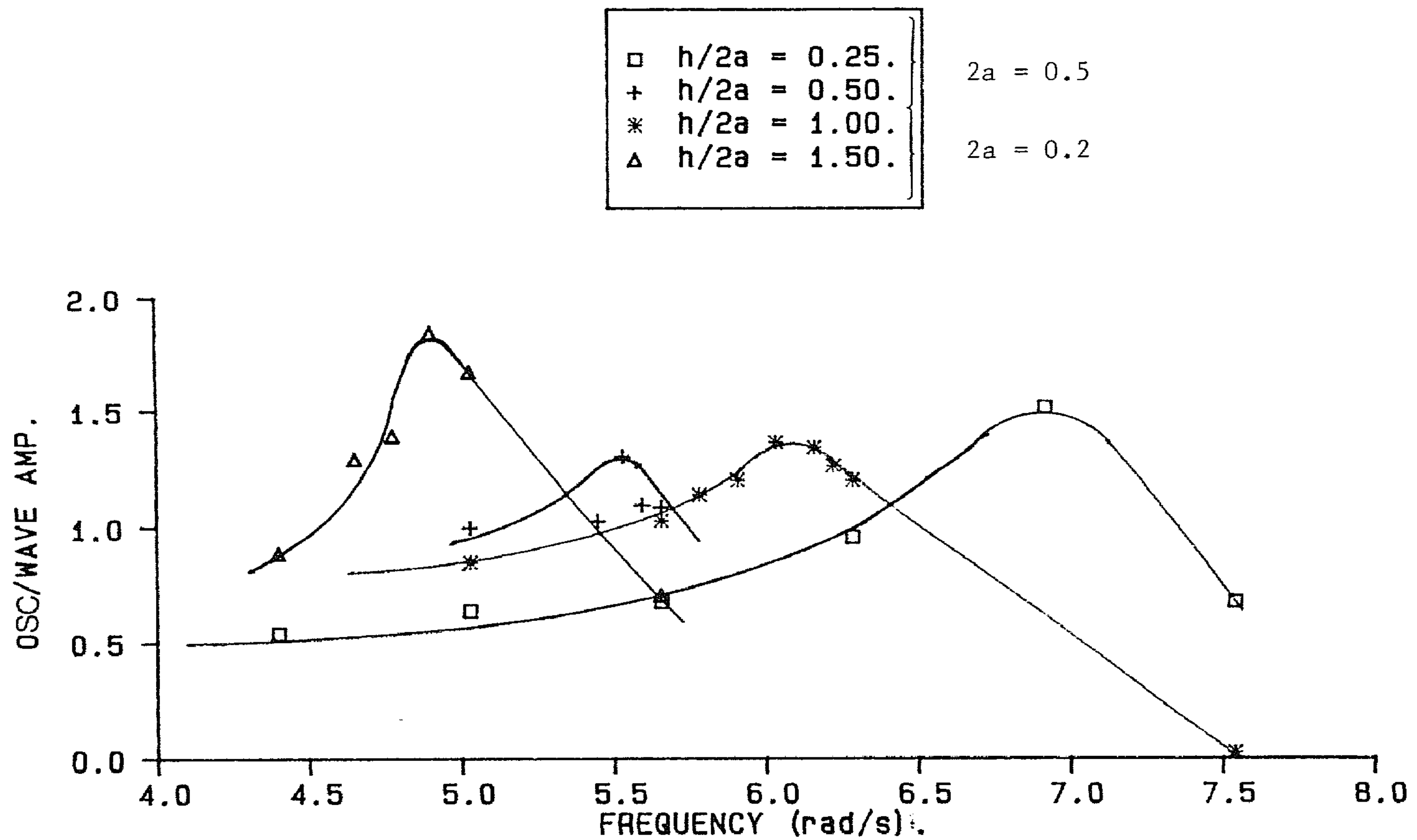

16

A PLOT OF FREQUENCY OF WAVE versus THE RATIO OF AMPLITUDE OF OSCILLATION: WAVE AMPLITUDE FOR DIFFERENT ASPECT RATIO .

USER: CLHV02 FILE: PLOTLIB PLOT NO: 1

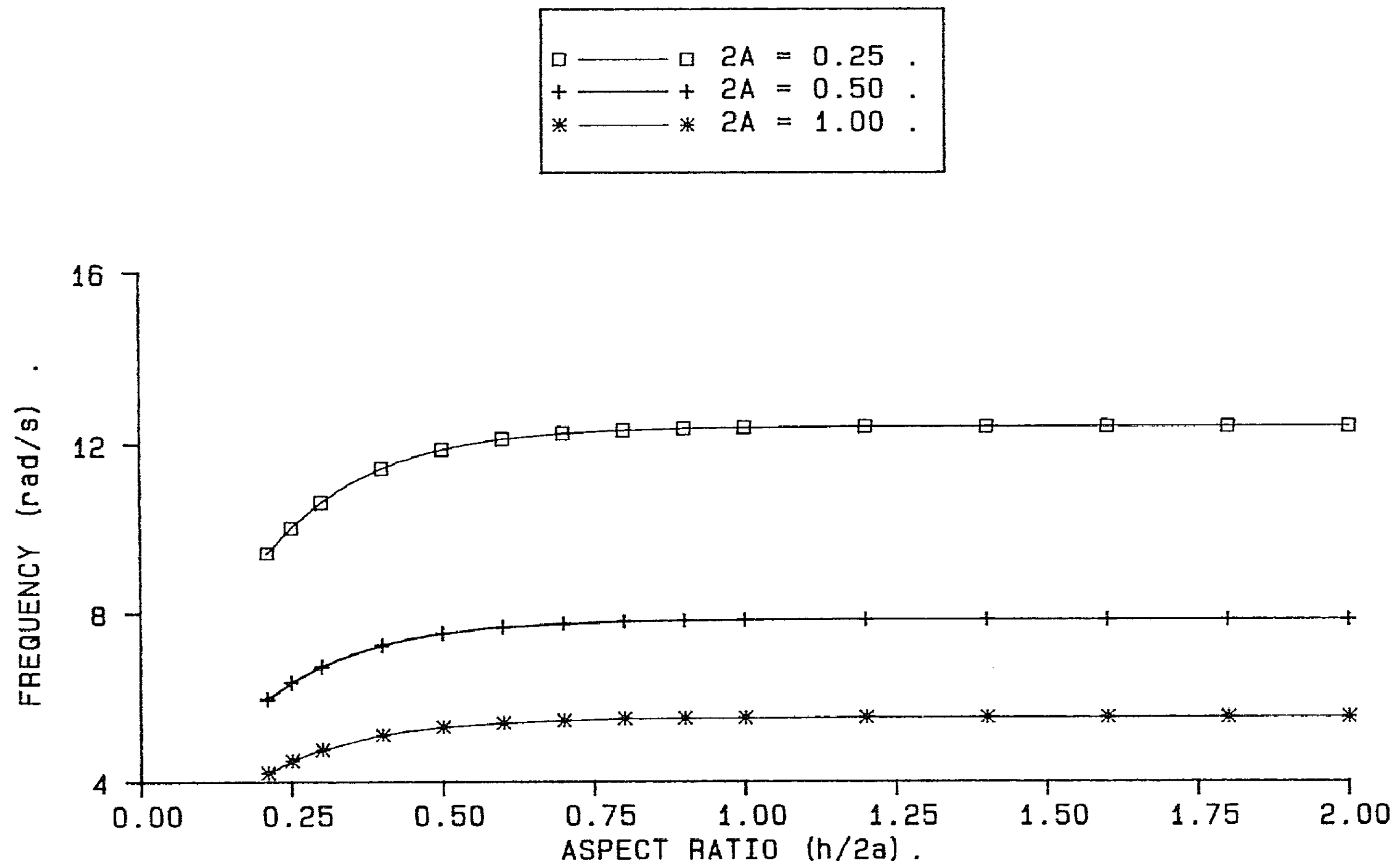

17 A THEORETICAL PLOT OF RESONANCE FREQUENCY versus ASPECT RATIO FOR DIFFERENT WIDTHS.

7.0 GENERAL OBSERVATIONS/CHARACTER OF FLUID TANK/ MOONPOOL BEHAVIOUR

The sloshing motion observed in the tank was similar to that of the moonpool. The general pattern in which water displayed its motions during excitation will be described as follows: At very low excititation frequencies, a small amount of water movement was observed at the model side wall interfaces. This observation is technically a standing wave with a node (N) at the centre of the model and the antinodes (A) at the side wall interfaces. See fig. 7.1.

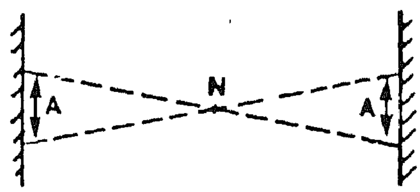

Fig. 7.1 ↔ = Movement N = Node A = Antinode

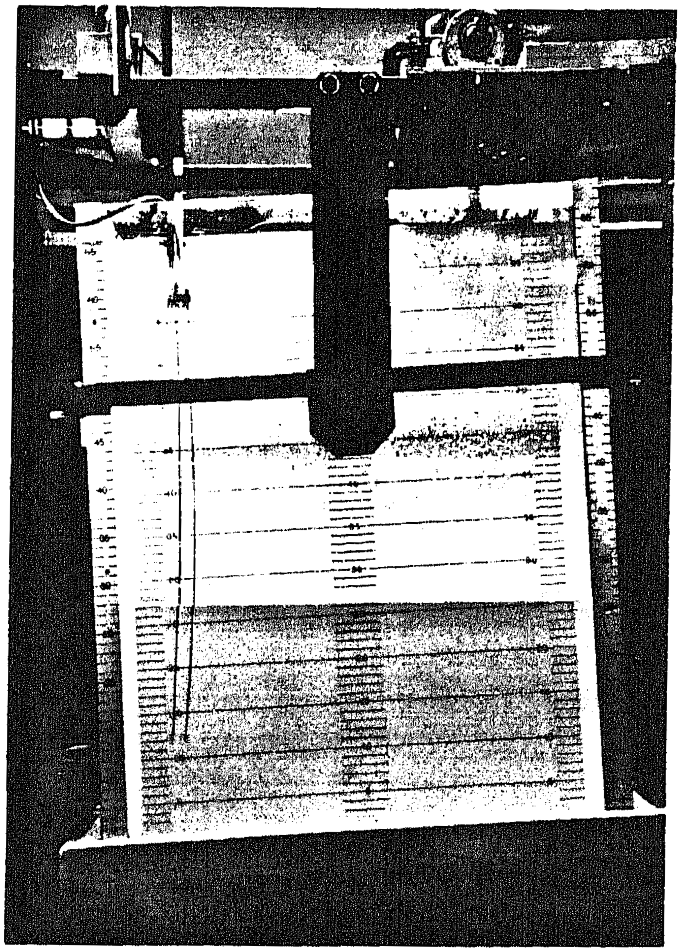

Fig. 7.2 : Tank undergoing low frequency roll motion

As the excitation frequency increases, the standing wave momentarily appears to have more than one node. It would be described as one of its homonics. This observation is not easily detected. See fig. 7.3.

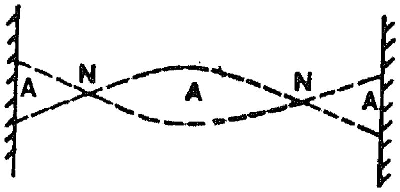

Fig. 7.3

A sudden transformation of a standing wave equal to half its wavelength takes place. At this stage the amplitude begins to dramatically expand along the tank wall interfaces, oscillating vertically like a spring mass system. See fig. 7.4 and 7.5.

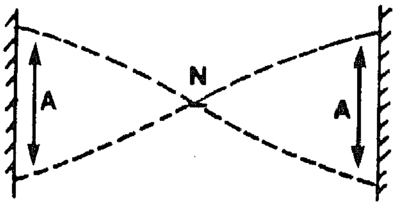

Fig. 7.4

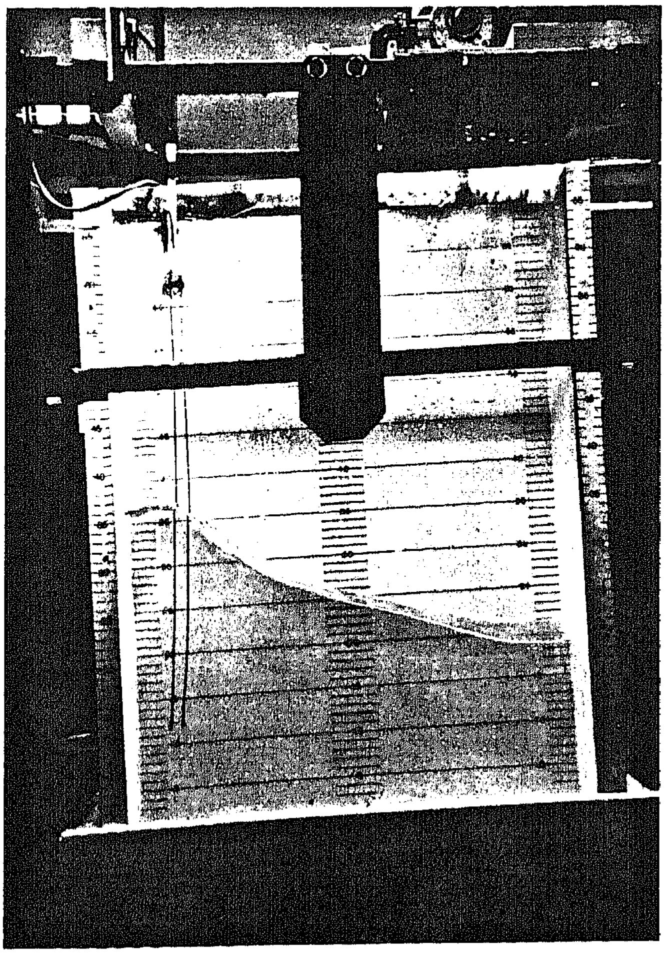

Fig. 7.5

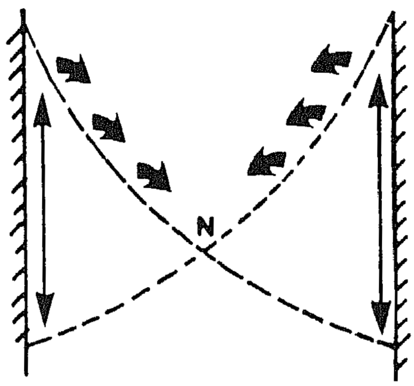

Waves breaking

Fig. 7.6

As resonance is approached, the combination of the roll motion and the stiffness of the water produce a curling motion with often resulted in spillage over the top of the model. The contribution to the curling effect is basically due to the waves breaking once a certain value has been reached. See figs. 7.6 - 7.10.

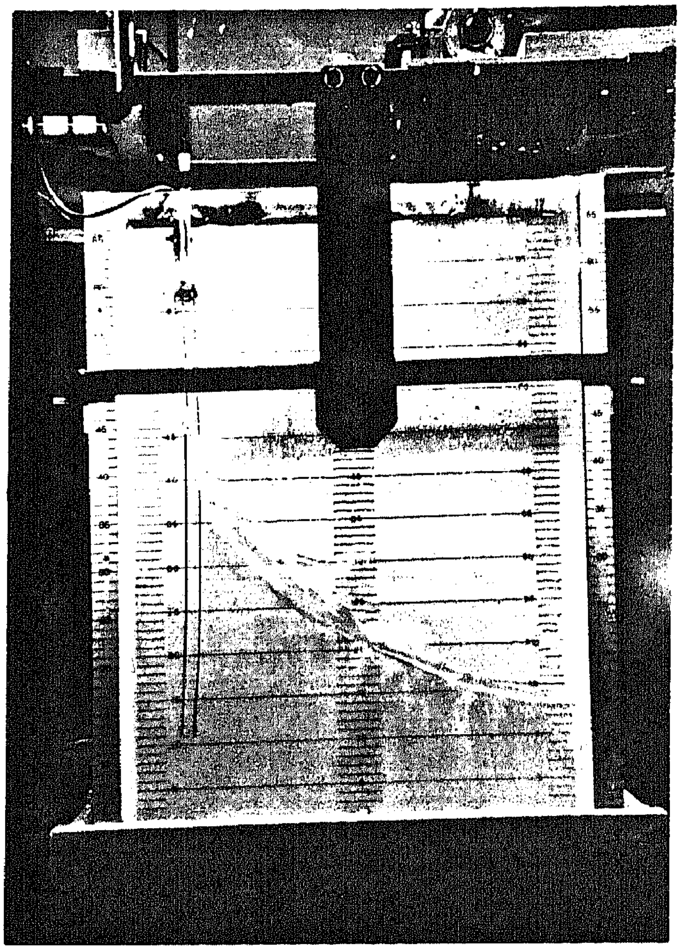

Fig. 7.7 : Shows resonance condition being approached (Aspect Ratio h/2a=0.5) by the rolling tank.

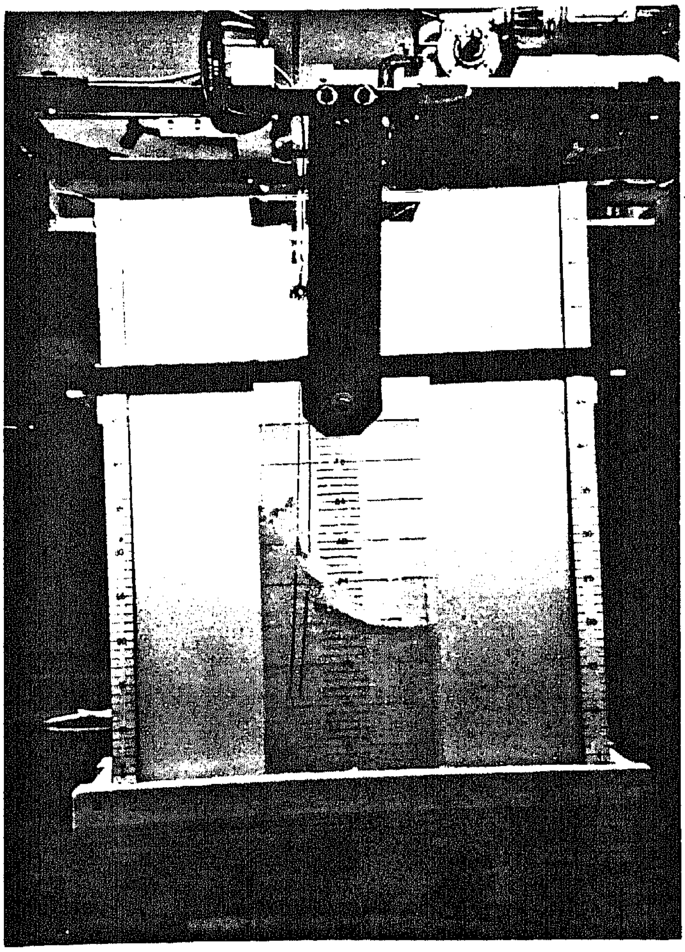

Fig. 7.8 : Shows the water in the tank is approaching 'resonance' (Aspect Ratio h/2a=1.0)

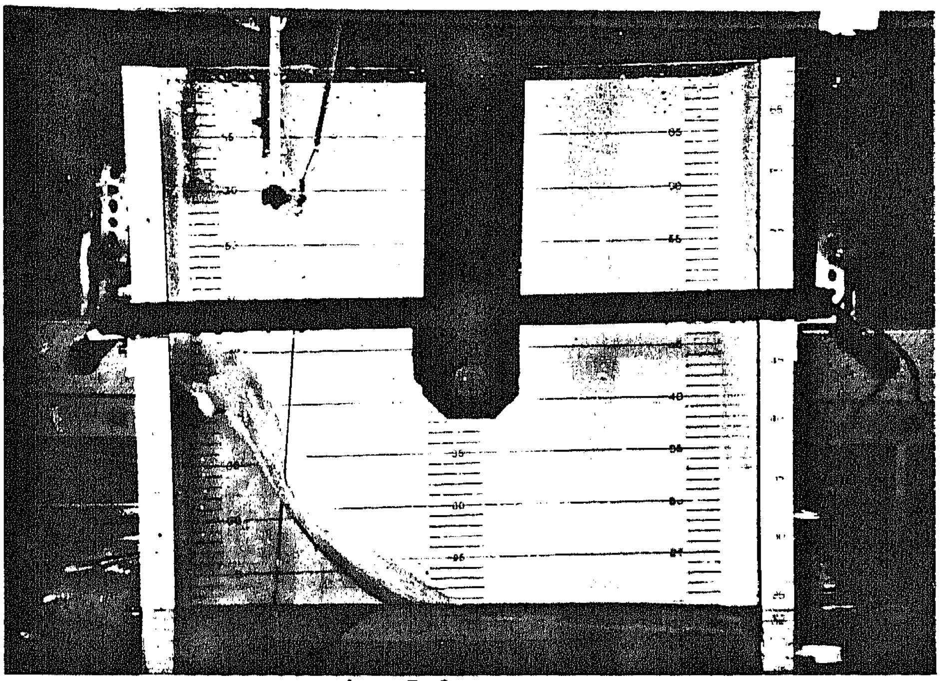

Fig. 7.9

Photos above and below shows that the water motions in moonpool reaching Resonance.

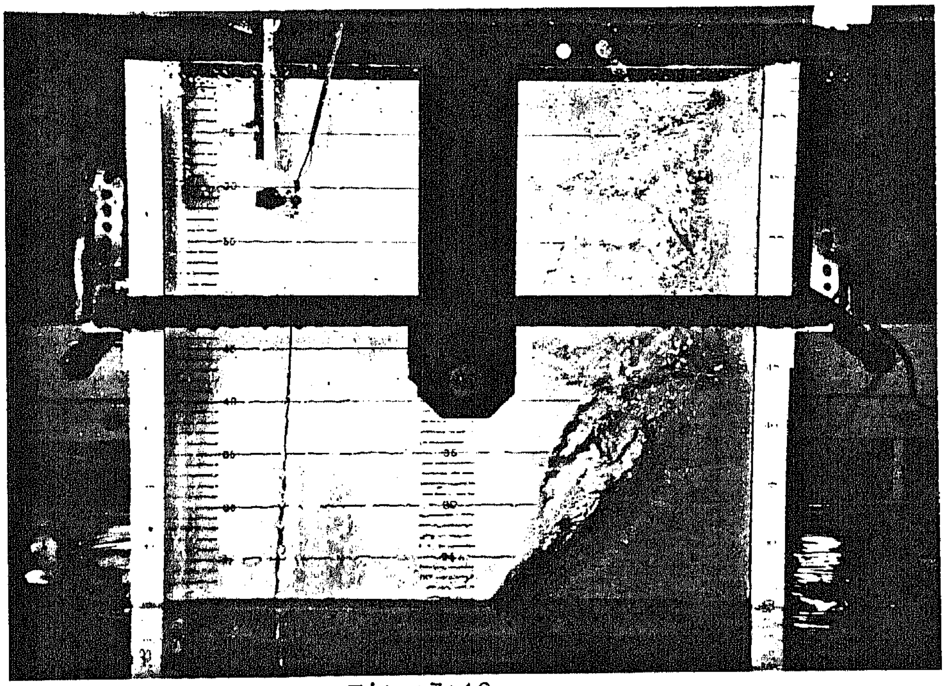

Fig. 7.10

Just past resonance a small travelling wave was set up as shown in fig. 7.11 below:

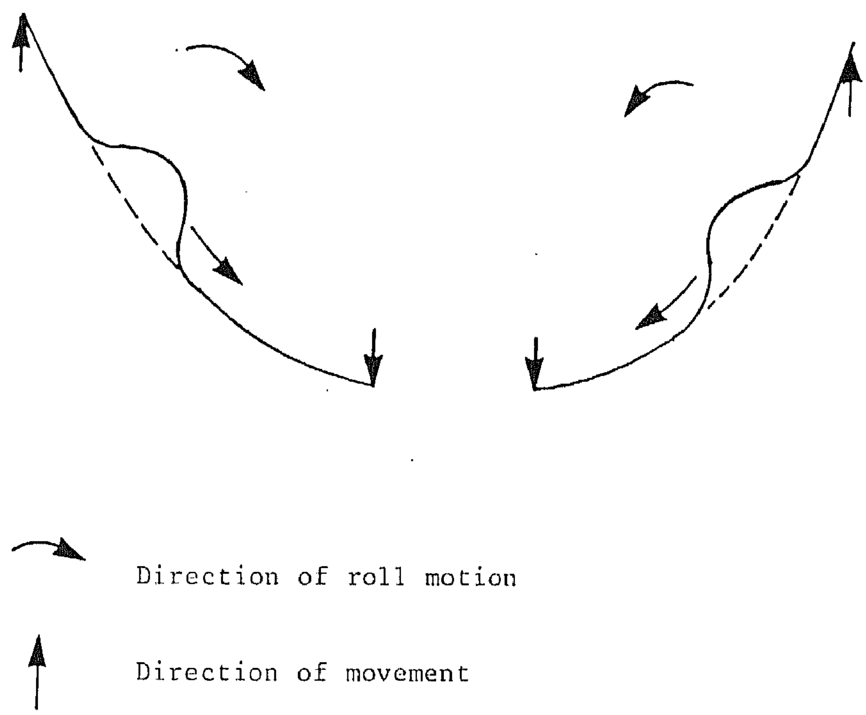

Fig. 7.11

A further increase in the excitation frequency simply distorts the water into small turbulent waves with defined peaks. See fig. 7.12 and 7.13.

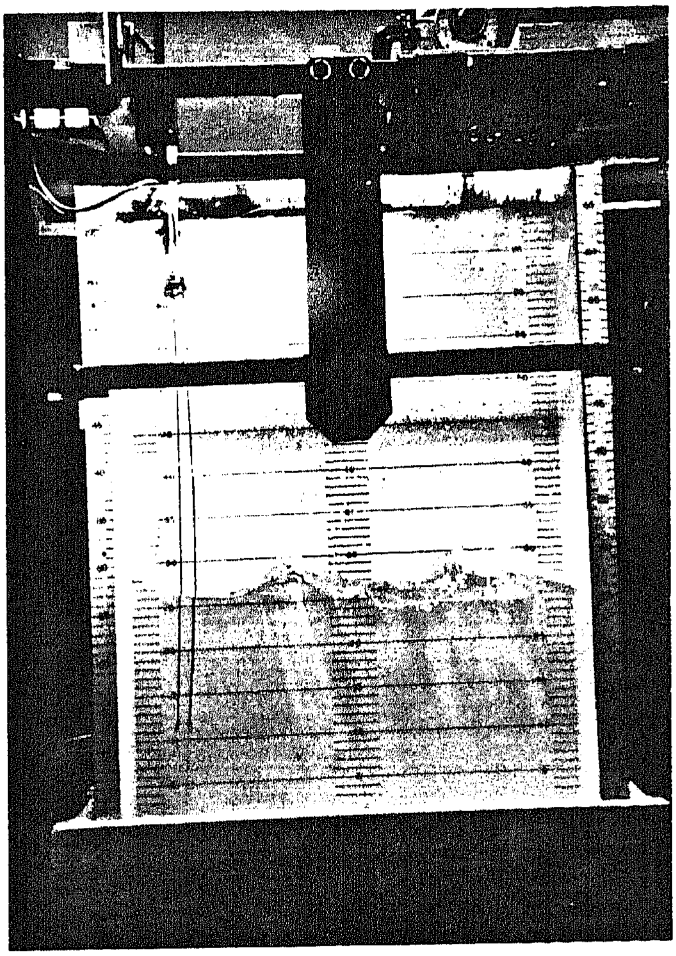

Fig. 7.12

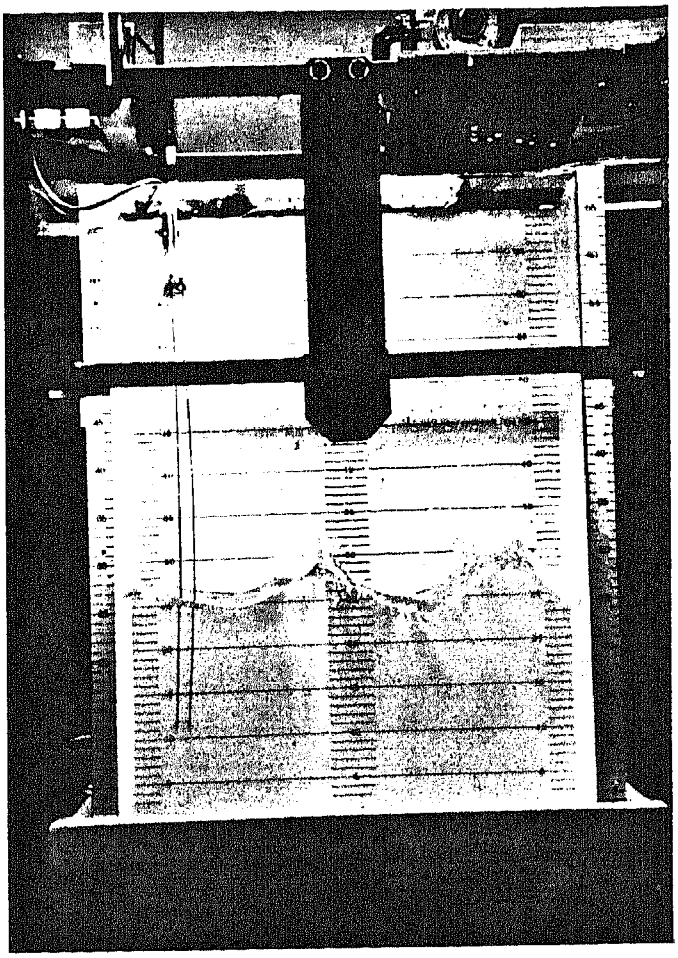

Fig. 7.13

In order to gain a deeper understanding of the water sloshing in the tank and moonpool, consider a beam with a particular stiffness experiencing a coupling effect as shown below:

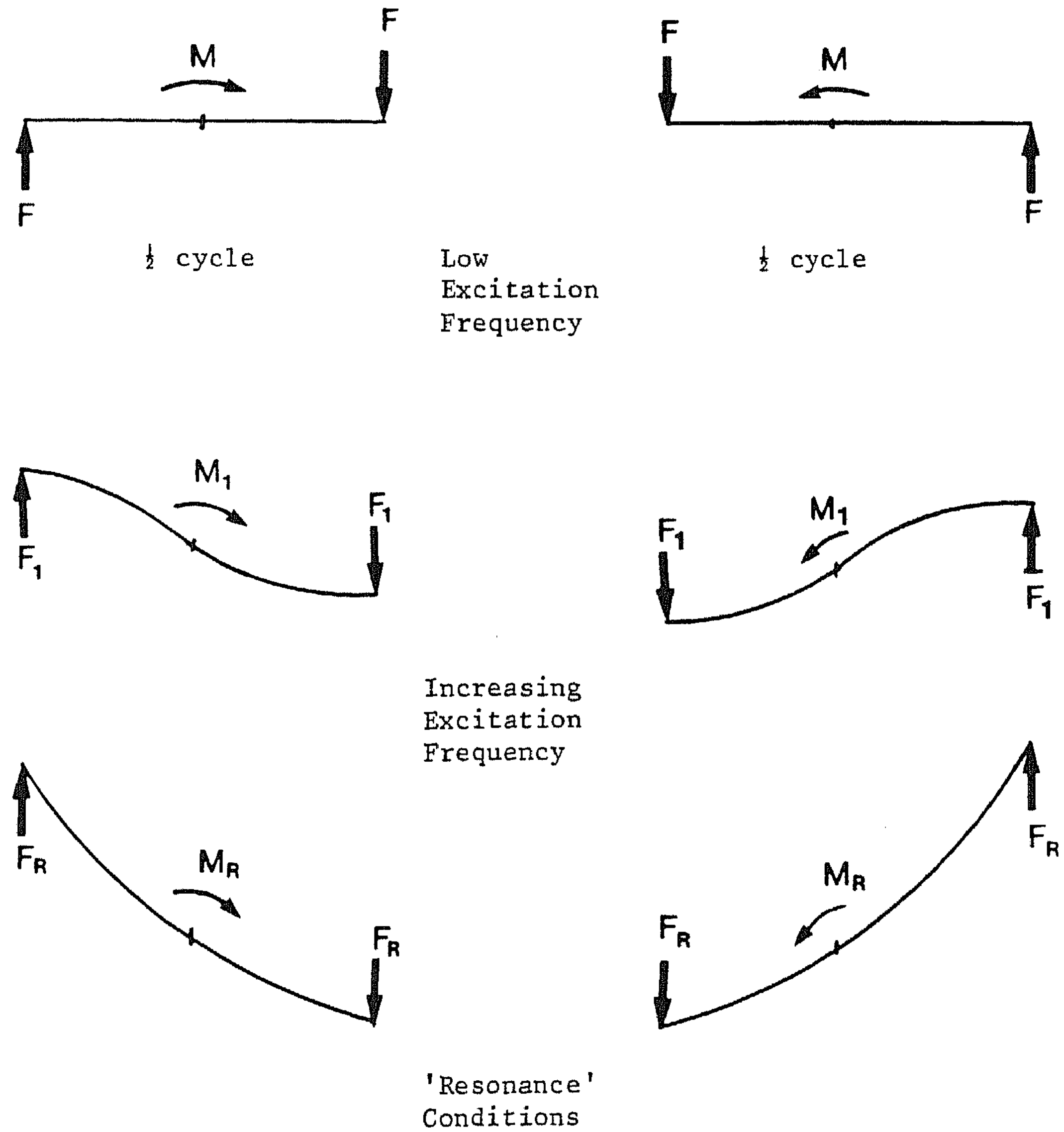

F represents the force

M represents the moment

Fig. 7.14

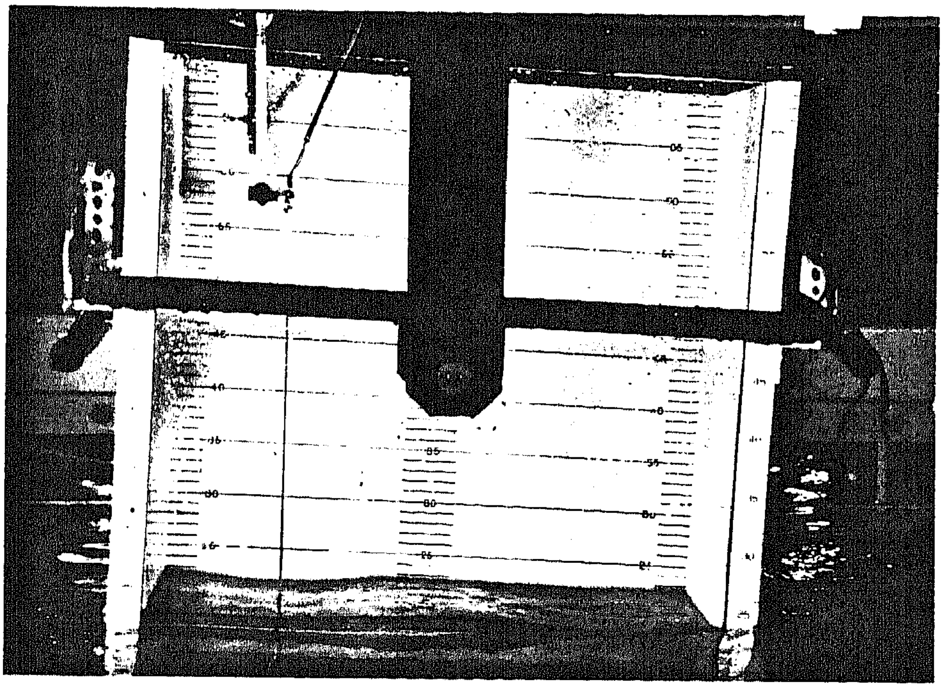

Fig. 7.15

During the Moonpool Experiments with waves producing vertical oscillation only, observation clearly shows that the oscillating mass of water has the behaviour of a spring mass system. However, when rising it was noticed that the water surface took the shape of a slight hump at the centre. Similarly when falling the hump was replaced by a level. It appeared that at the centre region of the moonpool the water surface was leading the motions, giving the impression that the water was dragging along the side walls due to shear stresses. See fig. 7.15 and 7.16.

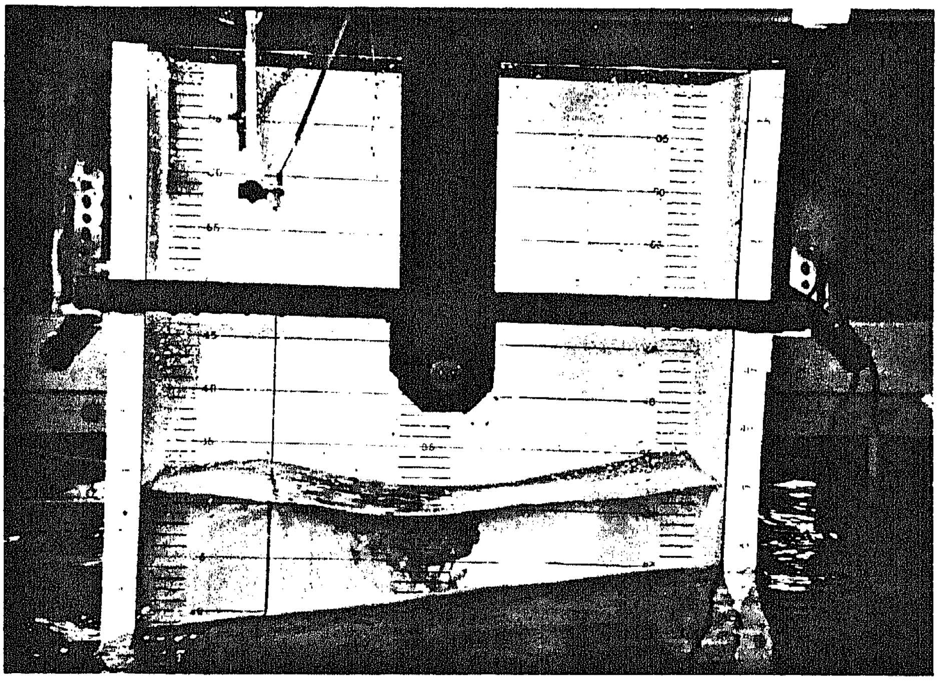

Fig. 7.16

When the moonpool was forced to roll in addition to the waves being generated, at low excitation frequencies the combination of the standing wave and vertical oscillation gave the effect such that the profile of the water surface had a slight curvature (see fig. 7.17).

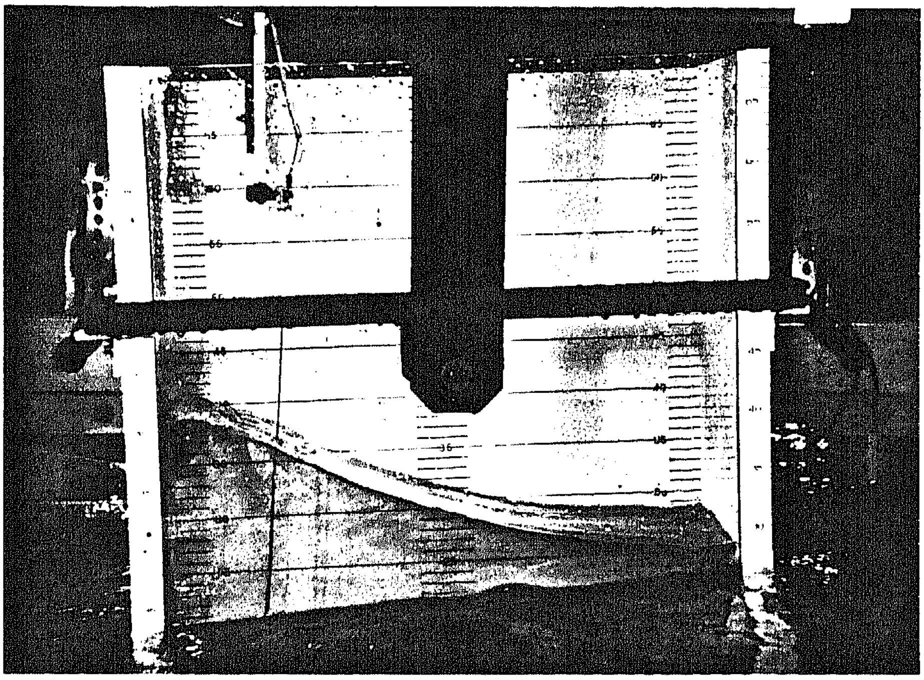

Fig. 7.17

As the speed of the rolling mechanism increased, this well defined profile gradually disappeared and invariably a small travelling was evident. See fig. 7.18.

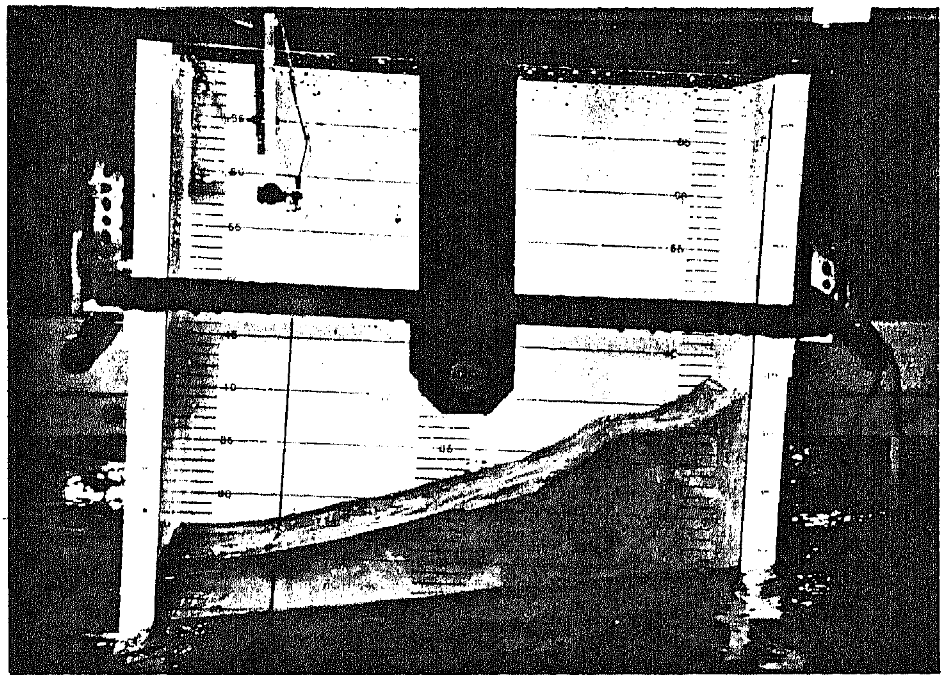

Fig. 7.18

Near resonance the behaviour of water motions showed certain similarities with Water Sloshing due to pure rolling excitation. However, in addition, the coupling effect of vertical oscillation and sloshing motion resulted in much more movement, especially along the side waves of the moonpool. See fig. 7.19.

Generally, it was observed that at low rolling excitation frequencies, vertical oscillation dominated the scene and near resonance the sloshing motion became the critical factor.

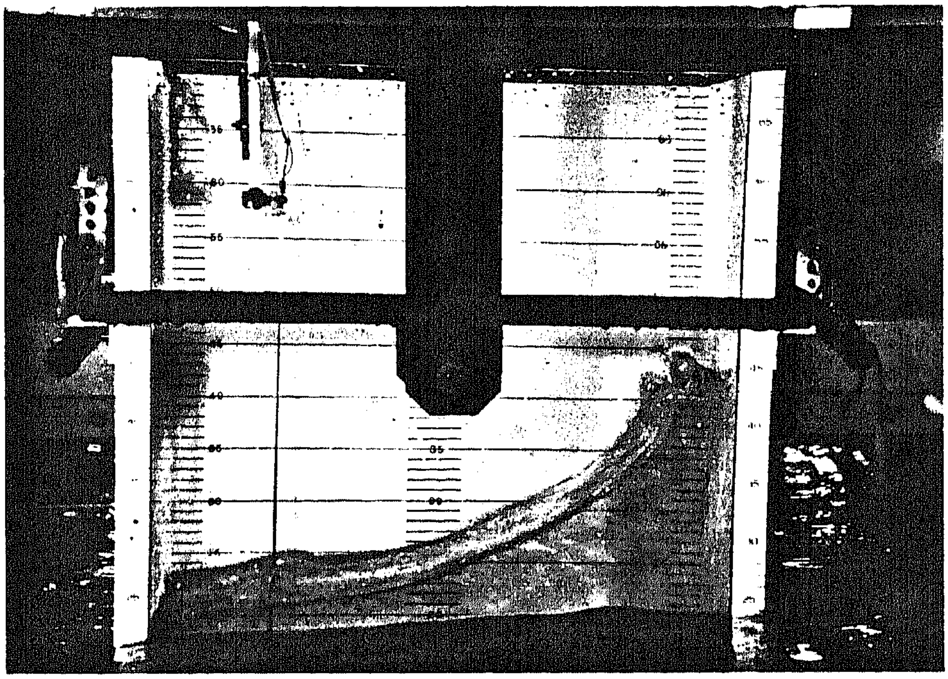

Fig. 7.19

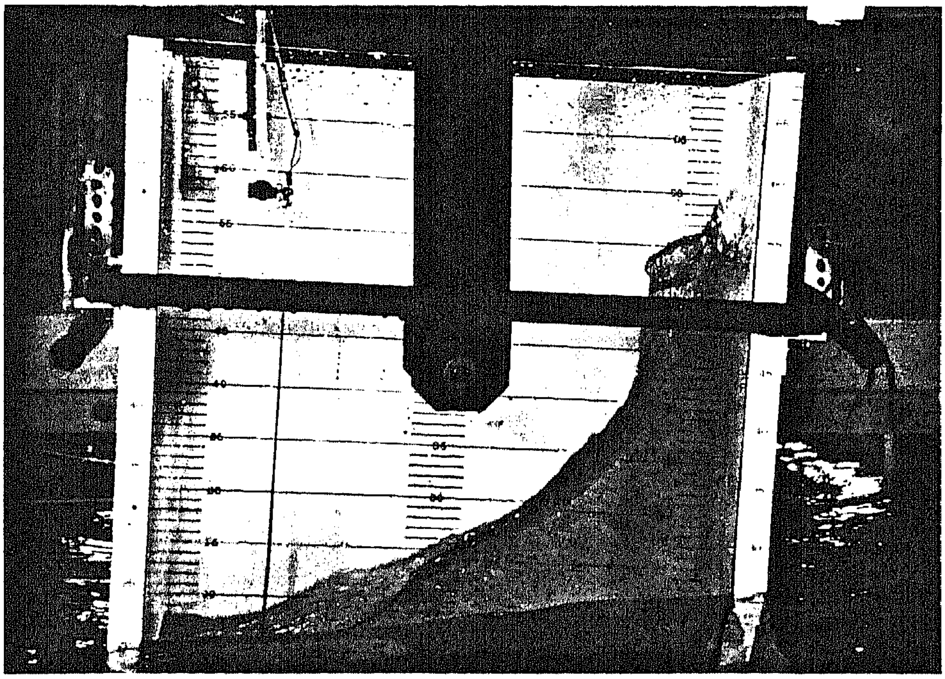

Fig. 7.20

Overall, the experiment conducted with baffles showed that at low rolling frequencies, the baffles effectively appeared to dampen the motions. (See fig. 7.21).

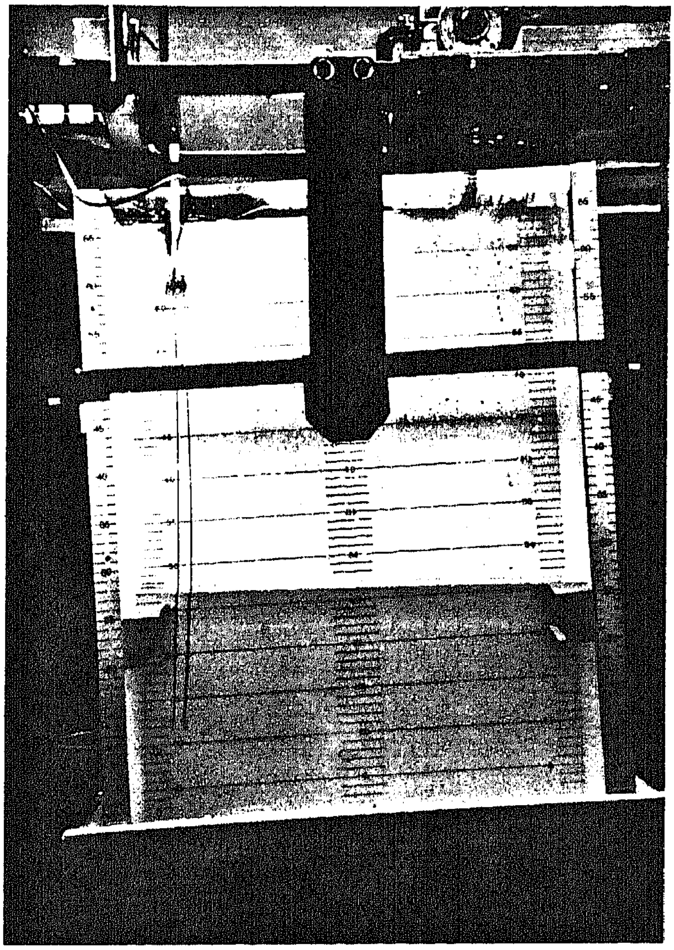

Fig. 7.21

However, as the frequency of the rolling mechanism increased, especially near resonance, although damping was considerable, a fair amount of turbulence was present. This was in the form of vortex trapping beneath and between as well as above the baffles.

The vortex motions can be seen in fig. 7.22 - 7.24 in the case of the tank, and fig. 7.25 - 7.26 in the case of the moonpool.

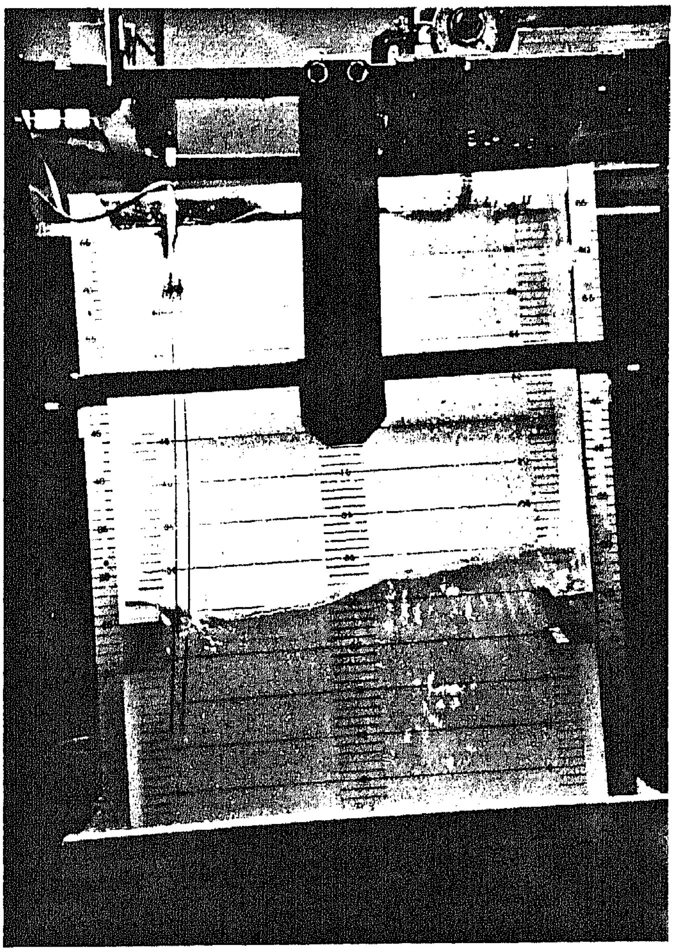

Fig. 7.22

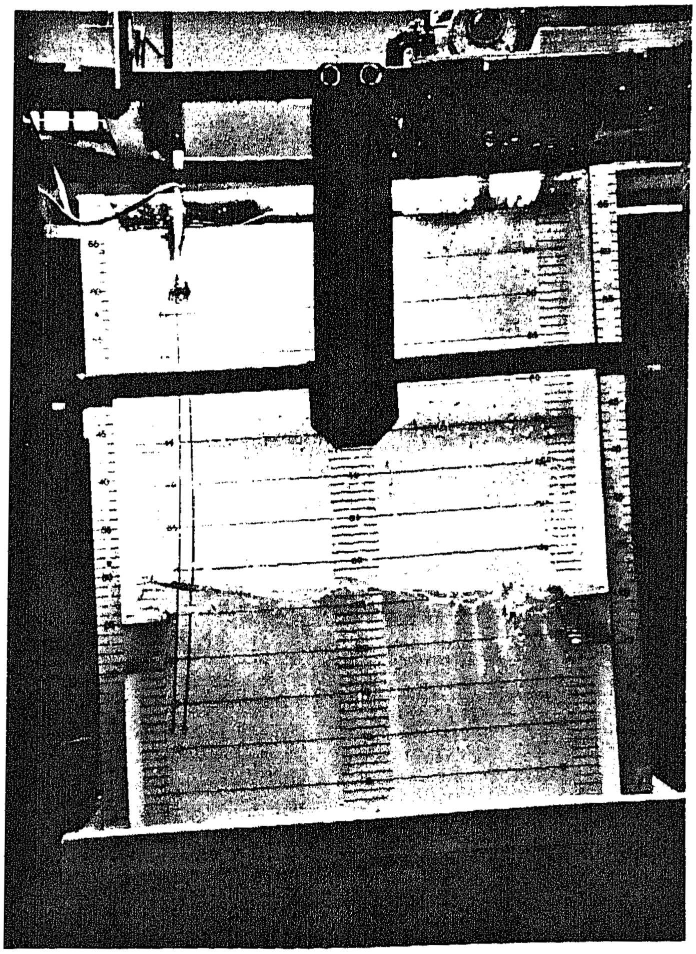

Fig. 7.23

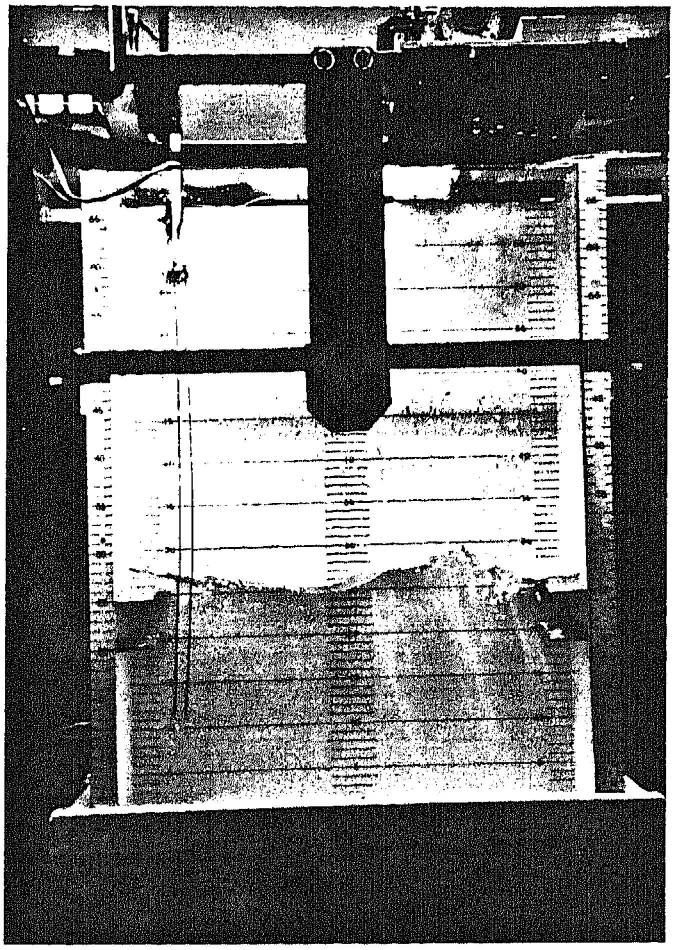

Fig. 7.24

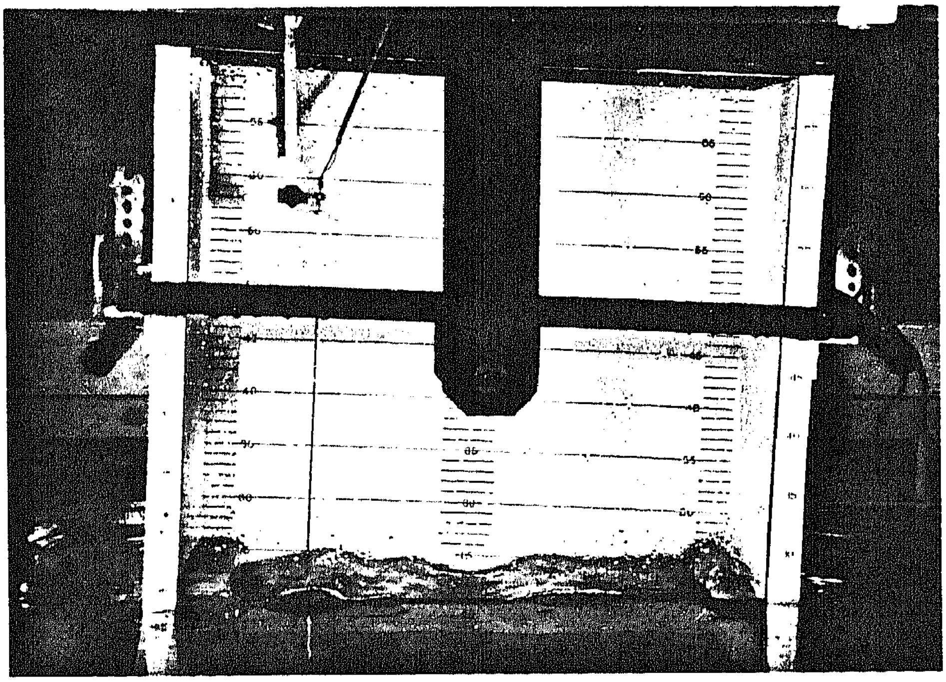

Fig. 7.25

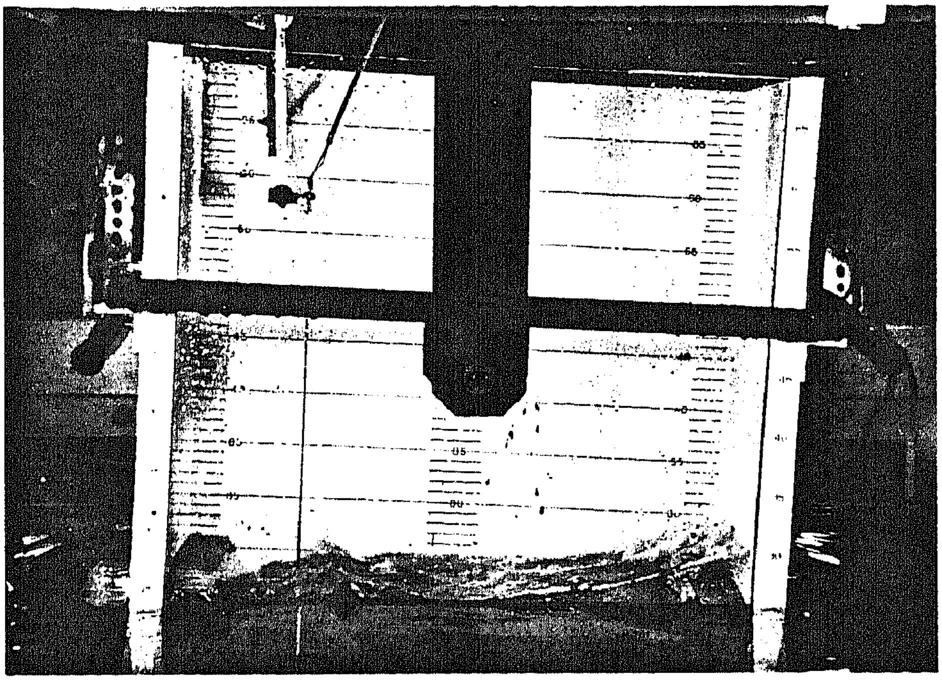

Fig. 7.26

As the model continued rolling the vortex motions released itself violently onto the water surface producing a mass of turbulence. See fig. 7.27/8 and fig. 7.29 for the tank and moonpool respectively.

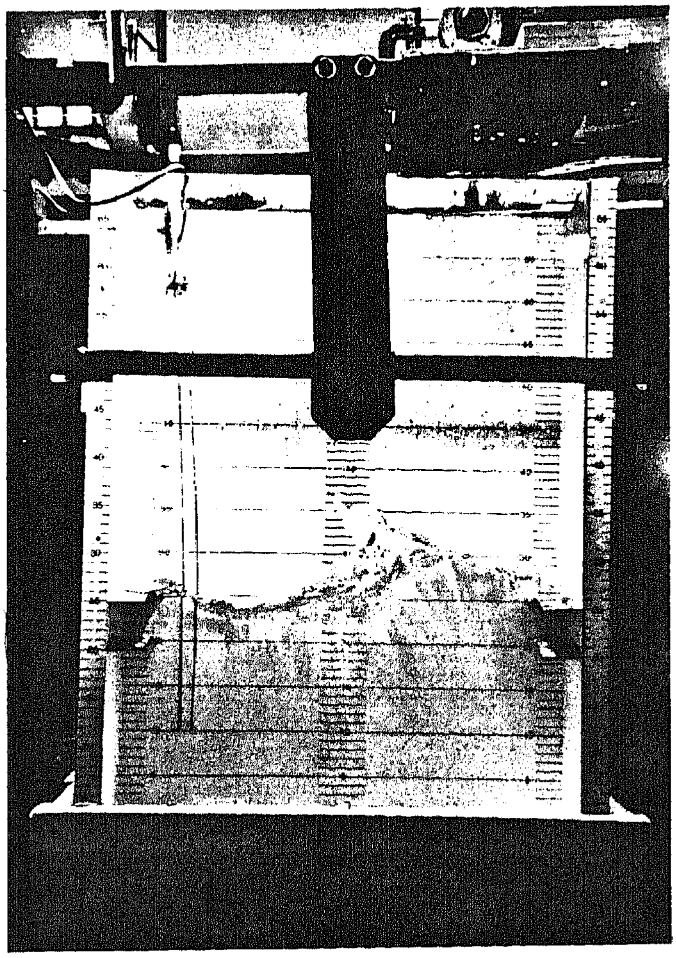

Fig. 7.27

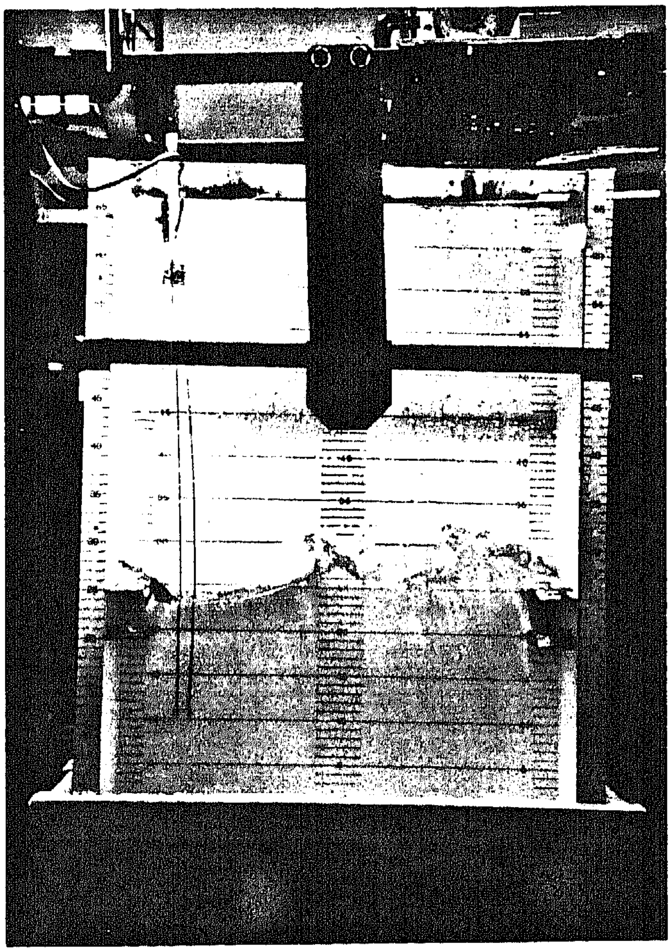

Fig. 7.28

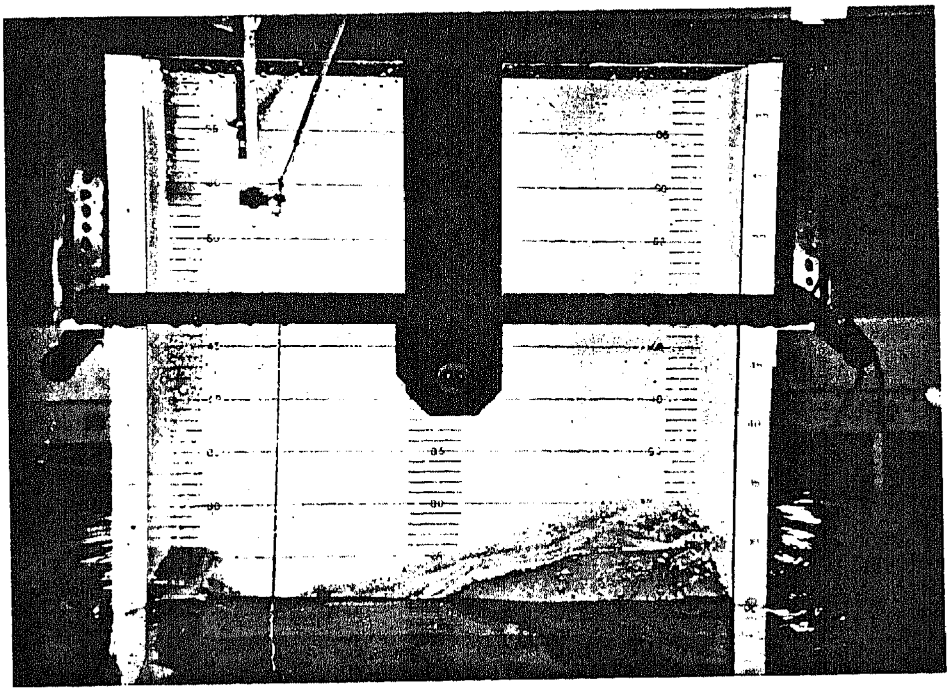

Fig. 7.29

8.0 DISCUSSION AND KEY FINDINGS

Following the project strategy, the behaviour of sloshing in moonpools was investigated through theoretical and experimental studies with stronger emphasis on the latter.

In the theoretical study, the wavemaker theory was applied to the moonpool problem by considering the generation of water waves by two barriers undergoing roll motion. This approach was taken on the basis that the water waves generated in the moonpool by the rolling motion, i.e. standing waves are formed. The solution was tested by evaluating the amplitude of the wave at the side wall, near resonant. The result showed that the amplitude acquires an infinite value. It must be empasised that the interest is not in the response amplitude but the wavelength at the frequency of resonance. It is to be pointed out, however, that further studies are necessary to fully investigate the potential of this approach.

The theory has its restrictions in that it is based on linearised hydrodynamics and sloshing phenomenon is demonstrably non-linear in character. It may be that a numerical study based on a non-linear model will be necessary to investigate this problem to any degree of accuracy.

The key objective of the experimental study was to make comparisons between the water sloshing motions in a tank and moonpool. This was achieved by comparing resonant frequencies and in turn comparisons were also made with the estimated values.

Ideally, the experiments should have included a greater range of aspect ratios for a given width. However, the present width of the model comfortably accommodated aspect ratios of, and up to, 0.5. This meant that this was adequate from a practical point of view where, say, a typical diving support vessel has an aspect ratio of approximately 0.5, taking full advantage of a larger width. However, a further increase in the aspect ratio indicated that the height of the model had to be extended. This would have caused problems in allowing for adequate clearance between the bottom of the towing tank and the moonpool. Furthermore, only limited resources were available in handling a much larger volume of water. It therefore appeared to be reasonable to use sections in reducing the width of the model in order to cater for higher aspect ratios.

Generally, it was observed that as the moonpool draft increases i.e. aspect ratio $h/2a$ is reduced, the resonant frequency appears to be higher in the case of a moonpool. In a practical situation, this could be useful. For example, in a design of ships with flatter hulls, and in turn the moonpool will have a shallow draft. As a result the water in the moonpool will be excited at a higher frequency, possible avoiding the clash with the wave dominant frequency.

Water sloshing is a relatively new problem and the contributions of this research has hopefully overcome the initial stages of the problem. In other words, this thesis has provided a possible theoretical approach and in addition experimental studies which will enhance the understanding of the problem. This work will therefore provide a good foundation for future work.

9.0 AREAS FOR FUTURE RESEARCH

The sloshing motions of water coupled with vertical oscillations in moonpool is a complex problem and the study is far from being completed. Generally the problem requires a more comprehensive theoretical analysis backed by additional experiments. The complexity and nature of the problem obviously needs simplification in the initial stages and as the investigation advances, the complexity can be gradually tackled and overcome. The ultimate aim in continuing the research should be in determining the forces, moments and pressures caused by the sloshing motions. This will aid designers in the design of a multi-purpose moonpool. The relevant areas of future research are discussed below:

(1) A Complete Theoretical Solution

Basically the problem of sloshing in moonpools is non-linear and hence further studies are required to investigate a numerical solution which involves a non-linear model.

The present, theoretical study deals with the interior fluid domain, and this approach requires further conformation.

In addition, the outer fluid domain still has to be considered. The derived velocity potential will then enable the pressures due to the sloshing motions to be calculated. This can be compared with the results obtained from the moonpool experiment by employing pressure/force transducer on the side walls.

The formula for evaluating resonant frequencies proved to be within close limits with the results obtained from the moonpool experiments for aspect ratios of, and greater than, 0.5. However, experimental results for lower aspect ratios showed the formula to be unsatisfactory and therefore an additional equation needs to be sought.

(2) Inclusions of Other Modes of Motions

It is apparent that the roll motion is the most important mode influencing the sloshing motions, and the effects of other modes of motions, including their combined effects needs to be investigated. This will either confirm or highlight the worst case.

(3) Explore Methods of Damping and Moonpool Geometry

As the dimensions of the moonpool increases, this will in effect, reduce the resonant frequency. Therefore it is inevitable that some form of damping system is required to improve the performance of launching and retrieving operations during a range of seastates. In addition, this will involve in determining the best configuration for the moonpool geometry.

The experiments conducted in increasing damping with the aid of baffles, showed to be inadequate in reducing the motions near resonant, especially near the centre region of the moonpool, thus a more effective damping system is required. For example, a combination of baffles with a perforated bulkhead may be more successful. There are other damping devices which are employed in an attempt to reduce water oscillations in moonpools with smaller dimensions. Whether it will be suitable and effective to moonpools with relatively arger dimensions is another matter which needs to be studied.

10.0 CONCLUSIONS

The main conclusions of this research are as follows:

(1) For aspect ratios (h/2a) greater than 0.5 the resonant frequencies obtained from the tank and moonpool experiments are to within a few percent, and these are in accordance with the theoretical values. However, lower aspect ratios appear to display a different trend, in that the resonant frequencies are higher in the case of the moonpool.

(2) The theory proposed involves idealising the moonpool as a two-dimensional system represented by two surface piercing parallel barriers of width 2a. The resonant frequencies estimated using this approach show fairly good agreement to experimental results.

(3) The parameters that appear to have a strong influence on the characteristics of the sloshing motion of water in moonpools are the width (distance between barriers) and the depth of water.

(4) A moonpool with relatively large dimensions require some form of sophisticated method of damping. The experiments show that although combination of baffles are effective to a degree at lower excitation frequencies, the fluid motions at the centre of the moonpool near resonant conditions are worse than the case without the baffles.

REFERENCES

1. LEE, B.S. "On The Properties of Vertical Oscillation in a Moonpool", PhD Thesis July 1982 Strathclyde University.

2. MOISEEV, N.N. "On The Theory of Non Linear Vibrations of a Liquid of Finite Volume", Appl. Math. Mech. 1958 N.Y.22,612.

3. FALTINSEN, O.M. "A Non Linear Theory of Sloshing in Rectangular Tanks", Jou of Ship Res. 18, 224, 1974.

4. FALTINSEN, O.M. "A Numerical Method of Sloshing in Tanks with Two Dimensional Flow", Jou of Ship Res. 22, 193, 1978.

5. CHU, B.T. & YING, S.J. "Thermally Driven Non Linear Oscillations in a Pipe with Travelling Shock Waves", Physics Fluids 6, 1625, 1968.

6. CHESTER, W. "Resonant Oscillations of Water Waves", Proc. R. Soc. 306A, 5, 1968.

7. VERHAGEN, J.H.G. & WIJNGAARDEN, V.L. "Non Linear Oscillations of Fluid in a Container", J. Fluid Mech. 22, 737, 1965.

8. WIJNGAARDEN, V.L. "Non Linear Acoustics", In Symp. on Appl. Math", edited by Hermans A.J. and Oosterweld, M.W.C. Delft, the Netherlands.

9. CHUL, W.H., DALZELL, J.F. & MODISETTE, J.E. "Theoretical and Experimental Study of Ship Roll Stabilisation", Jou. of Ship Res. 12, 165.

10. DEMIRBILEK, Z. "Energy Dissipation in Sloshing Waves in a Rolling Rectangular Tank", Ocean Eng., Vol.10, No.5 pp347-358 1983.

11. HAVERLOCK, T.H. "Forced Surface-Waves on Water", Philosophical Magazine 8, pp569-576 Oct. 1929.

12. BASS, R.L. BOWLES, E.B. & COX, P.A. "Liquid Dynamic Loads in LNG Cargo Tanks", Trans SNAME Vol. 88, pp103-126.

13. URSELL, F., DEAN, R.G. & YU, Y.S. "Forced Small-Amplitude Water Waves : A comparison of theory and experiment", Fluid Mech. 7, April, 1959.

14. McCORMICK, M.E. "Ocean Eng. Wave Mech", A Wiley-Intersience Publication.

15. MECHAUTE, B. "An Introduction to Hydrodynamics & Water Waves", Spinger-Verlag Publication.

A P P E N D I C E S

APPENDIX 1 - DESCRIPTION OF EXPERIMENTAL FACILITIES USED IN THIS STUDY

All the experiments were performed in the laboratory of the University of Strathclyde.

(a) Towing Tank

The main dimensions of the tank are:

length 25m

breadth 1.5m

depth 0.8m

normal water depth 0.6m

At one end of the tank a wave absorbing beach is installed. This is made of steel frames filled with aluminium mesh. At the other end the wavemaker consist of five flaps which are driven by d.c. motor with positional feedback facilities. The motors themselves are driven by power amplifiers which receive command signals from a frequency analyser for simple harmonic waves.

(b) Instrumentation System

i. Frequency Analyser SM2001

Manufactured by SE labs (EMI), its signal generators part can generate a range of sinusoidal signals in hertzs and voltage (amplitudes). This equipment was used to generate simple harmonic waves in the towing tank.

ii. Roll Forcing Mechanism

The roll forcing mechanism consists of an a.c. synchronous motor connected to an off centre flywheel assembly. The speed of the motor can be varied by a thyristor-based motor controller.

iii. Wave Monitor

The monitor is supplied by Churchill Controls Ltd., and its sensing part consists of two stainless steel wires. It measures the variation of conductucity between two wires due to the variation of depth of immersion when placed in the wave-field. The monitor module supplies a high frequency excitation signal across two wires and amplifies the signal obtained by the probe.

iv. Roll Measurement

This was achieved by an a.c. linear variable differential transducer. (LVDT) manufactured by Sangams Transducers. The a.c. energising current is supplied by a transducer conditioner model C33 made by the same Company.

v. Pen Recorder

A three channel pen recorder type CR533, manufactured by J.J. Lloyd Instruments Ltd., was used to record all the information obtained through the measuring instruments described above. Recording paper speed of 10mm/secs was used throughout the experiment.

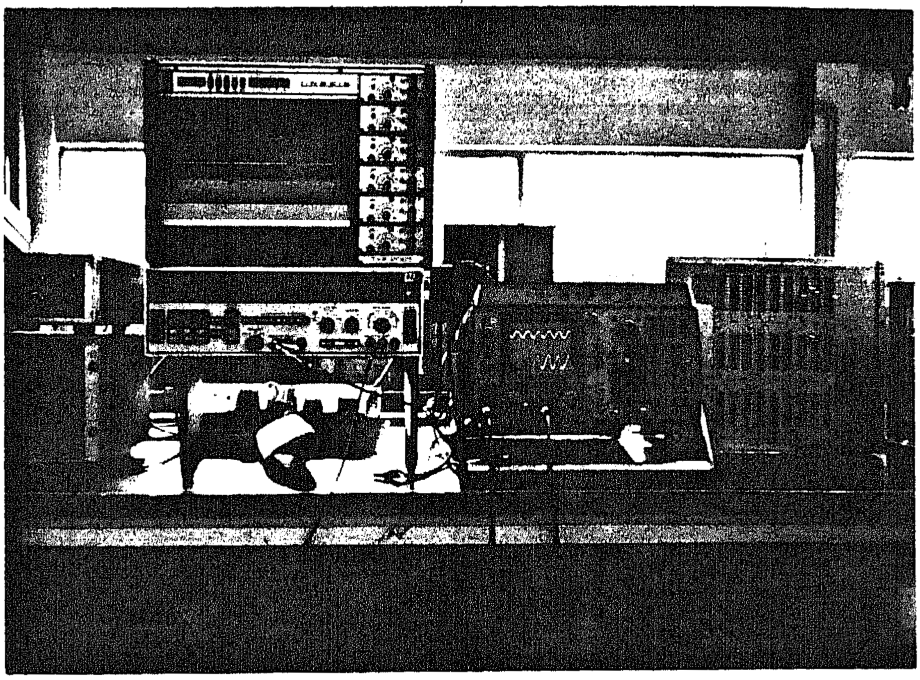

Fig. A1.1

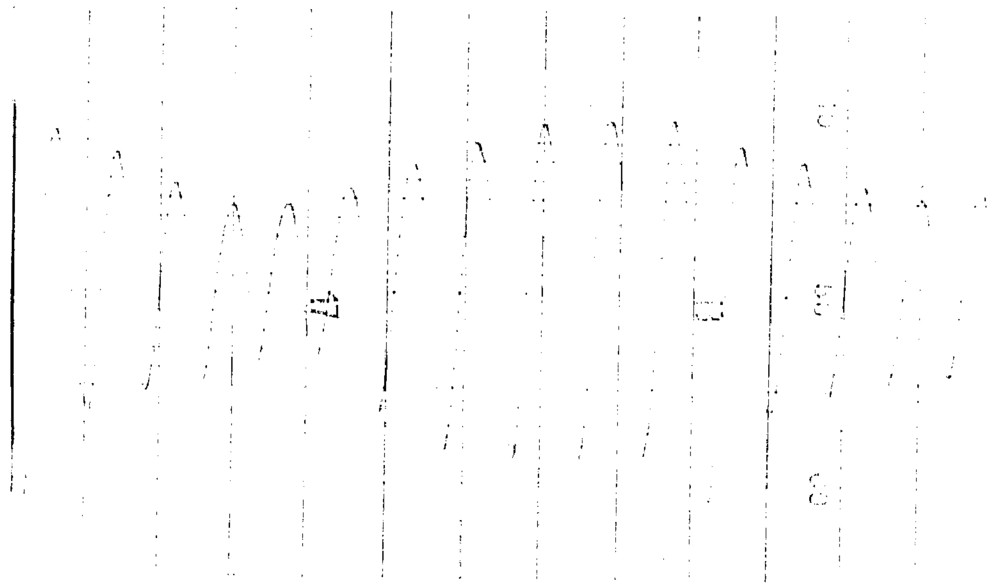

Fig. A1.2 An example of waves breaking Scale x 4
Approaching resonance (h/2a = 0.5)

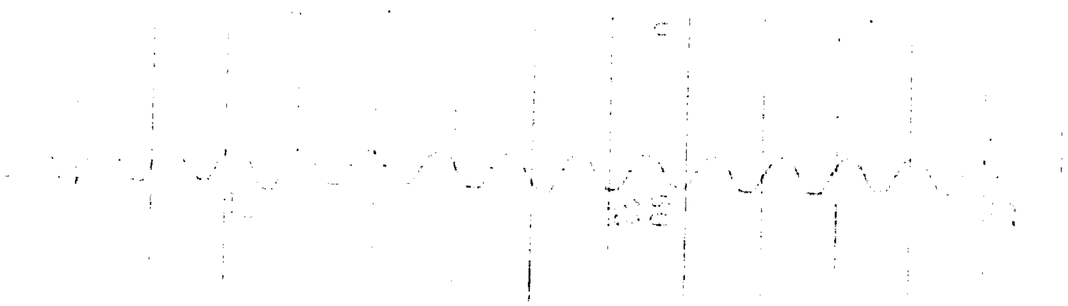

Fig. A1.3 Tank : Resonant Frequency = 7.1 rad/s

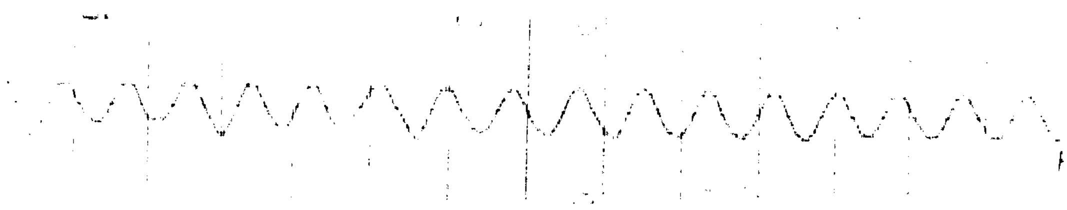

Fig. A1.4 Moonpool : Resonant frequency = 7.62 rad/s

Aspect Ratio (h/2a) = 1.0 Resonance Scale x 4

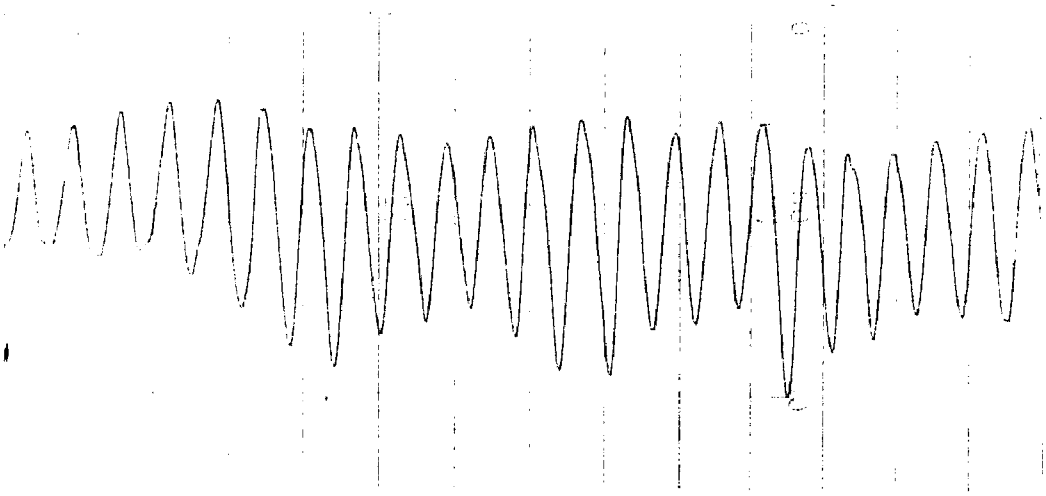

Fig. A1.5 Tank : Resonant frequency = 10.57 rad/s

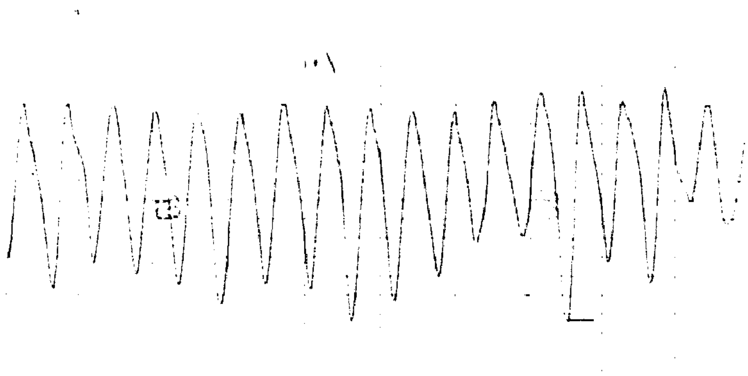

Fig. A1.6 Moonpool : Resonant frequency = 11.04 rad/s

Aspect Ratio (h/2a) = 0.25 Resonance Scale x 4

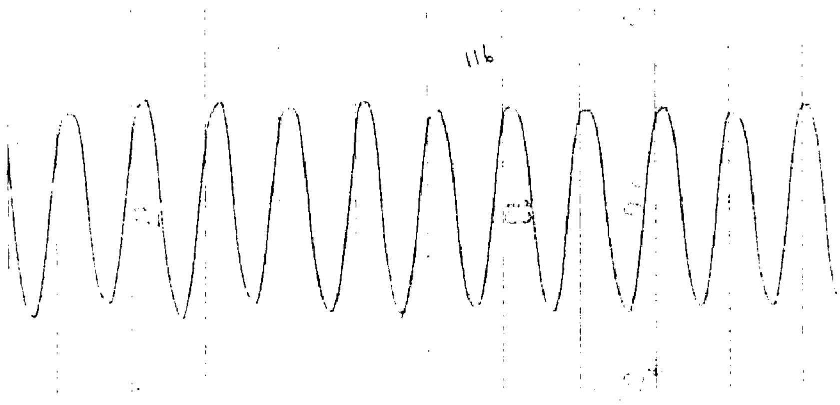

Fig. 12.7 Tank : Resonant frequency 0 6.29 rad/s

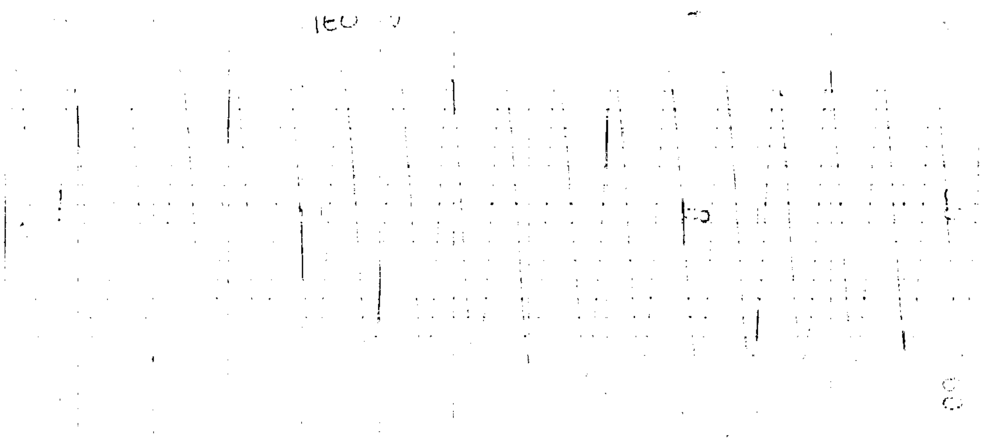

Fig. A1.8 Moonpool : Resonant frequency = 8.68 rad/s

Aspect Ratio (h/2a = 1.5) At Resonance Scale x 4

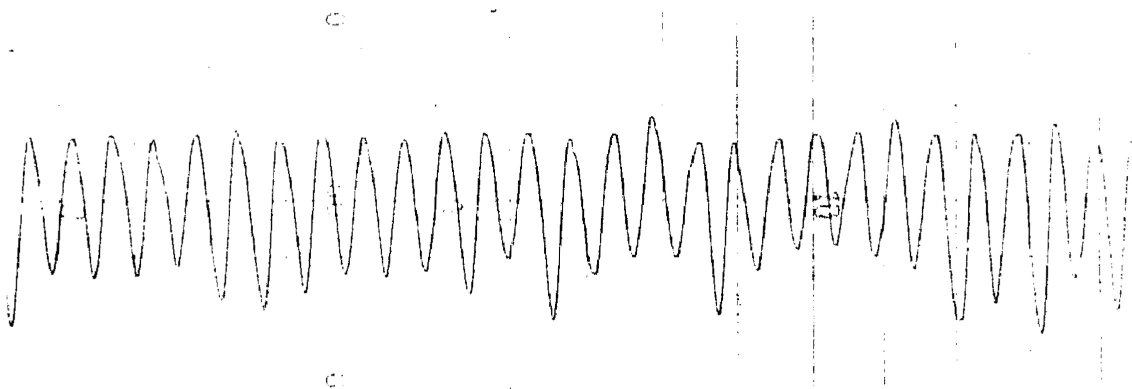

Fig. A1.9 Tank : Resonant frequency = 10.89 rad/s

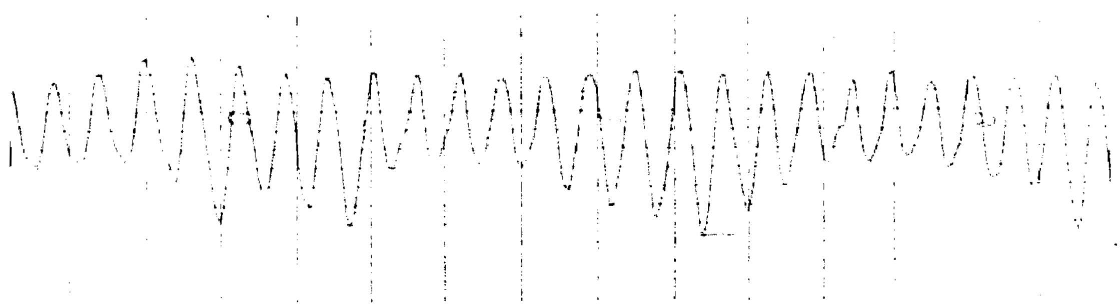

Fig. A1.10 Moonpool : Resonant frequency = 11.31 rad/s

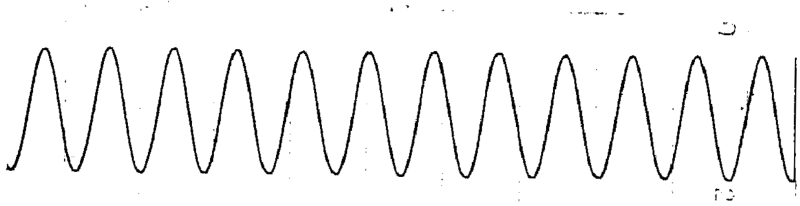

Fig. A1.11 An example of forced roll oscillation
Scale x 2

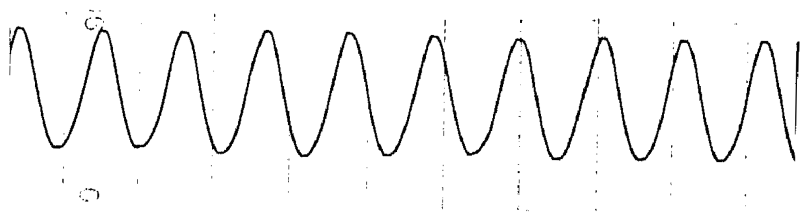

Fig. A1.12 An example of waves generated by wavemaker

Aspect Ratio (h/2a) = 0.5

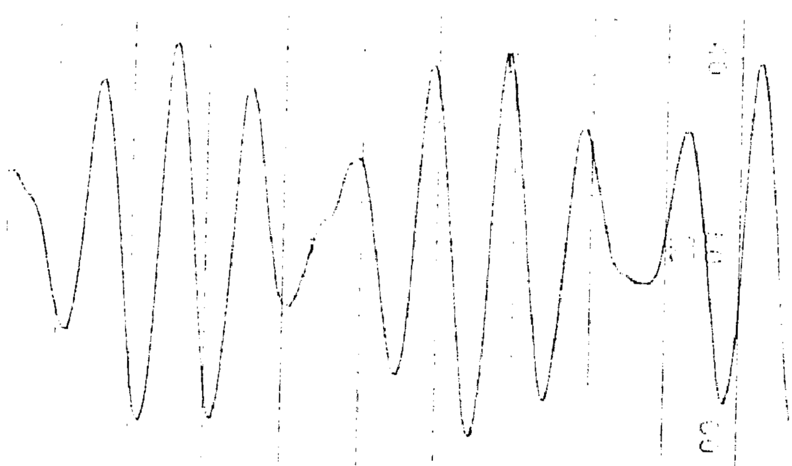

Fig. A1.13 Just before resonance scale x 4

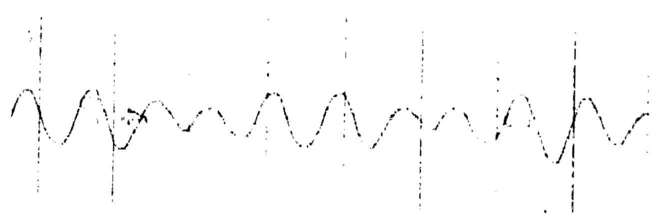

Fig. A1.14 Just before resonance scale x 40

APPENDIX II - WAVEMAKER THEORY APPLIED TO MOONPOOL

For a plate oscillating in roll mode, at finite depth, the solution for velocity potential is in the form of:

$$\Phi = \left[\frac{A}{K} \text{ Cosh } K(y-h) \sin (wt-kx) + \frac{An}{Kn} e^{-kx} \text{ CosKn}(y-h) \text{ Cost } wt\right] \qquad \ldots\ldots (1)$$

The expression for equation (1) consists of waves produced by small oscillations of a solid body. The first part of the equation represents a progressive wave, and the second part refers to local oscillations. The term (y-h) satisfy the bottom condition of $\partial\phi/\partial y = 0$.

For a moonpool section the problem will have to be formulated as shown below:

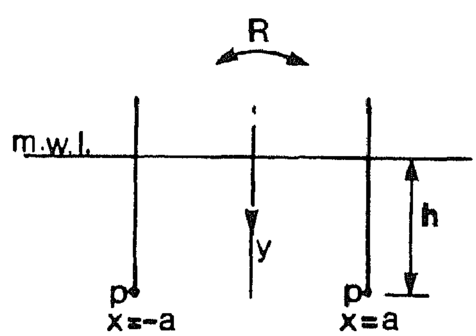

Fig. A2.1

It is possible to adapt the equation to crudely represent the moonpool situation without satisfying the bottom condition.

i.e the expression for Φ when the moonpool section is subject to rolling will comprise of a standing wave plus local oscillation.

$\Rightarrow \Phi = \Phi_1 + \Phi_2$

$$\Phi_1 = \frac{A}{K} \text{ Cosh } Ky \; [\text{Sin}(K[x+a]-wt) - \text{Sin } (K[a-x]-wt]$$

$$\Phi_2 = \frac{An}{Kn} \text{ Cos } Kny \; [e^{-kn(a+x)} + e^{-kn(x-a)}] \text{ Cos } wt$$

Where $Kn = (2n-1) \; \pi/2a$.

Notes

(1). A standing wave can have many modal points. However near resonance, at $\lambda/2 = 2a \Rightarrow \; = 4a$; $x = o$: hence $y = o$.

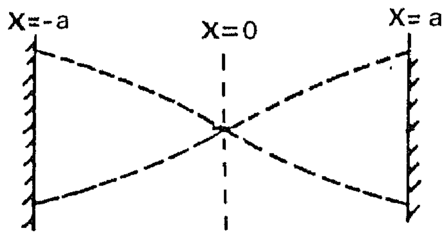

Fig. A2.2

(2). $\text{Sin}[K(x+a)-wt] - \text{Sin } [K(a-x)-wt] = 2 \text{ Sin } Kx \text{ Cos}Ka \text{ Cos } wt.$

$$\therefore \Phi_1 = \frac{2A}{K} \text{ Cosh } Ky \text{ Sin}Kx \text{ Cos}Ka \text{ Cos}wt$$

$$\Rightarrow \Phi = \left[\frac{2A}{K} \text{Cosh}Ky \text{ Sin}Kx \text{ Cos}Ka \text{ Cos}wt + \sum_{n=1}^{\infty} \frac{An}{Kn} \text{ Cos}Kny \; [e^{-Kn(a+x)} + e^{Kn(x-a)}] \text{ Cos}wt \right] \quad \ldots\ldots.(2)$$

In order to proceed with the problem solving, the boundary conditions have to be satisfied.

i.e. $\partial\Phi/\partial x = \mp \; U(y) \text{ Cos}wt \quad$ at $x = \pm a$

where $U(y)$ is the orizontal velocity.

From (2) $\partial\phi/\partial x$ = 2A CoshKy CosKx CosKa Coswt

$$+ \quad An\ CosKny\ [e^{Kn(x-a)} - e^{-Kn(a+x)}]\ Coswt$$

at $x = a;\ y = o;\ \partial O/\partial x = -U(y)$ Coswt

$$\therefore\ U(y) = 2A\ CoshKy\ Cos^2Ka + \sum_{n=1}^{\infty} An\ CosKny\ e^{-2Kna} \quad \ldots\ldots\ldots (3)$$

at $x = -a$

$$U(y) = 2A\ CoshKy\ Cos^2Ka + \sum_{n=1}^{\infty} An\ CosKny\ e^{-2Kna} \quad \ldots\ldots\ldots (4)$$

The functions on the right form a complete orthogonal set. If $2ACos^2Ka$ and Ane^{-2Kna} are replaced by constants the equations are very much the same and those shown in Ref (1), (2) and (3). With this in mind, it appears to be reasonable to adapt the same manner of solving the equations in order to determine the constants.

From equation (3)

$$\int_o^h U(y)\ CoshKy\ dy = -2\int_o^h A\ Cos^2Ka\ Cosh^2Ky\ dy$$

$$\Rightarrow -2\ ACos^2Ka = \frac{\int_o^h U(y)\ Cosh\ Ky\ dy}{\int_o^h Cosh^2\ Ky\ dy}$$

$$\int^h Cosh^2Ky\ dy = \frac{1}{2}\int_o^h (e^{ky}+e^{-ky})^2\ dy = \tfrac{1}{2}\int_o^h (Cosh2Ky + 1)dy$$

$$= \tfrac{1}{2}\left[\frac{Sinh2Ky}{2K} + y\right]_o^h = \tfrac{1}{2}K[Sinhkh\ CoshKh + Kh]$$

$$\Rightarrow \quad A = -\frac{2K\int_o^h U(y)\ Cosh\ Kydy}{Cos^2Ka(SinhKh\ CoshKh + Kh)} \quad \ldots\ldots\ldots (5)$$

Similarly for the second part of the expression of equation (2)

$$\int_0^h U(y)\ \mathrm{Cos}Kny\ dy = Ane^{-Kn2a}\int_0^h \mathrm{Cos}^2\ Kny\ dy$$

$$\Rightarrow Ane^{-Kn2a} = \frac{\int_0^h U(y)\ \mathrm{Cos}\ Kny\ dy}{\int_0^h \mathrm{Cos}^2 Kny\, dy}$$

$$\Rightarrow An = \frac{4Kn \int_0^h U(y)\ \mathrm{Cos}Kny\ dy}{e^{-Kn2a}\ (\mathrm{Sin}\ Knh\ \mathrm{Cos}Knh + Knh)} \qquad \ldots\ldots.(6)$$

To evaluate the constants we need to find U(y)
Consider the following:
Assume that the barriers are allowed to pivot as shown in Fig. A2.3

If $\tan\theta = -s/h$ if θ is small $\Rightarrow \theta = -s/h$ let x be any point the distance between the => rotated and original position.

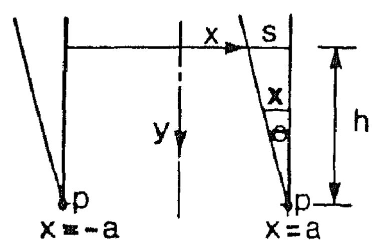

Fig. A2.3

hence $\frac{X}{h-y} = \theta \Rightarrow X = \theta(h-y)$

or $X = -s/h\ (h-y) = -s(1-y/h)$

$\therefore\ U(y) = -S(1-y/h)\ We$ at $x = a$ $0<Y<h$

In other words the multiplication frequency of the barriers oscillation by the displacement gives velocity of the particles. Note: at x=a it can be seen that $\partial\phi/\partial x$ will be negative and at $x = -a$, $\partial\phi/\partial x$ will be positive at $x = a$.

$U(y) = -S(1-y/h)We$ at $x=a$ $0\leqslant y\leqslant h$

At $x = a$ equation (5) and (6) yields

$$A = \frac{2K \int_0^h WeS\ (1/y/h)\ \text{Cosh}Ky\ dy}{\text{Cos}^2 Ka\ (\text{Sinh}Kh\ \text{Cosh}Kh + Kh)}$$

$$A = \frac{2KWeS \left[\int_0^h \text{Cosh}Ky\ dy - \int_0^h y/h\ \text{Cosh}Ky\ dy \right]}{\text{Cos}^2 Ka\ (\text{Sinh}Kh\ \text{Cos}kh + Kh)}\ .$$

$$A = \frac{2KWeS \left[\text{Sinh}Kh/K - 1/h\ (h/k\ \text{Sinh}Kh - \text{Cosh}Kh/K^2) \right]}{\text{Cos}^2 Ka\ (\text{Sinh}Kh\ \text{Cos}Kh + Kh)}$$

$$A = \frac{2KWeS\ (1/hK^2\ \text{Cosh}Kh)}{\text{Cos}^2 Ka\ (\text{Sinh}Kh\ \text{Cosh}Kh + Kh)}$$

$$A = \left[\frac{2WeS\ \text{Cosh}Kh}{Kh\ \text{Cos}^2 Ka\ (\text{Sinh}Kh\ \text{Cosh}Kh + Kh)} \right] \qquad \ldots\ldots\ldots(7)$$

and

$$An = -\frac{2Kn \int_0^h SWe\ (1-y/h)\ \text{Cos}Kny\ dy}{e^{-Kn2a}\ (\text{Sin}Knh\ \text{Cos}Knh + Knh)}$$

$$An = \left[\frac{-2KnSWe \int_0^h \text{Cos}Kny\ dy - \int_0^h y/h\ \text{Cos}Kny\ dy}{e^{-Kn2a}\ (\text{Sin}Knh\ \text{Cos}Knh + Knh)} \right]$$

$$An = \left\{ \frac{-2Kn\ SWe \left[\frac{\text{Sin}Knh}{Kn} - 1/h \left(\frac{h\text{Sin}Knh}{Kn} + \frac{\text{Cos}Knh}{K^2 n} \right) \right]}{e^{-Kn2a}\ (\text{Sin}Knh\ \text{Cos}Knh + Knh)} \right\}$$

$$An = \frac{+2SWe\ CosKnh}{Knhe^{-Kn2a}\ (SinKnh\ CosKnh + Knh)} \qquad \ldots.(8)$$

hence for X>O

$$\Phi = \left[\frac{2WeS\ CoshKh\ CosKy\ SinKx\ Coswt}{K2h\ Cos^2 Ka\ (SinhKh\ CosKh + Kh)} + \frac{2SWe\ CosKnh\ \left(e^{-Kn(a+x)} + e^{Kn(x-a)}\right)\ CosKny\ Coswt}{K^2 nhe^{-Kn2a}\ (SinKnh\ CosKnh + Knh)}\right]$$

When x = a

$$A = \frac{2K \int_0^h U(y)\ CoshKy\ dy}{Cos^2 Ka\ (SinKh\ CosKh + Kh)}$$

$$A = \left[\frac{2K \int_0^h SWe\ (1-y/h)\ CoshKy\ dy}{Cos^2 Ka\ (SinKh\ CosKh + Kh)}\right] \text{as before} \qquad \ldots.(9)$$

$$An = \left[\frac{4Kn \int_0^h U(y)\ CosKny\ dy}{e^{-Kn2a}\ (SinKnh\ CosKnh + Knh)}\right]$$

$$An = \left[\frac{4Kn \int_0^h SWe\ (1/y/h)\ CosKny\ dy}{e^{-Kn2a}\ (SinKnh\ CosKnh + Knh)}\right] \qquad \ldots..(10)$$

From (9), A yields

$$\frac{2WeS \cosh Kh}{Kh \cos^2 Ka \, (\sin Kh \cosh Kh + Kh)}$$

and (10), An yields

$$\frac{-2WeS \cos Knh}{Knhe^{-Kn2a} \, (\sin Knh \cos Knh + Knh)}$$

Now surface elevation $|\zeta| = \frac{1}{g} \quad \frac{\partial \phi}{\partial t}$

$$\left.\frac{\partial \phi}{\partial t}\right|_{\substack{x = a \\ y = o}} = \left[\frac{2We \cosh Kh \cosh Ky \sin Kx \sin wt}{K^2 h \cos^2 Ka \, (\sinh Kh \cos Kh + Kh)} - \frac{2SWe \cos Knh \, e^{-Kn2a} \cos Kny \sin wt \, (W)}{K^2 nhe^{-Kn2a} \, (\sin Knh \cos Knh + Knh)} \right]$$

W = Natural frequency of water

We= Excitation frequency

$$|\zeta| = \left[\frac{2WeS\ \mathrm{Cosh}Kh\ \mathrm{Sin}Ka\ \mathrm{Sin}Wt\ (W)}{K^2 h\ \mathrm{Cos}^2 Ka\ (\mathrm{Sinh}Kh + Kh)} + \sum_{n\,1}^{\infty} \frac{2SWe\ \mathrm{Cos}Knh\ \mathrm{Sin}wt\ (W)}{K^2 nh\ (\mathrm{Sin}Knh\ \mathrm{Cos}Knh + Knh)} \right]$$

$$|\zeta| = \left[\frac{2WeS\ \mathrm{Sin}wt(W)}{h} \left(\frac{2\mathrm{Cosh}Kh\ \mathrm{Sin}Ka}{K^2\ \mathrm{Cos}^2 Ka\ (\mathrm{Sinh}Kh + \mathrm{Cosh}Kh + Kh)} + \sum_{n=1}^{\infty} \frac{\mathrm{Cos}Knh}{Kn^2\ (\mathrm{Sin}Knh\ \mathrm{Cos}Knh + Knh)} \right) \right] \quad \ldots\ldots(11)$$

Subst. numerical values *i.e.* $h/2a = 0.5$, at resonance $We = w$ where $W = \left[\frac{g\pi}{2a} \tanh \frac{\pi h}{2a}\right]^{1/2} = 7.52$ rad/s $(2a=0.5)$ $h=0.25$m

$K = 2\pi/\lambda = \pi/2a$ (at resonance $\lambda = 4a$)

hence subst. in equation (11) yields the following:

(A) approaches infinity and (B) becomes very small. In other words (A) is more dominant then (B), where (A) represents the formation of the standing wave, and (B) local disturbances. Thus if (B) is ignored

$$\therefore\ |\zeta| = \frac{2We\ \mathrm{Sin}\ wt\ (W)}{h} \; \frac{\mathrm{Cosh}Kh . \mathrm{Sin}Ka}{K^2 a\ \mathrm{Cos}^2 Ka\ (\mathrm{Sinh}Kh\ \mathrm{Cosh}Kh + Kh)} \quad \ldots.(12)$$

Furthermore this applies to the range $x = -a$ to $x = +a$.

APPENDIX III - BACKGROUND TO THEORETICAL STUDY

In the case of irrotational, two dimensional flow, a velocity potential has been defined by

$$\mu = \frac{\partial \phi}{\partial x} \quad W = \frac{\partial \phi}{\partial z}$$

By introducing the above into the continuity relationship ie.

$$\frac{\partial \mu}{\partial x} + \frac{\partial w}{\partial z} = 0$$

hence

$$\frac{\partial^2 \phi}{\partial x^2} + \frac{\partial^2 \phi}{\partial z^2} = 0 \qquad \ldots\ldots (1)$$

Which is the well known Laplace equation, which a solution has to satisfy.

Other conditions which have to be satisfied are as follows:

1. At the free surface : Two conditions must be satisfied, these are the dynamic condition stating the value of pressure, and the Kinematic condition with the particle remain at the free surface.

Dynamic free surface condition

$$\frac{\partial^2 \phi}{\partial t^2} + g\frac{\partial \phi}{\partial z} = 0 \qquad \ldots\ldots (2)$$

Kinematic free surface condition:

$$\frac{\partial \eta}{dt} - \frac{\partial \phi}{\partial z} + \frac{\partial \phi}{\partial x} \quad \frac{\partial \eta}{\partial x} \qquad \ldots\ldots (3)$$

Here g is the acceleration of gravity, $z = \ (x,t)$ the free surface shape, and t is the time.

2. Solid boundary, since the fluid cannot pass through or escape from the boundary.

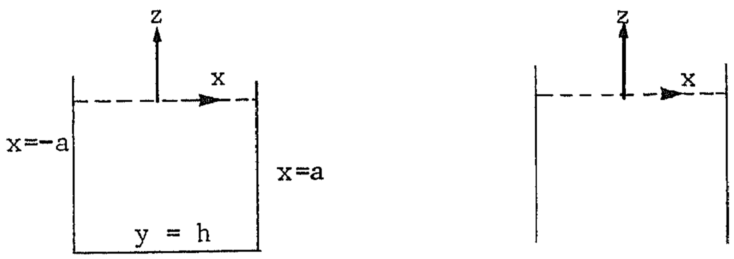

Tank
(1)

Moonpool
(2)

Co-ordinate system

ie. $\frac{\partial \phi}{\partial x} = 0$ on $x = \pm a$

(1) $\partial\phi/\partial z = 0$ on $z = -h$

Bernoulli's equation:

$$\frac{\partial \phi}{\partial t} + g\eta + \tfrac{1}{2} V^2 = 0$$ (is another form of equation (2)

ignoring $\frac{1}{2}V^2$ ie, linearised

=> $\frac{\partial \phi}{\partial t} + g\eta = 0$

=> $\eta = -1/g\ \partial\phi/\partial t$:

Assume the following:

$\phi = X(x)\ Z(z)\ T(t)$ ..... (4)

hence $\frac{\partial^2 \phi}{\partial X^2} = \frac{\partial^2 X}{\partial x^2}\ Z(2)$ ..... (5)

$\frac{\partial^2 \phi}{\partial Z^2} = \frac{\partial^2 Z}{\partial z^2}\ X(x)\ T(t)$ ..... (6)

The solution for X and Z will be in the form

$Z(z) = \text{Cosh}\ (Kztd)$ ..... (7)

and

$X(x) = \text{Sin}\ (Kx+\beta)$ ..... (8)

If a condition is applied as in fig.1, ie, $\frac{\partial \phi}{\partial z} = 0$ at $Z=-h$

$\frac{\partial z}{dz} = \text{Sinh}\ (-Kh + \alpha) = 0 \Rightarrow \alpha = Kh$

hence $Z(z) = \text{Cosh}K\ (z+h)$ ..... (9)

Otherwise if we let phase angle $B = 0$, and $= 0$

=> $Z(z) = \text{Cosh}\ KZ$ ..... (10)

and similarly

$$X(x) = \operatorname{Sin} Kx \qquad \ldots\ldots \quad (11)$$

Now $K = 2\pi/\lambda$ where $\lambda =$ wavelength
near resonance $\lambda = 4a \Rightarrow K = \frac{2\pi}{4a} = \pi/2a$

The time dependent function T(t):
from free surface condition

$$\frac{\partial^2 \phi}{\partial t^2} + \frac{g\partial\phi}{\partial z} = 0 \quad \left(\frac{\partial\phi}{\partial z} = w^2/g\right), \; z = 0$$

$$\text{ie. } T''(t) + w^2 T(t) = 0 \qquad \ldots\ldots \quad (12)$$

where

$$w = \left[\frac{g\pi}{2a} \tanh \frac{\pi}{2a} h\right]^{1/2} \qquad \ldots\ldots \quad (13)$$

is the first natural circular frequency.
Now solution for (12) is in the form

$$T(t) = \operatorname{Sin}(wt + \gamma) \qquad \ldots\ldots \quad (14)$$

by letting $\gamma = 0$, as combining with equation (9)/(10) and (11)

$\phi = \operatorname{Cosh} \pi/2a\,(Z+h)\,\operatorname{Sin}(\pi/2a\; x)\,\operatorname{Sin} wt$ See fig. 1
or $\phi = \operatorname{Cosh} \pi/2a\,(Z)\,\operatorname{Sin}(\pi/2a\; x)\,\operatorname{Sin} wt$ See fig. 2

Further studies will involve introducing a forcing term i.e., θ Coswt as in the case of rolling. The above analysis is as in the case of free vibrations.

This theory can also be extended to include damping. For example in equation (2) if a damping term say $\mu\, \partial\phi/\partial t$ is introduced.

ie, $\frac{\partial^2\phi}{\partial t^2} + \frac{\mu\partial\phi}{\partial t} + g\frac{\partial\phi}{\partial y} = 0$ ..... (15)

=> $T''(t) + \mu T'(t) + w^2 T = 0$ ..... (16)

Using Vector Algebra to find an Unknown Wave Source

$$\iiint_V \text{div}\ \underline{F}\ dv = \iint_S \underline{F}\ \underline{n}\ ds$$

$\underline{F} = \phi\ \text{grad}\phi$ $\qquad$ $\text{grad}\ \phi = \left(\frac{\partial\phi}{\partial x}, \frac{\partial\phi}{\partial y}, \frac{\partial\phi}{\partial z}\right)$

$$\text{Div}\ \underline{F} = \frac{Fx}{\partial x} + \frac{Fy}{\partial y} + \frac{Fz}{\partial z}$$

$$\text{Div}\ (\phi\ \text{grad}\phi) = \text{grad}\phi\ .\ \text{grad}\phi + \phi\nabla^2\phi$$
$$\text{Div}\ (\phi_1\text{grad}\phi_2) = \text{grad}\ \phi_1\ \text{grad}\phi_2 + \phi_1\nabla^2\phi_2$$
$$\text{Div}\ (\phi_2\text{grad}\phi_1) = \text{grad}\ {}_2\ \text{grad}\ {}_1 + \phi_2\nabla^2\phi_1$$

$$\iiint_V \text{div}\ (\phi_1\ \text{grad}\phi_2) - \text{div}\ (\phi_2\ \text{grad}\phi_1)\ dv = 0$$
$$\therefore \iint_S (\phi_1\ \underbrace{\text{grad}\phi_2 . n}_{\partial\phi_2/\partial n} - \phi_2\ \underbrace{\text{grad}\ \phi_1 . n}_{\partial\phi_1/\partial n})\ ds = 0$$
$$\iint_S (\phi_1\ \partial\phi_2/\partial n - \phi_2\partial\phi_1/\partial n)\ ds = 0$$

let ${}_1$ = unknown = & ${}_2$ known wave source

ie. $\iint_S (\phi\partial\phi_2/\partial n - \phi_2\partial\phi/\partial n)\ ds = 0$

can be written

$$\int_{body} (\phi\ \partial\phi_2/\partial n - \phi_2\ \partial\phi/\partial n)\ ds = 0$$

Consider a point distance r

hence $2\pi\phi r(x,y)\ \frac{1}{r} + \int_{body} \phi_2\ \partial\phi/\partial n\ \ ds$

APPENDIX IV - EXPERIMENTAL RESULTS

ASPECT RATIO (h/2a) = (h/2a) = 0.5

Forced Frequency (rad/s)	Tank Wave Amplitude (mm)
0	0
3.029	8.0
3.040	3.0
4.283	5.0
5.096	9.0
5.497	14.0
5.650	16.0
5.872	17.0
6.042	18.0
6.053	18.5
6.283	23.0
6.246	24.0
6.443	32.0
6.663	35.0
6.656	40.0
6.852	48.0
6.905	56.0
6.943	59.0
7.044	112.0
7.132	110.0
7.681	100.0
7.854	80.0
8.107	68.0
8.491	67.0
9.093	52.0
9.534	46.0
10.134	42.0
10.578	36.0
11.260	30.0

(Free Oscillation Frequency = 7.536 rad/s)

Forced Frequency (rad/s)	Moonpool Wave Amplitude (mm)
0	0
3.142	1.0
3.982	8.0
4.959	8.0
5.546	10.0
5.786	12.0
5.984	14.0
6.196	15.0
6.372	16.0
6.567	16.5
6.734	22.0
6.935	24.0
6.981	24.0
7.092	30.0
7.214	35.0
7.281	37.0
7.349	44.0
7.498	60.0
7.543	92.0
7.616	125.0
7.672	121.0
7.691	120.0
7.923	110.0
8.097	86.0
8.457	80.0
8.607	80.0
8.727	68.0
9.200	44.0
9.666	40.0
9.926	32.0
10.889	34.0
11.424	32.0
11.508	24.0
14.120	12.0

(Free Oscillation Frequency = 8.062 rad/s)

ASPECT RATIO (h/2a) = (h/2a) = 0.25

Forced Frequency (rad/s)	Tank Wave Amplitude (mm)	Forced Frequency (rad/s)	Moonpool Wave Amplitude (mm)
0	0	0	0
3.222	1.0	5.236	5.0
3.540	4.0	6.283	8.0
3.848	4.5	6.498	9.0
4.610	7.0	6.749	12.0
4.947	8.5	7.140	15.0
4.987	8.5	7.392	17.0
5.280	16.0	7.662	24.0
5.585	17.0	7.691	25.0
5.802	26.0	7.805	30.0
5.950	31.0	7.913	36.0
6.106	38.0	8.378	74.0
6.240	57.0	8.739	80.0
6.353	58.0	8.976	76.0
6.545	52.0	9.226	56.0
6.935	38.0	9.420	48.0
7.392	34.0	9.848	39.0
8.045	30.0	10.368	32.0
8.702	22.0	11.081	26.0
10.183	20.0	12.060	26.0

(Free oscillation frequency = 6.406 rad/s)

(Free oscillation frequency = 8.729 rad/s)

ASPECT RATIO (h/2a) = (h/2a) = 1.0

Forced Frequency (rad/s)	Tank Wave Amplitude (mm)	Forced Frequency (rad/s)	Moonpool Wave Amplitude (mm)
0	0	0	0
3.142	1.0	3.491	1.5
5.075	2.0	5.180	2.5
5.984	5.0	6.981	4.0
6.756	5.0	8.235	7.5
7.116	5.2	9.308	9.0
7.653	6.0	9.989	12.0
7.933	7.0	10.134	14.0
8.378	9.0	10.368	16.0
8.666	12.0	10.472	20.0
9.711	12.5	10.525	44.0
9.973	15.0	10.613	50.0
10.134	19.0	10.777	54.0
10.250	21.0	11.043	60.0
10.368	63.0	11.280	52.0
10.472	72.0	11.362	50.0
10.525	73.0	11.679	56.0
10.889	58.0	11.877	56.0
11.487	52.0	12.393	25.0
12.037	58.0	12.771	24.0
12.417	37.0	13.228	24.0
13.340	25.0	13.870	28.0
14.280	34.0		
16.111	26.0		

(Free Oscillation Frequency = 12.593 rad/s)

(Free Oscillation Frequency = 12.375 rad/s)

ASPECT RATIO (h/2a) = 1.5

Forced Frequency (rad/s)	Tank Wave Amplitude (mm)
0	0
2.532	0.7
4.423	1.5
5.642	2.0
6.283	6.0
7.150	4.0
7.854	6.0
8.269	7.0
9.199	7.0
9.821	10.0
10.474	15.0
10.562	16.0
10.593	16.0
10.612	18.0
10.813	48.0
10.908	59.0
11.065	49.0
11.159	50.0
11.385	43.0
11.680	42.0
11.988	44.0
12.271	34.0
12.566	26.0
13.396	24.0
15.991	19.0

(Free Oscillation Frequency = 12.504 rad/s)

Forced Frequency (rad/s)	Moonpool Wave Amplitude (mm)
0	0
4.833	2.0
6.905	6.0
8.160	6.0
8.976	6.0
9.593	8.0
10.005	8.0
10.351	12.0
10.472	12.0
10.613	14.0
10.772	16.0
10.777	38.0
11.023	39.5
11.571	43.0
11.923	30.0
12.060	33.0
12.393	32.0
12.668	22.0
13.228	21.0
14.151	14.0
15.708	12.0

(Free Oscillation Frequency = 12.177 rad/s)

TANK EXPERIMENT WITH BAFFLES

ASPECT RATIO (h/2a) = 0.5

4cm baffles: @ MWL and 30mm below		4cm baffles: @ MWL and 50mm below on both sides		4cm baffles: @ MWL and 100mm below	
Forced Frequ. (rad/s)	Tank Wave Ampl. (mm)	Forced Frequ. (rad/s)	Tank Wave Ampl. (mm)	Forced Frequ. (rad/s)	Tank Wave Ampl. (mm)
0	0	0	0	0	0
4.260	6.0	5.027	7.0	3.443	2.4
4.959	7.0	5.712	14.0	5.129	8.0
5.818	14.0	6.283	20.0	6.203	18.0
6.283	18.0	6.734	24.0	6.614	26.0
6.089	24.0	7.181	32.0	6.927	29.0
7.060	27.5	7.588	44.0	7.222	42.0
7.214	48.0	7.933	46.0	7.445	45.0
7.462	58.0	8.149	46.0	7.616	46.0
7.786	60.0	8.192	47.0	8.235	48.0
8.066	56.0	8.311	44.0	8.514	38.0
8.862	52.0	9.054	42.0	9.420	30.0
9.420	46.0	9.578	39.0	9.989	28.0
10.053	40.0	9.756	35.0	10.777	24.0
10.777	36.0	10.472	32.0		
		11.788	24.0		

TANK EXPERIMENT WITH BAFFLES

ASPECT RATIO (h/2a) = 0.5

4cm wide baffles: 10mm below MWL on either side.		4cm wide baffles: 50mm below MWL		4cm wide baffles: at the MWL	
Forced Frequ. (rad/s)	Tank Wave Ampl. (mm)	Forced Frequ. (rad/s)	Tank Wave Ampl. (mm)	Forced Frequ. (rad/s)	Tank Wave Ampl. (mm)
0	0	0	0	0	0
3.142	2.0	4.054	4.0	4.543	6.0
5.027	8.5	5.096	8.0	5.911	10.0
5.464	11.0	5.712	11.0	6.042	16.0
5.712	12.0	6.130	17.0	6.614	29.0
6.042	18.0	6.392	29.5	6.981	42.0
6.283	22.5	6.830	38.0	7.181	45.0
6.822	40.0	7.140	47.0	7.392	50.0
6.905	53.0	7.446	55.0	7.580	46.0
7.036	70.0	7.672	51.0	7.796	56.0
7.392	62.0	8.149	41.0	8.107	62.0
7.662	50.0	8.457	37.0	8.479	50.0
7.933	42.0	9.199	30.0	8.976	44.0
8.378	35.0			9.563	40.0
8.976	26.0			10.118	34.0
9.563	22.0			10.871	24.0

TANK EXPERIMENT WITH BAFFLES

ASPECT RATIO (h/2a) = 0.5

2cm wide baffles: 100mm below MWL		2cm baffles: at MWL		2cm baffles: @ MWL and 100mm 100mm below		2cm baffles @ MWL 50mm below	
Forced Frequ. (rad/s)	Tank Wave Ampl. (mm)	Forced Frequ. (rad/s)	Tank Wave Ampl (mm)	Forced Frequ. (rad/s)	Tank Wave Ampl (mm)	Forced Frequ. (rad/s)	Tank Wave Ampl. (mm)
0	0	0	0	0	0	0	0
3.927	7.0	4.054	6.0	3.879	8.0	4.488	5.0
5.236	9.0	4.959	9.0	5.129	9.0	5.347	10.0
5.984	19.0	5.712	13.0	5.802	16.0	5.712	13.0
6.525	24.0	6.130	18.0	6.160	19.0	6.203	20.0
6.793	44.0	6.498	25.0	6.471	30.0	6.830	40.0
6.852	50.0	6.545	26.0	6.793	40.0	7.060	68.0
6.981	86.0	6.682	35.0	7.124	60.0	7.230	80.0
7.392	68.0	7.068	68.0	7.298	58.0	7.480	76.0
8.025	50.0	7.247	66.0	7.767	52.0	7.672	64.0
8.607	39.0	7.516	60.0	8.107	50.0	7.854	60.0
9.477	30.0	7.561	60.0	8.378	44.0	8.192	45.0
		7.854	52.0	8.887	32.0	8.800	40.0
		8.837	37.0	9.477	24.0	9.549	28.0
		9.308	34.0				
		10.472	27.0				

MOONPOOL EXPERIMENT WITH BAFFLES

ASPECT RATIO (h/2a) = 0.5

4cm baffles: 100mm below MWL		4cm baffles: 50mm below		4cm baffles: at MWL	
Forced Frequ. (rad/s)	Moonpool Wave Ampl. (mm)	Forced Frequ. (rad/s)	Moonpool Wave Ampl. (mm)	Forced Frequ. (rad/s)	Moonpool Wave Ampl. (mm)
0	0	0	0	0	0
4.833	4.0	5.236	9.0	5.284	6.0
5.236	8.0	5.928	11.0	6.160	14.0
5.712	10.0	6.283	12.0	6.545	16.0
6.283	12.0	6.734	24.0	6.905	22.0
6.614	18.0	7.050	26.0	7.181	28.0
6.981	32.0	7.306	30.0	7.392	32.0
7.140	52.0	7.480	40.0	7.498	38.0
7.392	50.0	7.854	44.0	7.757	48.0
7.662	49.0	7.994	46.0	7.854	50.0
8.055	40.0	8.055	48.0	8.160	58.0
8.376	32.0	8.300	44.0	8.192	60.0
8.976	26.0	8.572	44.0	8.378	56.0
10.472	20.0	8.976	37.0	8.727	50.0
		9.520	32.0	9.133	46.0
		9.817	28.0	9.666	44.0
				10.183	36.0
				11.219	30.0

MOONPOOL EXPERIMENT WITH BAFFLES

ASPECT RATIO (h/2a) = 0.5

4cm baffles: 50mm above MWL		4cm baffles: 100mm and 50mm below MWL		4cm baffles: 100mm below and at MWL	
Forced Frequ. (rad/s)	Moonpool Wave Ampl. (mm)	Forced Frequ. (rad/s)	Moonpool Wave Ampl. (mm)	Forced Frequ. (rad/s)	Moonpool Wave Ampl. (mm)
0	0	0	0	0	0
5.027	9.0	4.654	5.0	5.712	7.0
6.525	18.0	5.236		6.221	13.0
6.882	24.0	5.236	7.0	6.852	21.0
7.140	32.0	5.712	8.0	7.181	22.0
7.392	40.0	6.283	12.0	7.453	36.0
7.480	52.0	6.614	15.0	7.757	42.0
7.854	66.0	6.830	24.0	8.025	40.0
8.055	80.0	6.981	28.0	8.378	39.0
8.666	74.0	7.306	38.0	8.976	38.0
8.976	64.0	7.480	45.0	8.976	36.0
9.080	48.0	7.854	54.0	9.106	34.0
9.666	32.0	8.055	40.0	9.666	30.0
		8.976	25.0	10.250	30.0
				11.004	26.0

MOONPOOL EXPERIMENT WITH BAFFLES

ASPECT RATIO (h/2a) = 0.5

4cm baffles: 50mm and 20mm below MWL		4cm baffles: 40mm below and at MWL		4cm baffles: at MWL and 50mm below	
Forced Frequ. (rad/s)	Moonpool Wave Ampl. (mm)	Forced Frequ. (rad/s)	Moonpool Wave Ampl. (mm)	Forced Frequ. (rad/s)	Moonpool Wave Ampl. (mm)
0	0	0	0	0	0
5.347	6.0	5.075	7.0	5.775	9.0
6.203	12.0	6.411	14.0	5.984	12.0
6.852	20.0	7.181	24.0	6.411	14.0
7.181	25.0	7.392	26.0	7.060	25.5
7.392	30.0	7.854	46.0	7.306	27.0
7.662	40.0	8.107	58.0	7.579	30.0
8.267	51.0	8.491	62.0	7.854	30.0
8.378	52.0	8.763	60.0	8.107	38.0
8.763	54.0	9.080	54.0	8.457	46.0
9.106	46.0	9.563	50.0	8.666	46.0
9.420	40.0	9.817	50.0	9.080	44.0
10.053	36.0	10.300	48.0	9.420	44.0
11.004	32.0	10.472	46.0	9.772	42.0
		11.424	36.0	10.300	35.0
		11.968	22.0	10.472	33.0
				11.081	32.0
				11.877	16.0

MOONPOOL EXPERIMENT WITH BAFFLES

ASPECT RATIO (h/2a) = 0.5

2cm baffles: 100mm below MWL		2cm baffles 50mm below MWL		2cm baffles: at MWL	
Forced Frequ. (rad/s)	Moonpool Wave Ampl. (mm)	Forced Frequ. (rad/s)	Moonpool Wave Ampl. (mm)	Forced Frequ. (rad/s)	Moonpool Wave Ampl. (mm)
0	0	0	0	0	0
5.096	6.0	5.384	8.0	6.283	14.0
5.984	10.0	6.178	12.0	6.734	20.0
6.444	20.0	6.734	22.0	7.060	28.0
6.830	28.0	6.981	26.0	7.332	42.0
7.181	36.0	7.181	34.0	7.616	60.0
7.392	66.0	7.306	44.0	7.854	64.0
7.579	76.0	7.616	60.0	7.953	66.0
7.854	78.0	7.974	80.0	8.160	64.0
8.192	71.0	8.192	78.0	8.378	58.0
9.133	32.0	8.378	70.0	8.850	50.0
10.596	22.0	8.727	50.0	9.420	36.0
		9.364	32.0	10.053	27.0

MOONPOOL EXPERIMENT WITH BAFFLES

ASPECT RATIO (h/2a) = 0.5

2cm baffles: at MWL and 50mm below		2cm baffles: 20mm and 50mm below MWL		2cm baffles: 30mm below and at MWL	
Forced Frequ. (rad/s)	Moonpool Wave Ampl. (mm)	Forced Frequ. (rad/s)	Moonpool Wave Ampl. (mm)	Forced Frequ. (rad/s)	Moonpool Wave Ampl. (mm)
0	0	0	0	0	0
4.959	6.0	4.488	4.0	5.712	10.0
5.802	10.0	4.760	4.25	6.203	14.0
6.411	14.0	5.546	8.0	6.793	22.0
6.920	25.0	5.984	14.0	7.306	32.0
7.392	40.0	6.525	16.0	7.543	48.0
7.854	72.0	6.498	16.0	7.728	68.0
7.933	74.0	6.684	20.0	7.953	74.0
8.468	64.0	7.222	26.0	8.192	70.0
8.666	58.0	7.392	38.0	8.468	64.0
9.989	34.0	7.543	48.0	9.200	44.0
		7.728	74.0	9.420	40.0
		7.933	80.00	10.134	36.0
		8.192	74.0	10.833	29.0
		8.619	62.0		
		9.420	36.0		

MOONPOOL EXPERIMENT WITH BAFFLES

ASPECT RATIO (h/2a) = 0.5

2cm baffles: 10mm, 30mm and 50mm below MWL		2cm baffles: at MWL and 100mm below		2cm baffles: 50mm, 30mm and 10mm below MWL	
Forced Frequ. (rad/s)	Moonpool Wave Ampl. (mm)	Forced Frequ. (rad/s)	Moonpool Wave Ampl. (mm)	Forced Frequ. (rad/s)	Moonpool Wave Ampl. (mm)
0	0	0	0	0	0
5.236	6.0	4.928	5.0	5.712	6.0
6.082	13.0	5.872	11.0	6.283	14.0
6.498	18.0	6.283	12.0	6.981	20.0
6.830	22.0	6.684	18.0	7.306	30.0
7.076	28.0	7.140	28.0	7.570	40.0
7.281	33.0	7.392	40.0	7.974	36.0
7.543	47.0	7.662	50.0	8.107	69.0
7.662	83.0	7.854	53.0	8.572	71.0
7.963	82.0	8.055	50.0	8.976	50.0
8.107	78.0	8.378	50.0	9.520	42.0
8.727	64.0	8.666	46.0	9.989	38.0
9.578	34.0	9.054	40.0	11.220	32.0
		9.563	34.0		
		10.300	26.0		
		11.004	22.0		

MOONPOOL EXPERIMENT WITH WAVES GENERATED

ASPECT RATIO (h/2a) = 0.5

Waves generated (1.05V)
(0.8Hz/5.027 rad/s)

Forced Frequ. (rad/s)	Moonpool wave ampl. (mm)	Moonpool wave amp/wave amp
0	60	1.07
5.276	50.0	0.89
4.984	50.0	0.89
6.498	65.0	1.16
6.912	77.0	1.38
7.140	80.0	1.43
7.462	80.0	1.50
7.672	140.0	2.50
7.913	140.0	2.33
8.128	130.0	2.17
8.346	130.0	2.17
8.514	110.0	1.83
8.572	110.0	1.83
8.900	100.0	1.67
9.420	90.0	1.41
9.666	77.5	1.25
10.317	74.0	1.32
10.833	75.0	1.34

Waves generated (1.4V)
(0.88 Hz/5.529 rad/s)

Forced Frequ. (rad/s)	Moonpool Wave ampl. (mm)	Moonpool wave amp/wave amp
0	84.0	1.3
2.285	90.0	1.4
3.142	88.0	1.47
3.989	80.0	1.33
4.987	82.0	1.37
5.417	70.0	1.30
5.645	70.0	1.25
6.042	70.0	1.25
6.360	80.0	1.33
6.500	84.0	1.40
6.734	90.0	1.61
6.981	90.0	1.61
7.181	90.0	1.61
7.332	95.0	1.70
7.392	100.0	1.79
7.543	126.0	2.10
7.579	144.0	2.40
7.757	140.0	2.33
7.854	140.0	2.25
7.923	140.0	2.19
7.963	140.0	2.19
8.107	130.0	2.17
8.572	110.0	1.96
8.976	110.0	1.96
9.420	100.0	1.78
10.118	90.0	1.61
11.081	80.0	1.43

MOONPOOL EXPERIMENT WITH WAVES GENERATED

ASPECT RATIO (h/2a) = 0.5

Waves generated (1.1 V)
(087 Hz/5.466 rad/s)

Forced Frequ. (rad/s)	Moonpool wave ampl. (mm)	Moonpool wave amp/wave amp
0	66.0	1.00
5.027	60.0	1.07
5.712	60.0	1.07
6.082	64.0	1.14
6.100	66.0	1.17
6.545	68.0	1.21
6.614	72.0	1.29
6.927	76.0	1.36
7.132	84.0	1.50
7.332	88.0	1.57
7.462	90.0	1.61
7.543	136.0	2.43
7.672	140.0	2.50
7.953	140.0	2.33
8.267	128.0	1.94
8.800	106.0	1.66
9.213	90.0	1.57
9.240	94.0	1.57
9.989	80.0	1.43
10.596	72.0	1.29

Waves generated (1.05V)
(0.89 Hz/5.592 rad/s)

Forced Frequ. (rad/s)	Moonpool Wave ampl. (mm)	Moonpool wave amp/wave amp
0	70.0	1.09
5.236	80.0	1.25
5.712	80.0	1.25
6.360	80.0	1.25
6.392	88.0	1.38
6.830	100.0	1.47
6.852	94.0	1.47
6.981	94.0	1.47
7.247	94.0	1.50
7.543	110.0	1.62
7.616	150.0	2.34
7.805	150.0	2.34
7.953	160.0	2.50
8.107	140.0	2.06
8.300	140.0	2.06
8.800	120.0	1.76
8.763	115.0	1.69
9.308	100.0	1.39
10.053	90.0	1.32
10.596	90.0	1.28
11.160	86.0	1.26

MOONPOOL EXPERIMENT WITH WAVES GENERATED

ASPECT RATIO (h/2a) = 0.5

Waves generated (1.0V)
(0.9 Hz/5.655 rad/s)

Forced Frequ. (rad/s)	Moonpool wave ampl. (mm)	Moonpool wave amp/wave amp
0	70.0	1.09
5.464	76.0	1.14
6.283	80.0	1.25
6.411	84.0	1.31
6.734	87.0	1.36
6.981	90.0	1.42
7.067	92.0	1.44
7.332	102.0	1.59
7.543	116.0	1.81
7.690	140.0	2.19
7.854	180.00	2.64
8.025	140.0	2.19
8.267	140.0	2.19
8.727	120.0	1.87
9.420	92.0	1.40
10.317	88.0	1.33
11.023	78.0	1.15

ASPECT RATIO (h/2a) = 1.0

Waves generated (1.0V)
(0.9 Hz/5.655 rad/s)

Forced Frequ. (rad/s)	Moonpool Wave ampl. (mm)	Moonpool wave amp/wave amp
0	62.0	1.14
6.663	66.0	1.06
8.025	68.0	1.10
9.213	68.0	1.10
10.368	72.0	1.20
10.631	90.0	1.45
10.871	90.0	1.45
11.180	91.0	1.47
11.593	82.0	1.37
11.833	86.0	1.34
12.200	76.0	1.27
12.566	73.0	1.26
13.036	76.0	1.27
13.840	78.0	1.30
15.032	80.0	1.33
16.07	74.0	1.32

MOONPOOL EXPERIMENT WITH WAVES GENERATED

ASPECT RATIO (h/2a) = 1.0

Waves generated (1.02V)
(0.94Hz/5.906 rad/s)

Forced Frequ. (rad/s)	Moonpool wave ampl. (mm)	Moonpool wave amp/wave amp
0	66.0	1.18
7.214	72.0	1.20
9.200	70.0	1.25
9.989	72.0	1.38
10.334	73.0	1.40
10.631	90.0	1.50
10.927	94.0	1.57
11.280	90.0	1.61
11.636	92.0	1.64
12.083	84.0	1.40
12.566	78.0	1.39
12.982	79.0	1.36
13.172	84.0	1.35
13.963	82.0	1.32
15.20	80.0	1.29

Waves generated (1.2V)
(0.96Hz/6.032 rad/s)

Forced Frequ. (rad/s)	Moonpool Wave ampl. (mm)	Moonpool wave amp/wave amp
0	76.0	1.36
6.830	80.0	1.38
7.854	80.0	1.38
8.763	80.0	1.39
9.308	80.0	1.40
9.364	80.0	1.42
9.895	82.0	1.46
10.134	82.0	1.46
10.300	86.0	1.54
10.578	86.0	1.54
10.777	100.0	1.78
11.362	102.0	1.82
11.679	96.0	1.71
12.296	88.0	1.57
12.849	80.0	1.46
13.719	90.0	1.40
14.889	82.0	1.37

MOONPOOL EXPERIMENT WITH WAVES GENERATED

ASPECT RATIO (h/2a) = 1.0

Waves generated (1.1V)
(0.98Hz/6.158rad/s)

Forced Frequ. (rad/s)	Moonpool wave ampl. (mm)	Moonpool wave amp/wave amp
0	75.0	1.34
7.140	80.0	1.43
8.107	80.0	1.48
9.420	78.0	1.50
9.817	82.0	1.52
10.217	82.0	1.57
10.578	94.0	1.68
10.889	98.0	1.75
11.121	100.0	1.85
11.722	96.0	1.70
11.788	95.0	1.60
12.248	88.5	1.58
12.875	80.0	1.54
14.248	88.0	1.57

Waves generated (1.0V)
(1.0Hz/6.283 rad/s)

Forced Frequ. (rad/s)	Moonpool Wave ampl. (mm)	Moonpool wave amp/wave amp
0	66.0	1.27
7.060	72.0	1.44
7.994	74.0	1.48
8.976	70.0	1.46
9.477	75.0	1.50
9.848	75.0	1.50
10.151	77.0	1.54
10.385	77.0	1.54
10.796	100.0	1.78
11.043	110.0	1.96
11.321	88.0	1.69
11.877	86.0	1.65
12.248	80.0	1.54
12.248	72.0	1.38
12.771	74.0	1.37

MOONPOOL EXPERIMENT WITH WAVES GENERATED

ASPECT RATIO (h/2a) = 0.25

Waves generated (   )
(1.1 Hz/6.92 rad/s)

Forced Frequ. (rad/s)	Moonpool wave ampl. (mm)	Moonpool wave amp/wave amp
0	70.0	1.52
2.992	72.0	1.64
4.833	73.0	1.66
6.830	76.0	1.73
7.500	90.0	2.05
8.235	108.0	2.25
8.607	120.0	2.4
9.040	94.0	1.81
9.787	90.0	1.73
10.167	90.0	1.73
10.722	92.0	1.64
11.321	84.0	1.62
12.296	82.0	1.58
14.215	76.0	1.46

ASPECT RATIO (h.2a) = 1.50

Waves generated (
(0.78 Hz/4.901 rad/s)

Forced Frequ. (rad/s)	Moonpool Wave ampl. (mm)	Moonpool wave amp/wave amp
0	100.0	1.85
7.044	100.0	1.92
7.776	100.0	1.92
8.235	100.0	1.95
9.378	100.0	1.98
9.772	100.0	2.00
10.053	100.0	2.00
10.472	95.0	2.04
10.613	100.0	1.92
10.631	100.0	2.08
10.722	120.0	2.40
11.023	120.0	2.31
11.424	120.0	2.31
11.788	120.0	2.31
12.153	112.5	2.25
12.566	112.5	2.16
13.009	100.0	2.08
13.541	110.0	1.96
14.612	90.0	1.88
15.362	110.0	1.96
16.755	100.0	1.92
18.868	100.0	1.92

MOONPOOL EXPERIMENT WITH WAVES GENERATED

ASPECT RATIO (h/2a) = 0.25

VERTICAL OSCILLATION

Wave Frequency (rad/s)	Moonpool Wave Amplitude (mm)	Moonpool Wave Amp/ Wave Amp
0	0	0
7.540	38.0	0.68
6.912	70.0	1.64
6.283	54.0	0.96
5.655	38.0	0.68
5.027	36.0	0.64
4.398	30.0	0.54

MOONPOOL EXPERIMENT WITH WAVES GENERATED

ASPECT RATIO (h/2a) = 0.25

VERTICAL OSCIALLATION

Wave Frequency (rad/s)	Moonpool Wave Amplitude (mm)	Moonpool Wave Amp/ Wave Amp
0	0	0
5.654	40.0	0.71
5.027	94.0	1.68
4.900	106.0	1.85
4.775	78.0	1.39
4.650	72.0	1.29
43.98	50.0	0.89

MOONPOOL EXPERIMENT WITH WAVES GENERATED

ASPECT RATIO (h/2a) = 0.25

VERTICAL OSCILLATION

Forced Frequ. (rad/s)	Moonpool wave ampl. (mm)	Moonpool wave amp/wave amp
0	0	0
7.540	38.0	0.68
6.912	70.0	1.64
6.283	54.0	0.96
5.655	38.0	0.68
5.027	36.0	0.64
4.398	30.0	0.54

ASPECT RATION (h/2a) = 1.5

VERTICAL OSCILLATION

Forced Frequ. (rad/s)	Moonpool Wave ampl. (mm)	Moonpool wave amp/wave amp
0	0	0
5.654	40.0	0.71
5.027	94.0	1.68
4.900	106.0	1.85
4.775	78.0	1.39
4.650	72.0	1.29
4.398	50.0	0.89